IEEE Access
Multidisciplinary ⋮ Rapid Review ⋮ Open Access Journal

Received December 24, 2021, accepted January 18, 2022, date of publication February 15, 2022, date of current version March 8, 2022.

Digital Object Identifier 10.1109/ACCESS.2022.3151967

Wireless Transmissions, Propagation and Channel Modelling for IoT Technologies: Applications and Challenges

HAIDER A. H. ALOBAIDY[1], (Graduate Student Member, IEEE), MANDEEP JIT SINGH[1,2], MEHRAN BEHJATI[1], ROSDIADEE NORDIN[1], (Senior Member, IEEE), AND NOR FADZILAH ABDULLAH[1], (Member, IEEE)

[1]Department of Electrical, Electronic and Systems Engineering, Faculty of Engineering and Built Environment, Universiti Kebangsaan Malaysia (UKM), Bangi 43600, Malaysia
[2]Space Science Centre (ANGKASA), Institute of Climate Change, Universiti Kebangsaan Malaysia (UKM), Bangi 43600, Malaysia

Corresponding author: Rosdiadee Nordin (adee@ukm.edu.my)

This work was supported by the Malaysia's Ministry of Higher Education (MOHE) under Grant FRGS/1/2019/TK04/UKM/02/8.

ABSTRACT The Internet of Things (IoT) has rapidly expanded for a wide range of applications towards a smart future world by connecting everything. As a result, new challenges emerge in meeting the requirements of IoT applications while retaining optimal performance. These challenges may include power consumption, quality of service, localization, security, and accurate modeling and characterization of wireless channel propagation. Among these challenges, the latter is critical to establishing point-to-point wireless communication between the sensors. Channel modeling also varies depending on the features of the surrounding area, which have a direct impact on the propagation of wireless signals. This presents a difficult task for network planners to efficiently design and deploy IoT applications without understanding the appropriate channel model to analyze coverage and predict optimal deployment configurations. As a result, this challenge has attracted considerable interest in academic and industrial communities in recent years. Therefore, this review presents an overview of current breakthroughs in wireless IoT technologies. The challenges in such applications are then briefly reviewed, focusing on wireless channel propagation modeling and characterization. Finally, the study gives a generalized form of commonly used channel models and a summary of recent channel modeling developments for wireless IoT technology. The outcome of this review is expected to provide a new understanding of the propagation behavior of present and future wireless IoT technologies, allowing network engineers to undertake correct planning and deployment in any environment. Additionally, the study may serve as a guideline for future channel modeling and characterization studies.

INDEX TERMS Channel modelling, channel characterization, IoT applications, IoT challenges, wireless IoT technologies.

I. INTRODUCTION

Wireless Channel Characteristics are essential in any communication system since they directly affect wireless signals traveling from the transmitter (Tx) to receiver (Rx). On the other hand, wireless transmission has become the backbone for enabling wireless IoT applications. Thus, establishing and developing wireless networks relies on propagation models that consider geographical features, among other factors, that can contribute to signal loss [1]. As a result, there is a need to investigate the propagation channel parameters that directly impact wireless transmission performance. Failure to do so will impact the planning and deployment of any IoT application.

The associate editor coordinating the review of this manuscript and approving it for publication was Hongwei Du.

A. PROBLEM FORMULATION AND BACKGROUND

Besides, choosing an accurate channel model to represent the actual real-world wireless IoT deployment is challenging due to imperfection surrounding the deployment area. These imperfections might include the varying terrain, large objects (e.g., buildings and tall trees), and various moving objects

with variable speeds. In other words, the actual wireless IoT performance differs when used in environments that have different channel conditions from the original development environment. Furth, the ongoing expansion of wireless networks needs further signal propagation studies to assure an effective post-planning phase service coverage and efficiency [2].

In this sense, radio network engineers frequently employ PL models to predict coverage, optimize constrained network resources, and conduct interference feasibility studies [3]. As a result, numerous studies in recent years have focused on either surveying and evaluating current models; as in [2], [4]–[8]; or proposing/improving models for more accurate propagation estimation in a specific area; as in [1], [3], [9]–[11].

For example, [4] compared PL prediction from nine empirical PL models to observations from four television transmitters along five pathways in urban and rural areas. Similarly, [2] compared the performance of three PL models at a 5.8 GHz frequency band in 12 cities using RSSI from 335 fixed user locations. In [4], the Hata and Davidson models outperformed other models. Meanwhile, the SUI and Okumura models had the lowest prediction accuracy, ranging from 15% to 21%. In contrast, the SUI Model performed best in [2], with the lowest root mean square error (RMSE) of 7.22 dB and standard deviation (STD) compared to COST231-Hata and ECC-33.

On the other hand, [5] and [9] focused on studying the foliage impact. Reference [5] assessed foliage excess loss from 2 GHz to 18 GHz and 26.5 to 40 GHz mmWave frequency bands in a tropical outdoor canopy and thickly foliated trees. The Weissberger Modified Exponential Decay (W MED) and ITU-R showed the most optimistic estimate of the measured data, while COST 235 provides the most pessimistic estimate. FITU-R has the largest attenuation increment as a function of frequency. Thus, results disagreed with current empirical models built solely for their temperate measurement area. This study, however, did not consider a few other aspects, such as leaf size, foliage density, tree species, wind effect, and precipitation. As for [9], a new foliage empirical propagation model was proposed for two morphologies based on measurements made in outdoor tropical vegetation at 700-800 MHz. W MED, COST 235, and Chen & Kuo foliage models were also compared, revealing that the proposed model differs significantly over larger distances between Tx/Rx.

The authors of [10] and [1] analyzed an outdoor mixed path tropical Amazon region and developed a propagation model for Digital TV (DTV) services in the UHF band. The model in [10] was based on Geometrical Optics (GO) and the Uniform Theory of Diffraction (UTD). In contrast, [1] proposed a Machine Learning (ML)-based model for non-homogeneous paths and various climates. The model was then tested using measurements from two DTV stations, considering multiple paths, woodland, and freshwater. [10] showed that the attenuation of a forest proved to be greater than that of a suburban area, with the electric field being lower by 12 dB for a dense forest compared to a sparse forest. Compared to the Okumura-Hata, ITU-R P.1546, and Walfisch-Ikegami models, the proposed model had the lowest RMSE of 2.75 dB to 3.43 dB. Finally, compared to the Hata model, the proposed model in [1] had a lower RMSE in all cases, ranging from 1.67 dB to 4.25 dB.

On the other hand, [11] proposed a statistical propagation model to estimate Air-to-Ground (ATG) coverage and PL between a Low Altitude Platform (LAP) and a terrestrial terminal in an urban region. Instead of site-specific 3D models, the estimation relied on the elevation angle between terminal and LAP. However, the study's drawbacks are: 1) the Doppler effect caused by the hypothetical high speed of an aerial transmitter was not examined because the assumption primarily focused on a semi-stationary LAP; 2) the study was based on simulations with no physical verification; and 3) potential urban geometry influences, such as foliage, lampposts, and moving objects, were also ignored, presuming that the large-scale building geometry and its EM characteristics will dominate the average PL.

The forthcoming 5G-based IoT, with its numerous complex application scenarios, necessitates more effective channel estimates and modeling [6]. Accordingly, [12] surveyed and evaluated the applicability of existing propagation models for Industrial IoT (IIoT) applications. The evaluation utilized worst, median, and best case predictive behaviors. As case studies, NB-IoT, Sigfox, LoRa, ZigBee, and MIOTY IoT technologies' performance metrics such as cell radius, spectral efficiency, and outage probability were examined. The models considered include Free Space Path Loss (FSPL), 3GPP (indoor open and mixed hotspots, outdoor urban macro- and micro-cell, and outdoor rural), and industrial indoor channel model for ISM bands. Results showed that NB-IoT had the longest cell radius and the lowest outage probability in outdoor scenarios, Sigfox had the highest indoor spectral efficiency, and ZigBee had the widest working bandwidth. They argued that 3GPP models are the most suitable for estimating the examined communication metrics, with estimations frequently close to the median-predicted behavior.

Besides, [6] provided an outline of the ML conceptual framework for future radio propagation modeling and estimation. The study also introduced the 5G channel modeling domain and summarized current advances in applying ML-based channel modeling. Then, essential methods in ML were discussed, including regression analysis and how classification determines output data to estimate traffic flow. The study emphasized that much work is needed to overcome obstacles and achieve accurate modeling despite significant investment in ML. Nevertheless, ML techniques showed feasibility by estimating channel parameters and extracting channel information. Hence, it was concluded that successful predictive ML techniques would reduce complexity while increasing precision. Further, as the number of measurements is reduced, the use of ML approaches in wireless channel

modeling becomes increasingly important as generalization abilities improve.

Finally, [7] presented a comprehensive study of existing over-the-sea channel models used for Unmanned aerial vehicles (UAVs) and marine communication. Hence, the study targeted simplifying the model selection procedures according to the targeted application. Meanwhile, [8] provided a comprehensive overview of existing ATG channel measurement studies, large- and small-scale fading channel models, limitations, and future guidelines for UAV communication scenarios. Different UAV propagation scenarios were also explored, as well as critical elements for these measurements.

B. STUDY MOTIVATIONS AND CONTRIBUTIONS

In conclusion, most wireless channel characterization and modeling studies are limited to study area settings. Besides that, only one study, in [12], examined the suitability of current channel models for wireless IoT technologies, which is in turn explicitly limited to IIoT applications, considering few channel models. On the other hand, the remaining studies focus on performance evaluation and surveying the suitability of existing models for traditional communication technologies with high transmission power, high power devices, and high gain antennas without considering IoT-based application requirements. As a result, more research is needed to precisely evaluate the suitability of existing models for various wireless IoT technologies, particularly in regions known for their harsh environments, such as tropical climates with irregular terrain.

As such, this work builds on past research and presents a comprehensive review of recent advances in wireless channel characterization and modeling for wireless IoT technologies. Therefore, the contributions of this work can be summarized as follows:

1) Provide a rigorous survey of modern wireless IoT-based solutions.
2) Describe the most significant challenges in such applications, with a particular emphasis on wireless channel propagation modeling and characterization.
3) Briefly describe channel modeling, a generalized form of commonly used channel models, and lists 34 well-known path loss models for wireless IoT channel modeling under different communication scenarios and environments.
4) Finally, the study reviews recent advances in channel modeling for wireless IoT technologies, identifies gaps in existing research, and suggests future directions for developing a robust wireless IoT solution.

The rest of the paper is structured as follows: Section II examines wireless IoT technologies and potential IoT solutions. Section III discusses the challenges related to wireless IoT technologies. Section IV covers wireless channel propagation modeling concepts and provides detailed equations for well-known and commonly used models for wireless IoT technologies. Section V reviews the most recent studies on wireless IoT channel modeling and characterization. Finally, Section VI draws conclusions and suggests some future work directions. To further facilitate reading, Fig. 1 provides a detailed structure of the review, while Table 1 summarize the related works compared to the current review.

II. WIRELESS IoT TECHNOLOGIES AND POTENTIAL IoT SOLUTIONS

The Internet of Things (IoT) is a network that connects users and objects by using information sensing devices and actuators [13]–[15]. IoT has caught academic and industry interest for the past few years [16] due to the exponential rise of connected devices and the need for new or optimized methods to manage many connected devices [13]. As a result, the number of connected devices nowadays is expected to be between 26 to 50 billion [17]–[21]. This trend is anticipated to accelerate further, expected to reach around 75 to 100 billion connected devices by 2025 [13], [16], [21].

Various wireless IoT technologies and network topologies can support IoT [22]. Depending on the application requirements, operational restrictions, and coverage needs, these technologies can be classified into three categories. First is traditional short-range technologies, such as Wi-Fi, ZigBee, and Bluetooth, mostly utilized for high availability and low latency activities, whereas energy consumption is not a key issue [14], [23]. As such, they are unsuitable for long-range communication. Second is cellular-based solutions, such as 2G-4G and future 5G/6G, which provide greater coverage but demand excessive device energy. Finally, as a result of the crucial IoT application requirements [13], [20], Low Power Wide Area Networks (LPWANs) are emerging as an exciting new trend in the growth of wireless communication systems. Many LPWAN developments, such as Sigfox, LoRaWAN, and NB-IoT, have lately emerged in both unlicensed and licensed spectrum, becoming one of the leading novel technologies with numerous technological differences [16], [20], [21]. Its main features include large coverage area support and massive scale networking with low cost, long-life, and restricted data rate EDs [13], [16], [18].

Together, these wireless IoT technologies support various IoT solutions for outdoor and indoor scenarios, whether deployed in urban, suburban, or rural areas. Those applications cover many sectors of life, including those reviewed in the below subsections and as shown in Fig. 2.

A. SMART CITIES

These paradigms are primarily evolving to address the issues faced by the rising complexity of today's urban environments [22]. The essential characteristics of a smart city include a high level of technological integration and broad use of information resources [24]. Accordingly, IoT use in smart cities enables remote device monitoring, management, and control, along with new views and operational knowledge driven from enormous data streams.

One of these smart city IoT applications is smart lighting, which boosts the lighting infrastructure's efficiency by reducing electricity use using dimmers and task lighting.

TABLE 1. Summary of related works.

Ref	Targeted application	Study focus	Key contributions	Limitations
[2], [4]	Wireless broadband and broadcasting	Evaluation & comparison of existing channel models' performance.	Showed how different models perform in different environmental contexts, identifying the most suitable model.	It is limited to a few models concerning conventional communication technologies that might not suit IoT requirements.
[5]	WSN and wireless broadband	Evaluation & comparison of existing foliage models' performance.	The results showed disagreement with current empirical models built solely for their temperate measurement area.	It is limited to the characterization of foliage impact concerning a few models. Utilize conventional communication technologies that might not suit IoT requirements.
[9]	Cellular communication		Suggested a new foliage empirical propagation model for two morphologies.	
[10]	Wireless broadcasting	Analysis & development of a propagation model for tropical areas.	Propose a model based on geometrical optics and the uniform theory of diffraction, then compare it against conventional models.	The models proposed are site-specific, with few considered models for comparison. The models are targeted for conventional communication technologies and not suitable for IoT requirements.
[1]			Propose an ML-based empirical propagation model for non-homogeneous paths and various climates.	
[11]	LAP	Propose a statistical ATG propagation model.	Instead of site-specific 3D models, the estimation relied on the elevation angle between terminal and LAP.	Do not consider other models & limited to LAP use cases. Do not consider the doppler effect and ignore potential urban influences.
[12]	IIoT	Survey and evaluate the applicability of available propagation models for IIoT applications.	The evaluation considered several models (FSPL, 3GPP, & industrial indoor). They argued that 3GPP models are the most suitable, with estimations frequently close to the median-predicted behavior.	It is explicitly limited to IIoT applications, considering few channel models.
[6]	General 5G applications	Survey ML conceptual framework for future radio propagation modeling and estimation.	Introduced 5G channel modeling domain and summarized current advances in applying ML-based channel modeling. They emphasized that much work is needed to overcome obstacles and achieve accurate modeling despite significant investment in ML.	The survey scope is limited to a few 5G channel models. Do not cover wireless IoT applications, challenges, and channel modeling requirements.
[7]	Marine & UAV communication	Comparative survey concerning over-the-sea channel models.	Present a comprehensive study of existing over-the-sea channel models to simplify the model selection procedures according to the targeted application.	It is limited to marine and UAV, specifically over-the-sea communication scenarios. Do not cover wireless IoT applications, challenges, and channel modeling requirements.
[8]	UAV applications	A comprehensive survey of existing channel models for UAV communication	Review existing ATG channel measurement studies, large- and small-scale fading channel models, limitations, and future guidelines for UAV communication scenarios.	The survey is limited to UAV channel modeling and does not cover wireless IoT applications, challenges, and channel modeling requirements.
Current work	Wireless IoT applications for commercial & industrial use cases under different communication scenarios and environments.	Presents a comprehensive review of recent advances in wireless channel characterization and modeling for wireless IoT technologies.	• Provide a rigorous survey of modern wireless IoT-based solutions & describe the most significant challenges. • Lists 34 well-known path loss models for wireless IoT channel modeling under different communication scenarios and environments. • Reviews recent advances in channel modeling for wireless IoT technologies, identifies gaps in existing research, and suggests future directions for developing a robust wireless IoT solution.	• Focus on wireless IoT technologies, device-to-device communication, and 5G-based IoT. • Do not cover channel modeling approaches & recent advances in mobile broadband communication and future 6G technology. • Future studies may improve the current work by comprehensively reviewing advances in ML and deep-learning propagation modeling approaches and the future directions concerning 6G technology.

It can also serve as an access network for context-aware services such as smart parking. Hence, it has the potential for a significant economic impact. In 2014, for example, studies revealed that smart lighting infrastructure in Montechiarugolo, Italy [22] helped reduce electricity usage by 76%, resulting in a 73% cost savings compared to traditional lighting systems used in the city. Further, the combined effect of LED lighting and wireless remote control saved 224 TEP (a ton of oil equivalent) each year and avoided 500 tons of CO_2 emissions.

In a smart city paradigm, many other applications exist, such as automotive and intelligent transportation systems [25], [26], Remote Structural Health Monitoring (RSHM) [27], smart homes and buildings [22], [28], [29], metering monitoring [28], concrete surface WSN [30], and level of trash monitoring [31]; as shown in Fig. 2.

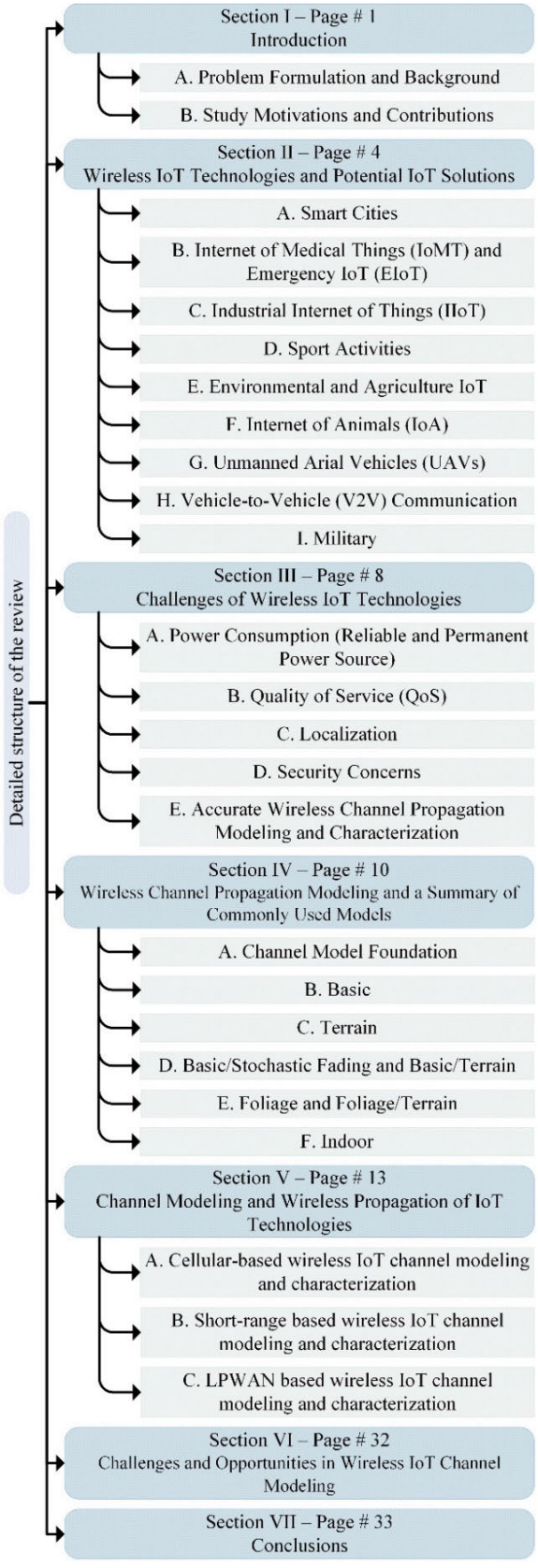

FIGURE 1. A detailed structure of the review.

B. INTERNET OF MEDICAL THINGS (IoMT) AND EMERGENCY IoT (EIoT)

The healthcare sector has recently experienced tremendous expansion and is estimated to be very large due to global aging [32] and corona-virus disease (COVID-19) [33], [34]. The healthcare sector has recognized the huge potential of IoMT technologies, often known as healthcare IoT, due to their effective collection, analysis, and transfer of health data. Thus, the IoMT has risen as a combination of medical equipment and software platforms to offer full healthcare services linked to healthcare IT systems [35].

In this way, IoMT monitors vital signs, instantly detects anomalies, and alerts parties concerned. Multiple sensors are embedded in garments, watches, wearable items, and even jewels in such a condition to continually monitor vital signs such as blood pressure, heart rate, blood glucose level, blood oxygen level, and standing position [36].

Besides, electrical bioimpedance methods require complex devices and measuring settings in medical and personalized healthcare systems. As such, various investigations were carried out in this context. For instance, [37] identified a standalone bioimpedance analyzer termed "Zink" with IoT monitoring features. The system allows users to obtain/perform single or multiple bioimpedance readings remotely. The device may also calculate bioimpedance synchronized with an electro-cardiogram (ECG) or electromyogram (EMG) readings. Similarly, [38] proposed an IoT-assisted ECG monitoring system with reliable data transfer for continuous cardiovascular health monitoring, enabling automated classification and real-time operation. Such a system has a high potential for defining clinical acceptance of ECG signals to improve an unsupervised diagnostic system's performance, accuracy, and reliability.

The IoMT may also be highly effective in emergency scenarios. For example, during the current COVID-19 pandemic, many innovators, medical authorities, and government agencies concentrated on harnessing IoMT resources to relieve pressure on medical systems. As a result, several IoMT technologies, such as smart thermometers and telemedicine (remote patient monitoring), have contributed to monitoring and, eventually, dealing with the COVID-19 pandemic impact [35].

Smart IoT-based fire-ground and firefighter monitoring system (IoT-FFM) suggested in [39] can also assist people in risky situations. It adds functions such as surveillance of fire environment gases, real-time danger notification, and transfer of firefighter location and health data to a remote command unit. As a result, the technology will aid in protecting people's lives (both firemen and victims) and avoid potentially hazardous situations.

Other IoMT and EIoT applications include medical bleeder [40], emergency & disaster monitoring [11], Wearable Body Area Networks (WBAN) [41]–[43], and Device-to-Device (D2D) & Device-to-Machine (D2M) based

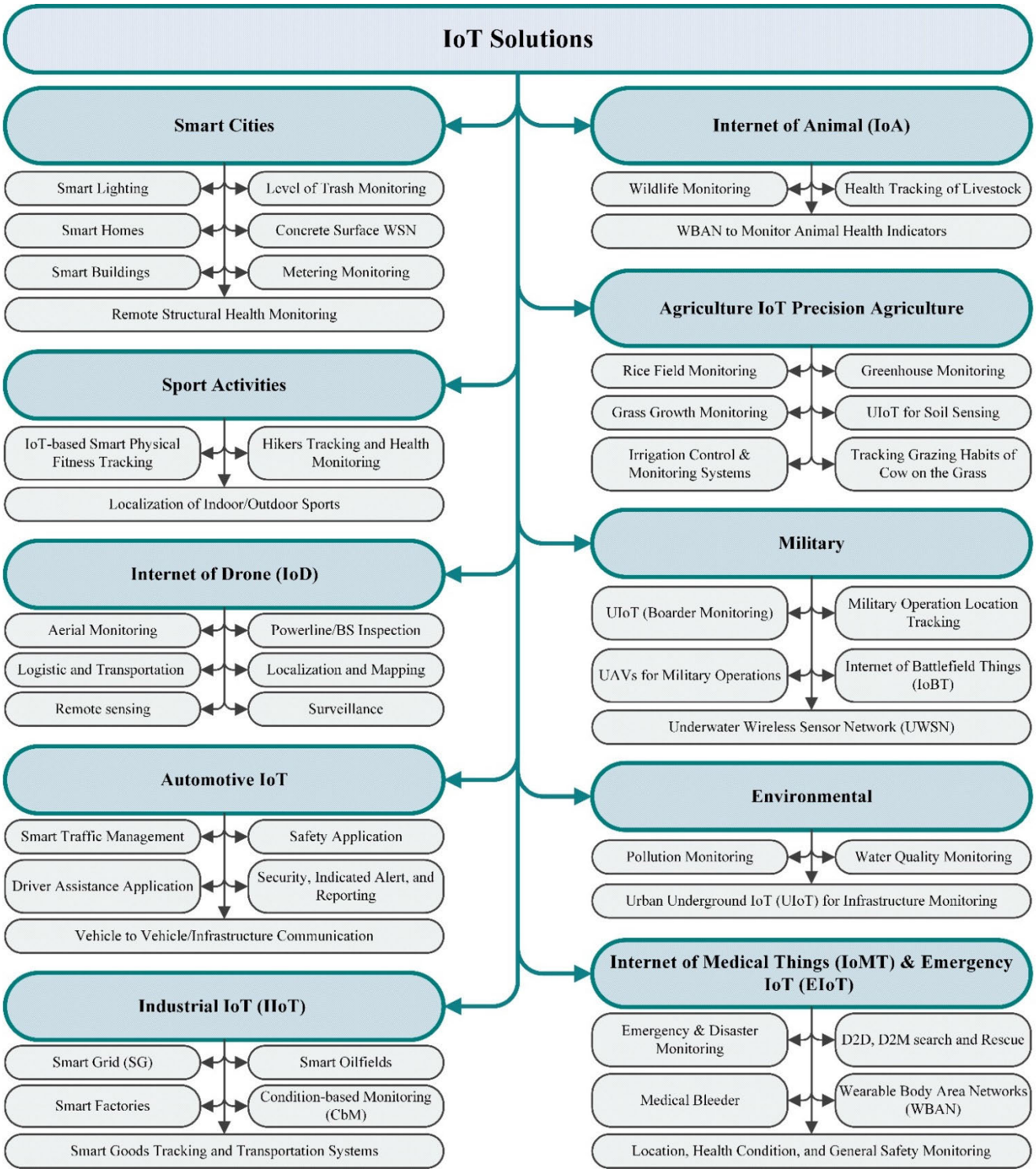

FIGURE 2. Several innovative IoT solutions from the reviewed literature.

communication devices to monitor and track devices during Search and Rescue (SAR) operations [44], as listed in Fig. 2.

C. INDUSTRIAL INTERNET OF THINGS (IIoT)

The IIoT and Industry 4.0 development goals include massively distributed smart computing and networking advances in industrial production and manufacturing systems for automation, quality, and control [45], [46]. IIoT has distinct features and requirements apart from commercial IoT, like specific built-in smart devices, network capabilities, QoS, and strict command and control standards [45]. Thus, IIoT helps reduce faults and costs and improves safety and performance

in manufacturing processes, giving the industry a consistent degree of precision, availability, and scalability [46], [47].

Among other features, IIoT allows control commands to be sent rapidly from a client device to anyplace in a facility, such as an oil rig or power plant, without requiring a physical presence. This ability to respond swiftly from any location may save the firm and the environment from costly damages or disasters like the 2015 oil spill in Santa Barbara, CA, USA [46].Another innovative use of IoT is in condition-based monitoring (CbM) applications to investigate vibration-based machine health. As such, the objective is to compare observed vibration to components that are vulnerable to common wear processes, such as bearings, gears, chains, belts, brushes, shafts, coils, and valves. These sensors can save money by detecting early warning signs of breakdown in industrial machinery and optimizing the maintenance schedule [48].

Other IIoT applications include industry risk management (to reduce infectious disease outbreaks such as COVID-19) [49], smart grid (SG) [50], [51], smart goods tracking and transportation systems [52], [53], smart oilfields [49], and smart factories [45]; as listed in Fig. 2.

D. SPORT ACTIVITIES

Another prominent application of IoT technology is in sporting activities [36]. Where gadgets such as IoT-based monitoring and tracking devices could, for example, monitor hikers' positions, health status, and overall safety while hiking [44]. D2D connectivity is favored for such situations with IoT, as small devices may be unable or need to connect with standard cellular infrastructure. As a result, such devices may communicate data on the positions of the various participants, allowing each to keep track of the others for either competition or safety [54].

Another example presented in [55] is an IoT-based smart physical fitness tracking device. The device comprises several portable sensors and RFID to adapt and control the physical load intensity in real-time, accurately, and efficiently, based on the physiological load within the human body, to meet the predetermined objectives of the training plan. Thus, athletes' physical fitness testing data may be saved and categorized with such a system then evaluated using the BP neural network approach. This can provide users and coaches with a highly matched training plan, generate scientific and routine physical fitness tests for athletes, give players maximum competitive potential, and improve physical fitness.

E. ENVIRONMENTAL AND AGRICULTURE IoT

Climate change, population expansion, demographic shift, urbanization, and resource scarcity imply that the world's largest cities will need to adapt to survive and grow in the future decades [56]–[58]. Cutting greenhouse gas emissions to avoid catastrophic global warming and sustaining or improving living quality, on the other hand, maybe an expensive and difficult task [56], [57]. For instance, factors directly impacting the quality of life, such as water and air quality, are routinely monitored using expensive systems [56], [59]. Such assessments, particularly for water quality monitoring, typically include on-site sample collection and subsequent laboratory analysis, which adds intense and costly labor [59]. Recent IoT advances have thus enabled unique methods and autonomous real-time monitoring of these factors by integrating low-cost sensor devices, machine-to-machine (M2M), and IoT technologies [56], [59].

Besides, IoT monitoring devices may track environmental impacts on urban underground infrastructure caused by excess storm and wastewater volumes entering pipelines, causing backups and sanitary sewer overflows. These systems, also known as urban underground IoT (UIoT), are required for controlling external water flow into pipelines and are enabled by merging underground wireless communication and sensor technologies [60].

Similarly, various studies have been conducted in agriculture IoT to digitalize the agricultural industry [61]. Thus, enabling the implementation of Precision Agriculture (PA) with increased financial returns, increased product quality and yield, and cost reduction [60], [62]. Besides, farming has recently become fairly reliant on processing production area information for various crops, utilizing actuators to remotely operate network equipment, consequently adopting two-way communication systems [62].

IoT usage in agricultural processes improves the traceability system and improves overall farming practices, effective land utilization, agricultural quality, and safety. As a result, internal traceability assures support for seedlings used in major crops across the whole agricultural sector. In this regard, [63] described an IoT-based greenhouse traceability system for tracking seedlings and other agricultural goods from germination to harvest. The system monitors luminosity, moisture, temperature, and water usage to indicate water consumption, plant development trends, and product harvesting timelines. The technology also allows for automatic monitoring of the indoor greenhouse environment via an irrigation system or temperature control and a vital overview of agricultural product internal traceability from seed to the final product.

Another example is automated irrigation monitoring and control systems, which can help identify the precise timing of watering and the amount of water required to meet crop water needs while improving water usage efficiency [64]–[67]. Other research looks into solutions like UioT to enable smooth access to data from agricultural fields, including in-situ soil sensing capabilities, communication through plants and soil, and supplying real-time environmental data, thus delivering useful information to farmers [60].

For example, [67] offered an open-source IoT-based smart irrigation architecture with a hybrid machine-learning-based strategy to predict soil moisture and watering requirements. The system uses sensor data such as soil moisture, soil temperature, ambient conditions, and weather forecast data to predict soil moisture for the next few days. Similarly, [68] uses an autonomous IoT-enabled WSN system comprising soil moisture & temperature, environmental

temperature & humidity, CO2, and daylight intensity sensors to obtain real-time farm data. Furthermore, farm history is saved to create relevant actions throughout the farming cycle. The study also uses neural networks to describe accurate water valve control based on soil water demand estimation one hour ahead. Accordingly, the structural similarity (SSIM) index-based soil moisture content shortage is calculated to control the specified valves and maintain uniform water needs over the entire farm area. Valve control commands are examined again using a fuzzy logic-based weather condition modeling approach to change control commands in response to changing weather conditions.

In contrast, [61] proposed a cloud-based greenhouse crop production solution to provide various services for the environmental and economic benefits of agricultural operations and improve system performance by offering recommendations for the use of water, pesticides, fertilization, or energy.

Other agricultural solutions (as listed in Fig. 2) could include tracking cows' grass grazing behaviors [69], [70], monitoring grass growth on major roadways, residential lawns, outdoor sports centers, and inaccessible areas [70], and rice field monitoring [71].

F. INTERNET OF ANIMALS (IoA)

In this context, IoT can be useful in a variety of applications. For instance, IoT monitoring and tracking devices could be used to track and monitor wildlife in rural or mountainous & rocky areas, like mountain lions [44], pink iguanas [72], and zebras [73]. WSN and MEMS advancements have also aided other solutions, such as remote monitoring of dairy cow health issues using IoT-based WBAN, as reported in [74]. Besides that, [75] described real-time IoT-based tracking systems leveraging sensors to enable large dairy farms to maximize revenue and improve cow welfare. The latter is done by monitoring ruminal temperature and pH, which are critical for monitoring the dairy cows' nutritional and health status and predicting anomalies (e.g., metabolic disorders after calving).

In contrast, [76] described an innovative IoT-based system with multiple sensors, wireless data transfer, and self-sustaining power for long-term and robust bee colony monitoring. The suggested system can detect hive temperature and humidity, bee comb weight, colony sounds, and the number of bees entering the hive. Long-term monitoring trials revealed that the system could run continuously without human intervention, and data can reveal bee colonies' activity and growth. Notably, data successfully identified a swarming behavior, indicating a high potential for recognizing specific bee colony activities. As a result, the suggested approach had a significant impact on verifying the activities and state of bee colonies, which could contribute to the evaluation of bee behavior and the enhancement of beekeeping quality.

G. UNMANNED AERIAL VEHICLES (UAVs)

Unmanned aerial vehicles (UAVs), commonly known as drones, have witnessed increased adoption in recent years, from agriculture to industry, government to private organizations, and smart cities to rural area monitoring. UAVs are becoming more maneuverable and intelligent with recent advances in IoT, cloud & edge computing, and wireless communication technologies. Hence, the Internet of Drones (IoD) is emerging as a promising technology and use case for UAVs. Many industries are projected to adopt IoD-based automation for smart monitoring, surveillance, and search and rescue via reliable mobile communications systems.

Drones have recently been used as flying cellular base stations (BSs) to deliver reliable and energy-efficient IoT communications [77], [78]. Such deployment of BSs would increase the probability of LOS communication and mitigate destructive effects such as shadowing and blockage, thereby increasing the reliability of communication links [79].

One application of IoD is remote sensing, which allows for easier measurements and monitoring in harsh or remote areas. For example, [80] presented an IoD-based system for livestock monitoring on large-scale rural farms, in which a fixed-wing UAV was equipped with a LoRa gateway and collected data from IoT-based monitoring equipment deployed across the farm. Disaster relief and management is another novel application of IoD. Reference [81] proposes a UAV-cloud framework for disaster sensing in disconnected, intermittent, and resource-constrained environments. Other UAV use cases include aerial entertainment [82], agriculture inspection [83], powerline/BS inspection [84], surveillance [85], aerial monitoring [86], radiation monitoring [87], logistics and transportation [88], and localization and mapping [89].

H. VEHICLE-TO-VEHICLE (V2V) COMMUNICATION

The automotive industry is currently undergoing a technological revolution fueled by IoT technologies. As a result, vehicles are going through a disruptive shift from manually driven vehicles to self-driving vehicles with varying degrees of autonomy, depending on the technology on-board and the situations encountered [90]. Existing Original Equipment Manufacturer (OEM) embedded systems use standard sensors such as GPS, camera, and proximity sensors, limiting their use to some basic applications such as sensing adjacent objects and crash detection. Hence, more advanced technologies are needed to achieve a high level of autonomy, safety, and traffic control.

V2V communication is a game-changing technology that connects vehicles and provides drivers with critical information about their vehicle, other nearby vehicles, and the surrounding environment, such as weather, roadblocks, and traffic [91]. This data will be utilized to warn drivers of potential hazards via a visual display, seat vibration, or tone. These warnings will assist drivers in responding more quickly and avoiding potential accidents [92]. Some examples of V2V-based driver assistance applications include the following:

- Intersection movement application; warns drivers when it is unsafe to enter an intersection.

- Do not pass applications; warns drivers when passing a slower-moving car is unsafe.
- Emergency electronic brake light application; notifies the driver when an out-of-sight vehicle several cars ahead is braking.
- Blindspot warning application; enables drivers to virtually view what is occurring in their blind spots.

On the other hand, V2V IoT services can continuously monitor the vehicle's condition and inform the driver in advance if something is likely to go wrong. Additionally, the IoT services can be used to notify medical personnel or the police in the event of an accident or emergency. Another application of V2V communication is path optimization, where critical travel-related information can be exchanged between vehicles to assist drivers in arriving at their destinations most efficiently.

I. MILITARY

Beyond traditional civilian contexts, IoT has many military and antagonistic uses. The US Army Research Laboratory (ARL), for example, has created an Enterprise strategy to deal with the complexities of the Internet of Battlefield Things (IoBT). ARL intends to build a new collaborative project (the IoBT CRA) to develop IoBT core capabilities for future military operations [93]. Similarly, IoT monitoring and tracking systems can enable connectivity during remote military operations via device-to-device and device-to-machine communications [44]. Furthermore, UioT can be used in border surveillance applications such as border enforcement and infiltration prevention [60].

On the other hand, UAVs have been widely used in military applications. When outfitted with various communication devices, UAVs working in tandem with satellites and BSs form a diverse three-tier (space-air-ground) network that provides seamless coverage and expands the capacity of increasingly profitable IoT networks [94].

Finally, the underwater wireless sensor network (UWSN) has been widely used for data collecting in an underwater environment for military and civilian uses. UWSN applications include tsunami and earthquake warning systems, undersea military monitoring, ocean exploration, navigation, environmental, and pollution management [95].

III. CHALLENGES OF WIRELESS IoT TECHNOLOGIES

With the technological advancements and current developments in the wireless IoT paradigm, various challenging factors must be considered while deploying precise, high-performance, and cost-effective IoT systems. As such, the following sub-sections summarize the most crucial challenges confronting any IoT solution:

A. POWER CONSUMPTION (RELIABLE AND PERMANENT POWER SOURCE)

In many cases, IoT systems are placed in locations with limited power resources, resulting in most IoT systems being battery-powered [96], [97]. Furthermore, the rising complexity of IoT data transmission, storage, and processing capabilities requires more power-intensive tasks. In this sense, the capacity of IoT devices to operate for long periods without recharging is a significant challenge [96], [98], [99]. Finally, the rise of IoT and the emergence of LPWAN IoT technologies, e.g., in traffic monitoring, PA and animal health monitoring, posed an additional challenge to power efficiency in long-range transmission situations [96], [100].

As a result, battery life and the ability of end nodes to communicate over long ranges is one of the most crucial and problematic issues, particularly for off-grid and wearable IoT applications [96], [97]. Many studies have focused on addressing this issue to analyze and optimize power performance for optimal IoT applications, considering both hardware and software perspectives [96]–[99], [101], [102]. Accordingly, low power systems or energy harvesting techniques such as micro-magneto-electric, thermoelectric, piezoelectric, or photoelectric technologies have lately been proposed as a feasible solution [99].

B. QUALITY OF SERVICE (QoS)

Conventionally QoS was mainly determined by factors such as bandwidth, jitter effect, packet loss, and network delay. To provide superior IoT services, however, various other characteristics of the IoT network must be considered, including network/server connection time, service level agreement compliance, availability, and reliability. The authors in [103] identified and classified major QoS metrics based on the main IoT components, including communication, things, and computing.

It is challenging to deliver guaranteed QoS, particularly for IoT applications distributed in harsh environments or when IoT nodes are placed near the ground, as in agricultural areas [62], [104]. In such conditions, communication suffers from severe attenuation due to obstacles [104], thus adding complexity to the network design phase [62]. Therefore, such an issue might impact the QoS, causing poor node communication and an unreliable IoT system that could increase the number of packet retransmissions and nodes' energy consumption, resulting in wireless link failure [104]. Consequently, providing the nodes with adequate resources to operate the system self-sufficiently without affecting QoS is another tricky task [101].

C. LOCALIZATION

IoT applications frequently demand location data from end devices [105], [106]. As a result, data obtained for various applications, such as animal tracking, surveillance, autonomous vehicle guidance, and patient monitoring [43], [101], [106]–[108], is only meaningful if the precise location of sensor nodes is known [105], [106].

Typically, the position can be obtained using Global Navigation Satellite Systems (GNSS), such as the Global Positioning System (GPS), which is viewed as an effective outdoor localization solution [106], [109]. These methods, however, are not always viable, particularly in indoor

environments [105], [106]. Where, for example, such environments may impose numerous multi-path effects due to obstacles between satellites and users [106], [109], resulting in significant signal degradation [106]. GPS is also recognized for its poor accuracy, which is limited to a maximum of five meters [109] and a solution that requires more energy and costs [105]. Aside from that, the cost, power, and size limitations of IoT technologies, particularly LPWAN, impose further constraints on embedding a GPS receiver into each end device [110]. Hence, localization is viewed as one of the most difficult IoT-related challenges [106], [109], [111].

Numerous IoT localization techniques have been developed recently [105], [110], [112], to address the existing challenges and introduce accurate, energy-efficient, low-cost localization techniques [105], [113]–[115]. These techniques are typically classified into three categories [43], [101], [107], as follows:

First is range-based localization techniques, which rely on the range to identify the position of nodes or objects after a series of ranging and computing phases [101], [107]. These techniques can thus be based on methods such as Time of Arrival (TOA), RSSI, weighted centroid-locating algorithm, Time Difference of Arrival (TDOA), Angle of Arrival (AOA), and Phase of Arrival (POA) [101], [106], [107].

Second is range-free localization techniques; these do not employ any measuring techniques and usually necessitate special hardware to do the ranging, which is subsequently used to compute coordinates [101]. Thus, these approaches prioritize cost-effectiveness over range-based methods [107] and are frequently utilized in mobile scenarios where the precise location of nodes is unknown [101].

Finally, the third category combines range-free and range-based techniques [107]. Among the three categories, range-based localization techniques are the most extensively utilized, particularly the RSSI-based localization technique [105]–[107], [110], which requires no additional hardware or synchronization in network end devices [105], [106].

D. SECURITY CONCERNS

Despite all-new IoT-enabled capabilities, there is an increased security risk [46], [47], which could be caused by device failure, malicious attacks, unauthorized access, or poor key management [46], [47], [116]. As a result, such security concerns will cause severe disruption to global IoT systems, potentially outweighing their benefits [47]. A wide-scale security attack on a large IoT network, on the other hand, can be costly and difficult to prevent. For instance, security attacks may result in factory shutdown and disruption to public safety [116].

On the other hand, wearable IoT devices are predicted to have weaker security features due to design compromises to accomplish lightweight and low power consumption. Maintaining low complexity in wearables is challenging with enhanced security standards [99]. In this regard, practical and reliable security algorithms must be considered, taking both security and reliability into account [116].

E. ACCURATE WIRELESS CHANNEL PROPAGATION MODELING AND CHARACTERIZATION

For wireless systems, the surrounding environment, such as terrain, plant height and density, and obstacles, can easily affect the received signal [71]. As a result, these channel imperfections cause signal power loss, which affects QoS, causing poor communication and thus a higher number of data packet retransmissions between nodes. Such issues ultimately result in higher power consumption in nodes and radio link failure, leading to an inefficient IoT application [104].

Wireless channel propagation modeling and characterization are thus required for the design and evaluation of robust wireless IoT systems [71], [104], [117]. Path loss (PL) modeling, in particular, enables an accurate estimation of IoT system propagation behavior and interference [71], [117]. Thus, this enables the best possible estimation of the range and coverage between adjacent IoT terminals, together with an estimate of the number of nodes required to cover a specific area [62], [104], [118], [119]. In agriculture IoT, for example, the widespread deployment of IoT-based WSNs would be reliant on unique factors impacting PL model accuracy in such situations, predicting nodes height and coverage range, and enhancing transmission quality [71].

In conclusion, wireless channel propagation modeling and characterization are crucial for sophisticated wireless IoT systems and related to the other challenges this section mentions. As a result, its accuracy is crucial for properly assessing and optimizing network efficiency amid deployment stages. It also contributes to energy savings, precise node localization (for RSSI-based techniques), reduced network interference, and enhanced network capabilities, all of which improve QoS in various deployment scenarios [119].

Due to the significance of this constraint, several studies have been conducted recently to evaluate the effectiveness of wireless channel models or propose optimized/new models for wireless IoT technologies. As such, the next sections will focus on this challenge, providing an overview of wireless channel modeling and characterization concepts, current well-known and regularly used models for wireless IoT technologies, and a survey of the most recent works aiming at wireless channel modeling.

IV. WIRELESS CHANNEL PROPAGATION MODELING AND A SUMMARY OF COMMONLY USED MODELS

The wireless channel is the physical link between the transmitter and the receiver through which the carrier signal transmits data [6]. The signal interacts with various obstacles on its path to the receiver, as shown in Fig. 3, leading to various impacts that cause the signal to be either destructive or constructive during propagation [6], [120]. These obstacles cause the signal to be reflected, refracted, or diffracted, resulting in signal attenuation (by absorption) and inducing scattering and secondary waves [120], [121]. Additionally, when an antenna radiates the signal, the signal can take several paths to the receiver. Each signal may interact chaotically with the environment and arrive at the receiver marginally delayed.

As a result, depending on whether the delayed signals are in or out of phase, they can introduce constructive or destructive interference. The spread of this delay is known as delay spread (DS), and the attenuation associated with it is known as multi-path fading [120].

Subsequently, propagation in wireless channels results in either large- or small-scale fading based on signal variations [6], [122]. In turn, large-scale fading can be caused by either PL as a function of distance or shadowing / slow-fading caused by big fixed obstacles such as mountains and buildings [6], [28], [123]. Meanwhile, destructive interference from multi-path effects and small scatterers causes small-scale fading / fast-fading / scattering [6], [120], [122], [123]. Small-scale fading is frequently used to evaluate link-level performance using bit error rates and average fading [6], [124]. In small-scale fading, the amplitude distribution of the received signal is typically modeled using a probability distribution, such as Rayleigh, Rician, and m-Nakagami. [6], [28], [122]–[124]. Signal delays caused by reflections, scattering, and diffraction, on the other hand, cause time dispersion, leading the signal to be distorted [6], [120]. Time dispersion may also cause inter-symbol interference (ISI). Moreover, distortion can arise due to object movement, resulting in frequency dispersion due to Doppler spread [6].

As a result, wireless channel propagation modeling, commonly referred to as ''channel modeling'' or ''propagation modeling,'' is essential for the design of wireless communication systems [6], [114], [120], [123]. It employs mathematical parameters to determine the impact of the channel medium on the transmitted signal [6], [31]. These models are classified into two groups: deterministic (theoretical) and stochastic channel models [6], [118], [119], which can contain a variety of randomly varying parameters [6].

Others may classify channel models into three groups: geometry-based deterministic models such as ray-tracing, non-geometric stochastic models such as empirical models, and geometry-based stochastic models (GBSM), also known as semi-empirical models, which combine deterministic and empirical models [6], [125].

The stochastic modeling approach is based on the statistical distributions of channel parameters and can be narrowband or wideband [6]. Meanwhile, deterministic relies on knowledge of the physical characteristics of the wireless channel [118], [119] and is based on Maxwell equations [6]. This approach has the drawback of increasing computing complexity and requiring costly site-specific designs and extremely accurate 3D maps [6], [118], [126]. In contrast, stochastic modeling approaches, such as empirical models, are based on real measurements of wireless channels. These models have the advantage of being simple to develop and flexible enough to incorporate all environmental factors influencing signal propagation during real-world measurements [118], [119]. However, such models only include frequency and distance, leaving out reflections, diffraction, and refraction characteristics. Another disadvantage of such models is the uniform representation of measurement data acquired in a specific area with varying terrain and climate [4].

Impulse response within a delay bin in the narrowband can result in non-selective flat or frequency fading. On the other hand, Wideband focuses on each channel response ray independently and can be signal dispersion or selective frequency fading. As a result, the stochastic narrowband model is commonly used to characterize fading statistics and the Doppler spectrum. The stochastic wideband model, on the other hand, often focuses on received power, delay, departure and arrival angle, and Doppler shift [6].

Having stated that, numerous channel models have been described in past years [28], [31]. However, there is a lack of studies in the literature that summarize and describe available channel models suitable for a broad range of wireless IoT-based systems. As such, this section summarizes several well-known and frequently used PL model equations for various communication scenarios and environments, as given in Table 2. Where 34 equations, from Eq. (1) to Eq. (34), are listed and classified according to model category (empirical, semi-empirical, or deterministic). For simplicity, the models are further categorized into eight sub-categories based on their intended use scenario, as follows:

A. CHANNEL MODEL FOUNDATION

This set of models includes those models driven purely from the idealized theory of electromagnetic propagation, including the Friis equation of Free Space Path Loss (FSPL), Eq. (1), and two-Ray (2-Ray) or Plane Earth (PE) model, Eq. (2), which treats the earth as a perfect conductor. These two models are considered deterministic (theoretical) and are widely used as baseline models in most comparison studies and more complex models derivation [123].

B. BASIC

This set of models includes commonly used models, typically empirical and based on basic inputs such as distance, frequency, antenna height, and gain, with measurement-based area-specific tuning [123]. The Okumura-Hata model, given in Eq. (3), is the most popular. It is an empirical model with environmental type parameters and is valid for frequencies ranging from 150 MHz to 1500 MHz, 30 m to 200 m Tx/GW, and 1 m to 10 m Rx/ED. One drawback of the Okumura-Hata model is that its estimation does not consider the terrain profile [31], [127]. Due to its popularity, several models adapted the Okumura-Hata model to expand its supported frequency, distance, and Tx/Rx height [120], [128]. These models include Hata-Davidson, ILORIN (an optimization of the Hata-Davidson model based on measurements in Nigeria), CCIR, COST231-Hata, Extended COST 231, ECC-33, Ericsson 9999, and ITU-R P.529-3, as given in Eq. (4) to Eq. (11), respectively.

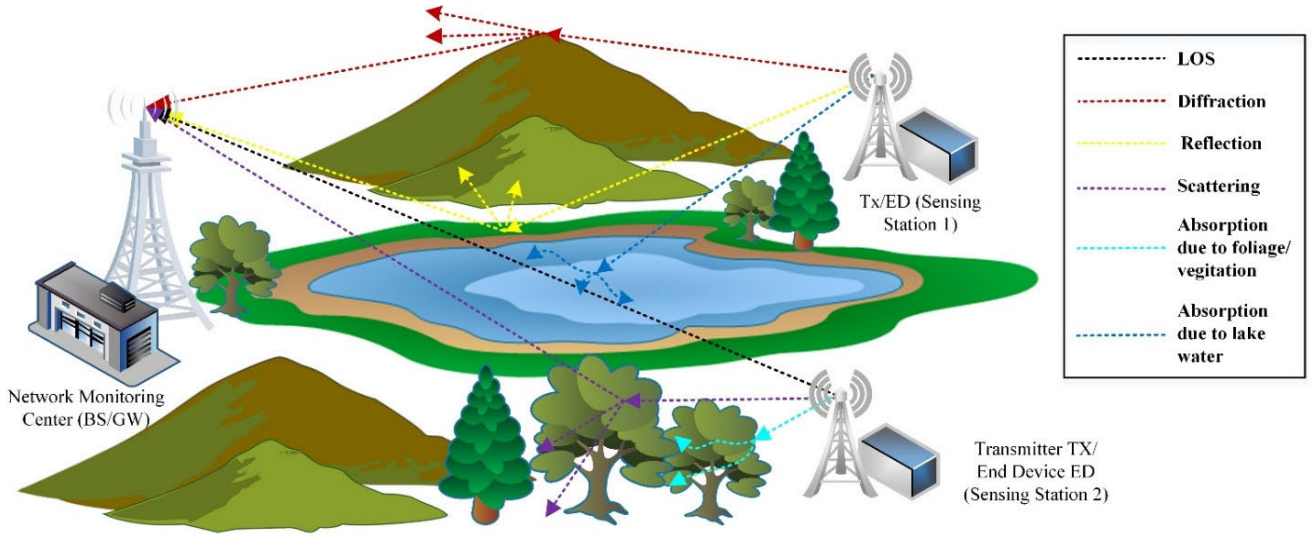

FIGURE 3. A basic wireless signal transmission with various attenuation scenarios due to channel imperfection.

C. TERRAIN

In contrast to the basic models, this set of models is commonly considered more complex and considers the estimation of diffraction losses due to terrain obstacles [123]. Empirical models, such as Okumura, Lee, and Stanford University Interim (SUI), and deterministic models, such as the Air-to-Ground (ATG) model, as given in Eq. (12) to Eq. (15), are examples of these models. There are also many more highly complex but extremely popular models in this category, such as the Longley-Rice Irregular Terrain Model (ITM) [31], [123], [127], and Irregular Terrain with Obstructions Model (ITWOM) [127], [129].

Despite their accuracy, empirical terrain models have several limits due to low antenna heights, limited prediction distances, and other area-specific limitations. Meanwhile, ray-tracing ATG epitomizes deterministic models by employing Maxwell's equations as well as the laws of reflection and diffraction. The ATG propagation model is widely used in Low Altitude Platforms (LAP) since it offers enhanced cell capacity and downlink coverage. PL is calculated using a closed-form approach between Tx and Rx based on two major ATG propagation categories. The first is LOS or near-LOS, whereas the second is NLOS but still receives signals with significant reflections and diffractions [130].

The ITM model is used at frequencies ranging from 20 MHz to 20 GHz. It is a two-part system with an ITM core and an input-output module. This model is generally used for point-to-point (P2P) communications and uses terrain data to measure PL in P2P mode. This model, however, is based on traditional diffraction theory, which does not incorporate precise radio wave calculations over irregular terrain. It also does not account for environmental factors near the Rx [31], [127]. ITWOM, on the other hand, is an extension to ITM that incorporates high location estimates and better accuracy into the ITM core. In addition, unlike ITM, it considers more than one obstacle in its diffraction calculations [127]. As a result, the latter two models are commonly utilized in ray-tracing and coverage estimation tools like Cloud-RF and Radio Mobile [31], [127], [129].

D. BASIC/STOCHASTIC FADING AND BASIC/TERRAIN

This set of models consists of two sub-categories of basic models. These models comprise Eq. (16) to Eq. (21), with the last equation being the Egli PL model, which combines a basic PL model with an empirical terrain loss factor, although diffraction losses are not explicitly considered [131].

On the other hand, stochastic fading models, as given in Eq. (16) to Eq. (20), are similar to basic models except that they incorporate one or more random variables to account for channel variance [123]. Numerous models fall into this category, with the Log-Normal Shadowing PL (LNSPL) model, as defined in Eq. (16), being the most widely used due to its simplicity and flexibility to account for a wide variety of environmental and propagation scenarios [117]. As a result, it is commonly applied in the PL modeling of most IoT-based wireless technologies [117], [114]. LNSPL is a one-slope model, typically known as a one-slope log-distance model if the PL estimation does not include the random variable. This model is also adopted in both WINNER II and 3GPP standards and is referred to as the Floating Intercept (FI) or Alpha-Beta (AB) PL model [132]–[135]. It is based on floating-intercept and line slope to provide the best minimum PL error fit. This model's parameters are usually derived through curve fitting and minimum mean square error (MMSE) approaches [132], [134].

Another common model in the category of stochastic fading models is the so-called Close-In (CI) PL model [6], [134], [136], as given in Eq (17). 3GPP adopts this model for Urban Microcell (Umi), Urban Macrocell (Uma), and Indoor Hotspot (InH) using a free-space reference PL at

a reference distance of 1 m [6], [136]. Therefore, it relies on a single parameter optimization of a distance-dependent PLE [134], [136]. CI model also has an intrinsic PL frequency dependence within the close-in (1 m) FSPL value [135]. It thus models frequency dependence across a wide range of frequencies and exhibits good precision and parameter stability across various outdoor settings, distances, and frequency ranges [136].

Several models have also been suggested to further modify the CI model, such as the Close-In with Frequency-Dependent Exponent (CIF) model [6], [132], [136], given in Eq. (18), and the Close-In with Hight Dependent Exponent (CIH) model [136], [137], given in Eq. (19). The CIF model was proposed to extend the CI model by modifying the PLE to compensate for frequency dependency empirically observed in the environment while maintaining a straightforward physical basis of frequency dependency due to Friis' equation at reference distances of 1 m [6], [137]. On the other hand, the CIH model modifies the CI model by adjusting the PLE to account for the Tx antenna height dependency in the PL calculation [136], [137]. Finally, Eq. (20) provides the Alpha-Beta-Gamma (ABG) PL model [6], [132], [134] that is a multi-frequency [132], [134] and the current 3GPP 3D model [6]. Due to its three parameters, it always has a lower shadow fading STD value than other models [6].

E. FOLIAGE AND FOLIAGE/TERRAIN

Another significant constraint in signal propagation is foliage attenuation. It is shown to be a function of various parameters, including frequency, foliage depth, tree species, foliage thickness, leaf density, leaf size, branches, trunks, humidity, wind speed, tree height relative to antenna heights, and foliage length [138]. Furthermore, foliage attenuation is expected to be greater in tropical areas where foliage is relatively comparable to or larger than wavelength plus humidity. Interestingly, recent field studies of tropical foliage attenuation showed that the presence of a single tree in a link could cause the signal to suffer foliage attenuation [5].

Numerous models exist to predict the excess loss due to foliage attenuation, referred to in this sub-category as foliage models. These models may include empirical foliage models such as Weissberger's Modified Exponential Decay (WMED), ITU-R, Fitted ITU-R (FITU-R), COST-235 [5], [9], [54], [139], and Chen & Kue [9], as specified in Eqs. (22), (23), (24), (25), and (26).

The W MED model was proposed for dense foliage areas in temperate climates with propagation paths blocked by dry-leaf trees [5], [9], [139]. By contrast, the ITU-R model was developed utilizing Weissberger's approach [9] and VHF / UHF frequency band measurements [5], [139]. The latter was then refined further using data from the VHF-mmWave frequency band, comprising trees with and without leaves over a short foliage depth [5]. Similarly, the COST-235 model was proposed utilizing Weissberger's method and mmWave measurements through a small grove of trees [5], [139]. Finally, the Chen & Kue model was proposed based on diffraction theory with a four-layer medium to address propagation impact in a forest environment utilizing measurements over frequencies from 1-100 GHz [9].

The latter exponential decay models are purely empirical and are therefore not constrained by inherent propagation mechanisms. As a result, several semi-empirical models have been proposed to address this issue [54]. These models may include the current ITU-R foliage model (P.833-9) [54], also known as the Maximum Attenuation (MA) model [54], [139], [140], as well as the Non-Zero Gradient (NZG) model [54] and the Dual Gradient (DG) model [139], as specified in Eqs. (27), (28), and (29). The MA model is recommended for terrestrial radio paths in wooded areas [140] and can operate at frequencies ranging from 30 MHz to 100 GHz [54]. Meanwhile, the NZG and DG models expand the MA model beyond 5GHz [54], [139].

The Tewari model, provided in Eq. (30), is an empirical model proposed for frequencies ranging from 50 MHz to 800 MHz, considering both terrain and foliage loss. Thus, this model is listed in Table 2 under the Foliage/Terrain subcategory. This model was further modified in the Extended Tewari model, as given in Eq. (31), by including an antenna height gain factor to account for the effect of Tx and Rx antenna height above terrain [54].

F. INDOOR

Propagation imperfections are primarily caused by reflection and diffraction from/around building objects, walls, and floors for indoor environments. Additional loss happens due to signals traveling through latter objects and moving objects, resulting in temporal and spatial signal fluctuation [141]. As a result, estimating and modeling indoor propagation is critical for indoor applications, gaining significant research and development interest [142]. Accordingly, several models have been proposed to compensate for these indoor propagation imperfections and model the PL in such environments. These models may include the COST231 Multi-Wall Multi-Floor (COST231-MWF) model [142], the ITU-R Indoor (P.1238-10) model [141], and the Multi-Wall Multi-Floor (MWMF) model [142], [143], as represented in Eqs. (32), (33), and (34).

Indoor PL is addressed in the COST231-MWF model by incorporating an FSPL with additional attenuation losses due to building walls and floors [142]. Meanwhile, the ITU-R P.1238-10 is a site-specific model that requires minimal information about the signal path and the site while spanning a broad frequency range of 300 MHz to 450 GHz. It is typically an empirical, basic PL model that considers the various attenuations of walls and floors and the shadowing impact under certain conditions [141]. On the other hand, the MWMF model was proposed utilizing ray-tracing measurements, considering the nonlinear relationship between total attenuation and the number of crossed walls or floors [142], [143].

Apart from the models discussed in the preceding subsections, various models have been introduced over the years. These models include 3GPP TR 38.901 and ITU-R M.2412,

TABLE 2. Well-known path loss models for wireless IoT channel modeling under different communication scenarios and environments.

Category/Type/Model			PL in dB	Eq.	Parameters
Foundational	Deterministic	FSPL [54],[130],[144],[145]	$PL_{FS}(f,d)=\begin{cases}32.44+20\log_{10}(f[MHz])+20\log_{10}(d[km])\\32.44+20\log_{10}(f[GHz])+20\log_{10}(d[m])\\92.45+20\log_{10}(f[GHz])+20\log_{10}(d[km])\end{cases}$	(1)	f is the frequency d is Tx-Rx separation distance
		2-Ray [54], [139]	$\begin{cases}PL_{2-Ray}=\begin{cases}PL_{FS}(f,d)\ for\ d<d_C\\PL_{PE}\ for\ d\geq d_C, d>h_{Tx},h_{Rx}\end{cases}\\PL_{PE}=40\log_{10}(d)-20\log_{10}(h_{Tx})-20\log_{10}(h_{Rx})\\d_C=(4\pi h_{Tx}h_{Rx})/\lambda\end{cases}$	(2)	d in m; d_C is Crossing distance or breakpoint; h_{Tx} and h_{Rx} are Tx and Rx antenna height in m.
Basic	Empirical	Okumura-Hata [144]–[146]	$\begin{cases}PL_{OH}=\begin{cases}PL_{OH_U}\ for\ Urban\\PL_{OH_U}-2(\log_{10}(f/28))^2-5.4\ for\ Suburban\\PL_{OH_U}-4.78(\log_{10}(f))^2+18.33\log_{10}(f)-40.94\ for\ Rural\end{cases}\\PL_{OH_U}=\begin{cases}69.55+26.16\log_{10}(f)-13.82\log_{10}(h_{Tx})\\-a(h_{Rx})+(44.9-6.55\log_{10}(h_{Tx}))\log_{10}(d)\end{cases}\\a(h_{Rx})=\begin{cases}8.29(\log_{10}(1.54h_{Rx}))^2-1.1\ Urban, f\geq 300\ MHz\\3.2(\log_{10}(11.75\,h_{Rx}))^2-4.97\ Urban, f\leq 300\ MHz\\(1.1\log_{10}(f)-0.7)h_{Rx}-(1.56\log_{10}(f)-0.8)\ for\ Suburban\ and\ Rural\end{cases}\end{cases}$	(3)	f is the frequency in MHz (except for ECC-33 and ITU-R P.529-3, where the frequency is given in GHz), d is Tx-Rx separation in km (except for ITU-R P.529-3, where the Tx-Rx separation distance is given in m), $a(h_{Rx})$ is the effective Rx antenna height correction factor in dB, h_{Tx} & h_{Rx} are Tx & Rx antenna heights in m, C_{HD} is Hata-Davidson correction parameter, $A(h_{Tx},d)$ and $S_1(d)$ are Hata-Davidson model correction factors to extend Okumura-Hata model maximum supported distance to 300km, $S_2(h_{Tx},d)$ is Hata-Davidson model correction factor that extends Okumura-Hata model supported Tx antenna height to 2500m, $S_3(f)$ and $S_4(f,d)$ are Hata-Davidson model correction factors to extend Okumura-Hata model frequency to 1.5GHz, b_ρ is the percent of the building covered area, C_m is an environment correction factor in dB, A_{bm} is a basic medium loss, G_{Tx} & G_{Rx} are Tx and Rx antenna height gain factor, $\propto_0$, $\propto_1$, $\propto_2$, and $\propto_3$ are different environment correction constants for Ericsson 9999 model, $G(f)$ is a frequency correction factor for Ericsson 9999 model, h'_{Tx} is a correction factor for Tx antenna height, b is a distance correction factor
		Hata-Davidson [130], [144]	$\begin{cases}PL_{HD}=PL_{OH}+C_{HD}\\C_{HD}=A(h_{Tx},d)-S_1(d)-S_2(h_{Tx},d)-S_3(f)-S_4(f,d)\end{cases}$	(4)	
		ILORIN [4]	$\begin{cases}PL_{ILORIN}=73.56+26.16\log_{10}(f)-13.82\log_{10}(h_{Tx})\\-a(h_{Rx})+30.5\log_{10}(d)+C_{HD}\end{cases}$	(5)	
		CCIR [4]	$PL_{CCIR}=PL_{OH_U}-(30-25\log_{10}(b_\rho))$ for Suburban	(6)	
		COST231-Hata [2], [144], [146]	$\begin{cases}PL_{C231\_H}=46.3+39.9\log_{10}(f)-13.82\log_{10}(h_{Tx})-a(h_{Rx})\\+(44.9-6.55\log_{10}(h_{Tx}))\log_{10}(d)+C_m\\a(h_{Rx})=\begin{cases}(1.1\log_{10}(f)-0.7)h_{Rx}-(1.56f-0.8)for\ Suburban\\3.2(\log_{10}(11.75\,h_{Rx}))^2-4.97\ for\ Urban\end{cases}\\C_m=0\ dB\ for\ Suburban\ and\ Rural, 3\ dB\ for\ Urban\end{cases}$	(7)	
		Extended COST 231 [145]	$PL_{Ex\_C231}=\begin{cases}PL_{C231\_H}\ for\ Urban\ Area\\PL_{C231\_H}-2(\log_{10}(f/28))^2-5.4\end{cases}$	(8)	
		ECC-33 [2], [146], [147]	$\begin{cases}PL_{ECC-33}=PL_{FS}(f,d)+A_{bm}-G_{Tx}-G_{Rx}\\A_{bm}=20.41+9.83\log_{10}(d)+7.89\log_{10}(f)\\+9.56(\log_{10}(f/28))^2\\G_{Tx}=\log_{10}(h_{Tx}/200)(13.958+5.8\log_{10}(d))^2\\G_{Rx}=\begin{cases}(42.57+13.7\log_{10}(f))(\log_{10}(h_{Rx})-0.585)\\0.759(h_{Rx})-1.862\ for\ larg\ city\end{cases}\end{cases}$	(9)	
		Ericsson 9999 [4], [147]	$\begin{cases}PL_{Er}=\propto_0+\propto_1\log_{10}(d)+\propto_2\log_{10}(h_{Tx})+\propto_3\log_{10}(h_{Tx})\log_{10}(d)\\-3.2(\log_{10}(11.75h_{Rx}))^2+G(f)\\G(f)=44.49\log_{10}(f)-4.78(\log_{10}(f))^2\end{cases}$	(10)	
		ITU-R P.529-3 [130]	$\begin{cases}PL_{P5293}=\begin{cases}PL_{P5293_U}\ for\ Urban\\PL_{P5293_U}-2(\log_{10}(f/28))^2-5.4\ for\ Suburban\\PL_{P5293_U}-4.78(\log_{10}(f))^2+18.33\log_{10}(f)\\-40.94\ for\ Rural\end{cases}\\PL_{P5293_U}=\begin{cases}69.55+26.16\log_{10}(f)-13.82\log_{10}(h_{Tx})\\-a(h_{Rx})+(44.9-6.55\log_{10}(h_{Tx}))(\log_{10}(d))^b\end{cases}\\a(h_{Rx})=(1.1\log_{10}(f)-0.7)h_{Rx}-(1.56\log_{10}(f)-0.8)\\b=\begin{cases}1\ for\ d\leq 20km\\1+(0.14+1.87*10^{-4}f)+(1.07*10^{-3}h'_{Tx})\\*(\log_{10}(d/20000))^{0.8}\ for\ 20km<d\leq 100km\end{cases}\\h'_{Tx}=h_{Tx}/\sqrt{1+(7*10^{-6}*h_{Tx}^2)}\end{cases}$	(11)	

TABLE 2. ***(Continued.)*** **Well-known path loss models for wireless IoT channel modeling under different communication scenarios and environments.**

Terrain	Empirical	Okumura [130]	$\begin{cases} PL_{Okm} = PL_{FS}(f,d) + A_{mu}(f,d) - G(h_{Rx}) - G(h_{Tx}) - G_{area} \\ G(h_{Tx}) = 20\log_{10}(h_{Tx}/200) \quad 30m < h_{Tx} < 1000m \\ G(h_{Rx}) = \begin{cases} 20\log_{10}(h_{Rx}/3) & for\ h_{Rx} \le 3 \\ 10\log_{10}(h_{Rx}/3) & for\ 3m < h_{Rx} < 10m \end{cases} \end{cases}$	(12)	f is the frequency in MHz, d is the Tx-Rx separation distance in km, A_{mu} is a medium attenuation factor relative to FS attenuation, $G(h_{Tx})$ & $G(h_{Rx})$ is the Tx/Rx antenna height gain factor, G_{area} is environment type gain, h_{Tx} and h_{Rx} are Tx and Rx antenna height in m
		Lee [145], [148]	$\begin{cases} PL_{Lee} = A + B\log_{10}(d/d_0) + 10n\log_{10}(f/900) + \alpha_0 \\ d_0 = 1.6\text{km} \end{cases}$	(13)	d_0 is the reference distance, A, and B are environment correction factors, n is a distance-dependent PL Exponent (PLE), α_0 is a correction factor to consider Tx and Rx antenna heights
		SUI [2], [147], [149]–[151]	$\begin{cases} PL_{SUI} = PL_{FS}(f,d_0) + 10\gamma\log_{10}(d/d_0) + X_f + X_{Rx} + X_\sigma \\ d > d_0, d_0 = 100m\ or\ 1m, \gamma = a - bh_{Tx} + (c/h_{Tx}) \\ X_f = 6\log_{10}(f(MHz)/2000) \\ X_{Rx} = \begin{cases} -10.8\log_{10}(h_{Rx}/2)\ for\ terrain\ type\ A\ \&\ B \\ -20\log_{10}(h_{Rx}/2)\ for\ Terrain\ type\ C \end{cases} \\ a = 4.6, b = 0.0075, c = 12.6, , for\ terrain\ type\ A \\ a = 4, b = 0.0065, c = 17.1, , for\ terrain\ type\ B \\ a = 3.6, b = 0.005, c = 20, , for\ terrain\ type\ C \end{cases}$	(14)	d is the Tx-Rx separation distance in m, γ is SUI effective PLE, $a, b, and\ c$ are model parameters for terrain type A (hilly, dense vegetation), B (hilly, rare vegetation), and C (flat, rare vegetation), X_f is the correction factor for frequency > 2 GHz, X_{Rx} is the correction factors for Rx antenna height, X_σ is the shadowing variable in dB, typically zero-mean Gaussian random variable with standard deviation σ in dB
	Deterministic	ATG [130]	$\begin{cases} PL_{ATG} = \rho_{LOS}PL_{LOS} + \rho_{NLOS}PL_{NLOS} \\ \rho_{LOS} = a - \dfrac{a-b}{1+\left(\dfrac{\theta-c}{d}\right)^2}, \quad \rho_{NLOS} = 1 - \rho_{LOS} \\ PL_{LOS} = PL_{FS}(f,d) + \eta_{LOS}, \ PL_{NLOS} = PL_{FS}(f,d) + \eta_{NLOS} \\ 3dB \le \eta_{LOS} \le 5dB, 8dB \le \eta_{NLOS} \le 12dB \end{cases}$	(15)	ρ_{LOS} and ρ_{NLOS} are the probability of having LOS/NLOS conditions at an elevation θ; PL_{LOS} and PL_{NLOS} is the PL for LOS/NLOS condition, η_{LOS} and η_{NLOS} are average additional loss depending on environment type, a, b, c, and d are ITU-R parameters for environment type (rural, suburban, urban)
Basic/Stochastic Fading	Empirical	LNSPL [6], [114], [133],	$PL_{LNSPL}(d) = PL(d_0) + 10n\log_{10}(d/d_0) + X_\sigma$ Known as Floating Intercept (FI) or Alpha-Beta (AB) PL model (for $d \ge 1m$), where: $\beta = PL(d_0), \alpha = n, \ X_\sigma^{FI} = X_\sigma$, $PL_{FI}(d) = \beta + 10\alpha\log_{10}(d/d_0) + X_\sigma^{FI}$	(16)	f is the frequency in GHz, d is the Tx-Rx separation distance in m, n is a distance-dependent PLE, n_{eff}^{CIF}, and n_{eff}^{CIH} are effective PLE for CIF and CIH model, b is the linear frequency-dependent factor of CIF PL over considered reference frequency, b_{Tx}, h_{Tx}, and h_{Tx0} are linear Tx height dependent PLE, Tx antenna height, average Tx antennas heights in a set of measurements, α, and γ are constant coefficients used to indicate dependencies of frequency and distance on PL, β is offset in PL, X_σ, X_σ^{FI}, X_σ^{CIF}, and X_σ^{CIH} are zero-mean Gaussian random variables with standard deviation σ in dB X_σ^{ABG} is a Gaussian random variable with a standard deviation σ^{ABG} in dB.
		CI [6], [132]–[136], [153]	$PL_{CI}(f,d) = PL_{FS}(f,d_0) + 10n\log_{10}(d/d_0) + X_\sigma$, d_0=1m	(17)	
		CIF [6], [132], [133]	$\begin{cases} PL_{CIF}(f,d) = PL_{FS}(f,d_0) + 10n_{eff}^{CIF}\log_{10}(d/d_0) + X_\sigma^{CIF} \\ n_{eff}^{CIF} = n(1 + b((f-f_0)/f_0) \end{cases}$, d_0=1m	(18)	
		CIH [136]	$\begin{cases} PL_{CIH}(f,d,h_{Tx}) = PL_{FS}(f,d_0) + 10n_{eff}^{CIH}\log_{10}(d/d_0) + X_\sigma^{CIH} \\ n_{eff}^{CIH} = n(1 + b_{Tx}((h_{Tx} - h_{Tx0})/h_{Tx0}) \\ d_0\text{=1m} \end{cases}$,	(19)	
		ABG [6], [132]–[135],	$PL_{ABG}(f,d) = 10\alpha\log_{10}(d/d_0) + \beta + 10\gamma(f/f_0) + X_\sigma^{ABG}$, d_0=1m, $f_0 = 1GHz$, $f \ge 1GHz$	(20)	
Basic/Terrain	Empirical	Egli [131], [154]	$\begin{cases} PL_{Egli} = 20\log_{10}(f) + 40\log_{10}(d) - 20\log_{10}(h_{Tx}) + C(h_{Rx}) \\ C(h_{Rx}) = \begin{cases} 76.3 - 10\log_{10}(h_{Rx})\ for\ h_{Rx} < 10m \\ 85.9 - 20\log_{10}(h_{Rx})\ for\ h_{Rx} \ge 10m \end{cases} \end{cases}$	(21)	f is the frequency in MHz, d is Tx-Rx separation in km, h_{Tx} and h_{Rx} are Tx and Rx antenna height in m, and $C(h_{Rx})$ is the Rx antenna height correction
Foliage	Empirical	W MED [5], [9], [139]	$\begin{cases} PL_{W\_MED} = \begin{cases} 1.33f^{0.284}d^{0.588}\ for\ 14m < d \le 400m \\ 0.45f^{0.284}d\ for\ 0m < d \le 14m \end{cases} \\ 230MHz \le f \le 95GHz \end{cases}$	(22)	f is the frequency in MHz (except for W MED, frequency is given in GHz), d is the tree depth in m
		ITU-R [5], [9], [139]	$\begin{cases} PL_{ITU-R} = 0.2f^{0.3}d^{0.6} \\ 200MHz \le f \le 95GHz, d \le 400m \end{cases}$	(23)	
		FITU-R [5], [9], [139]	$\begin{cases} PL_{FITU-R} = \begin{cases} 0.37f^{0.18}d^{0.59}\ for\ out\ of\ leaf \\ 0.39f^{0.39}d^{0.25}\ for\ in\ leaf \end{cases} \\ 10GHz \le f \le 40GHz, d \le 400m \end{cases}$	(24)	

TABLE 2. *(Continued.)* **Well-known path loss models for wireless IoT channel modeling under different communication scenarios and environments.**

Foliage	Empirical	COST-235 [5], [9], [139]	$\begin{cases} PL_{C235} = \begin{cases} 26.6f^{-0.2}d^{0.5} \; for \; out \; of \; leaf \\ 15.6f^{-0.009}d^{0.26} \; for \; in \; leaf \end{cases} \\ 9.6GHz \le f \le 57.6GHz, d \le 200m \end{cases}$	(25)	f is the frequency in MHz, d is the tree depth in m
		Chen & Kue [9]	$\begin{cases} PL_{C-K} = \begin{cases} (0.001f + 0.2)d + 0.5f + 3 \; vertical \; polarization \\ (0.002f + 0.2)d + 0.03f + 2 \; horizantal \; polarization \end{cases} \\ 1GHz \le f \le 100GHz \end{cases}$	(26)	
	Semi-Empirical	MA [54], [140]	$\begin{cases} PL_{MA} = A_m(1 - e^{-\left(\frac{\xi d}{A_m}\right)}) \\ A_m = A_1 f^{\propto_1} \\ 30MHz \le f \le 100GHz \\ A_1 = 0.18, \propto_1 = 0.752 \; for \; tropical \; trees \; at \; 900 - 1800MHz \\ @h_{Rx} = 2.4m \; with \; 15m \; average \; tree \; height \\ A_1 = 1.15, \propto_1 = 0.43 \; for \; mixed \; forest \; at \; 900 - 2200MHz \\ @h_{Rx} = 1.6m \; and \; h_{Tx} = 25m \; with \; 15m \; average \; tree \; height \\ A_1 = 1.37, \propto_1 = 0.42 \; for \; mixed \; forest \; at \; 105.9 - 2117.5MHz \\ @h_{Rx} = 1.5m \; with \; 14m \; average \; tree \; height \end{cases}$	(27)	A_m is the maximum attenuation in dB for a specific type of vegetation, ξ is the attenuation for a very short path via a specific type of vegetative in dB/m, d is tree depth in m (propagation distance through foliage), R_0 is the initial gradient of the attenuation curve, R_∞ is final attenuation in dB/m, k is final attenuation offset in dB, f is the frequency in GHz, w is the maximum effective width between Tx-Rx, a, b, and c are estimated constants
		NZG [54]	$PL_{NZG} = R_\infty d + k(1 - e^{-\left(\frac{R_0 - R_\infty}{k}\right)})$	(28)	
		DG [54], [139]	$PL_{DG} = \frac{R_\infty}{f^a w^b} d + \frac{k}{w^c}(1 - e^{-\left(\frac{(R_0 - R_\infty)W^c d}{k}\right)})$	(29)	
Foliage/Terrain	Empirical	Tewari [54]	$\begin{cases} PL_{Tewari} = -27.56 + 20\log_{10}(f) - 20\log_{10}(\frac{A_2 e^{-(\propto_2 d)}}{d} + \frac{B_2}{d^2}) \\ 50MHz \le f \le 800MHz, d \le 4000m \end{cases}$ f [MHz] | $\propto_2$ [Horizontal (H), Vertical (V)] | A_2 [H, V] | B_2 [H, V] 50 | -, - | 0, 0 | 7.367, 1.917 200 | 0.011, 0.0125 | 0.8201, 0.4989 | 5.045, 1.8358 500 | 0.0138, 0.0135 | 0.6571, 0.3658 | 1.4304, 0.904 800 | 0.0152, 0.014 | 0.4491, 0.2661 | 0.6291, 0.5331	(30)	f is the frequency in MHz, d in m, $\propto_2$ is attenuation rate in dB/m, A_2 and B_2 are empirically found constants for different frequencies and polarization, $G(h_{Tx}, h_{Rx})$ is the antenna height gain factor for both Tx and Rx, h_{Tx} and h_{Rx} are Tx and Rx antenna heights above terrain
		Extended Tewari [54]	$\begin{cases} PL_{Ext\_Tewari} = PL_{Tewari} + G(h_{Tx}, h_{Rx}) \\ G(h_{Tx}, h_{Rx}) = 14 + 4\log_{10}(f) - 20\log_{10}(h_{Tx}h_{Rx}) \\ 50MHz \le f \le 800MHz, d \le 4000m \end{cases}$	(31)	
Indoor	Empirical	COST231-MWF [142]	$PL_{C231\_MWF} = PL_{FS}(f, d) + L_c + \sum_{i=1}^{I} K_{wi}L_{wi} + K_f^{(\frac{K_f+2}{K_f+1} - b)} L_f$	(32)	L_c is a measurement-based constant loss, usually found using multi-linear regression method; K_{wi} and L_{wi} are the number and the loss of traversed walls of type i, respectively; K_f and L_f are number and loss of penetrated floors, respectively; b is an empirical accuracy adjustment factor, I is the number of wall types
		ITU-R Indoor (P.1238-10) [141]	$\begin{cases} PL_{P1238_{10}}(d) = PL(d_0) + N\log_{10}(d/d_0) + L_f(n) \\ PL(d_0) = 20\log_{10}(f) - 28, \quad for \; d_0 = 1m \\ L_f = 0dB, \quad for \; n = 0 \\ 300MHz \le f \le 450GHz, d > 1m, n \ge 0 \end{cases}$	(33)	$PL(d_0)$ is the basic transmission loss at the reference distance d_0, N is a distance-dependent power loss coefficient given in [141], d is the Tx-Rx separation distance in m, d_0 is the reference distance in m, L_f is the floor penetration factor in dB, given in [141], n is the number of floors between Tx and Rx, f is the frequency in MHz
		MWMF [142], [143]	$PL_{MWMF}(d) = PL(d_0) + 10n\log_{10}(d/d_0) + \sum_{i=1}^{I}\sum_{k=1}^{K_{wi}} L_{wik} + \sum_{j=1}^{J}\sum_{k=1}^{K_{fj}} L_{fjk}, \quad d_0 = 1\text{m}$	(34)	d is the Tx-Rx separation distance in m, d_0 is the reference distance, n is the PLE, L_{wik} is the loss in dB of the kth traversed wall of type i, K_{wi} is the number of traversed walls of type i, I is the number of wall types, L_{fjk} is the loss in dB of the kth traversed floor of type j, K_{fj} is the number of traversed floors of type j, J is the number of floor types

which support a wide range of transmission scenarios for a wide range of frequencies and bandwidths, such as Outdoor-to-Outdoor (O2O), Outdoor-to-Indoor (O2I), and Indoor-to-Indoor (I2I) [128].

Meanwhile, several other studies have been conducted over the past years mainly to propose new models or improve existing models by optimizing their parameters through different methods such as linear curve fitting. Hence, the next section will cover the most recent advances in wireless IoT channel modeling and characterization.

V. CHANNEL MODELING AND WIRELESS PROPAGATION OF IoT TECHNOLOGIES

This section thoroughly reviews the most recent developments and studies aimed at wireless channel modeling and characterization of wireless IoT technologies. For simplicity, the section will be divided into three sub-sections according to wireless IoT technology categories, as follows:

A. CELLULAR-BASED WIRELESS IoT CHANNEL MODELING AND CHARACTERIZATION

The wireless communications sector is undergoing significant growth. In this regard, the fifth-generation (5G) of mobile communication technology has been designed to address all wireless broadband communication needs and enable massive IoT deployments over the next decade [155], [156]. While spectrum in the existing sub-6 GHz band remains constrained, new frequency bands are required to enable the efficient design of IoT applications in 5G networks [155]. As a result of its vast bandwidth, which spans 30 GHz to 300 GHz, the mmWave band is regarded the leading choice for adoption [132], [155]. However, the electromagnetic (EM) wave characteristics of these bands present several challenges in terms of coverage limits, signal attenuation, PL, penetration loss, diffraction, and scattering [125], [155], [157]. Besides, buildings and other structures may block the mmWave band signal [125]. Accordingly, several studies have addressed these challenges and characterized the 5G frequency bands' wireless channel characteristics [156].

For instance, the studies in [132], [156], [158], [159] considered a variety of indoor scenarios and a broad range of frequencies to evaluate the channel's behavior. In [156], various channel models were studied for the 4.5, 28, and 38 GHz frequency bands, including CI, FI, and ABG. Then, a new hybrid probabilistic PL model was proposed, based on the CI PL model, for directional and omnidirectional antennas in LOS and NLOS scenarios. Meanwhile, [158] presented measurements of an indoor cellular system operating at 40 GHz in LOS and NLOS scenarios. A single frequency PL model was thus proposed, based on the CI and FI models, and the 2-Ray model was investigated. According to [156], the FI model does not physically represent either the LOS or NLOS channel. Also, the small STD difference shows that the CI model may be better suited for closed-form analysis than the FI and ABG models. The proposed model was compared to the CI, FI, and ABG models, which showed that the PL might be modeled more accurately utilizing the proposed model with a single parameter (PLE). According to [158], the PLE of the CI and FI were similar, around 1.8 and 2.9, respectively, for LOS and NLOS scenarios. Conversely, the results showed that the FI model gave the best minimum error fit and, just like the CI model, would be the most suitable for indoor PL modeling of a 5G network operating at 40 GHz.

In contrast, [132] conducted a comparative study for the indoor 5G channel, then proposed two models that addressed loss due to wall edge diffraction and high-frequency band. The results showed that the PLE values for the LOS were 1.6 and 1.3 at 3.5 and 28 GHz, respectively. However, the power received was dropped in the NLOS, with PLE values being 2.7 and 3.6 at 3.5 GHz and 28 GHz, respectively. The results also indicated that FI and ABG models provided reliable PL performance in the LOS scenario for single and multi-frequency models. At 3.5 GHz and 28 GHz, the average diffraction loss was 11.11 dB and 23.37 dB, respectively.

Meanwhile, the frequency-related loss, referred to as frequency drop, was 19.73 dB for the LOS and 32 dB for the NLOS. The root mean square delay spread (RMS-DS) values for the LOS and NLOS scenarios were less than 8 ns and 12 ns, respectively. These results indicated that the 5G channel has excellent PL performance and a very small DS, enabling future real-world deployments of 5G-based smart city IoT networks.

On the other hand, [159] presented an empirical characterization of the mmWave frequency bands, 6.5, 10.5, 15, 19, 28, and 38 GHz, in an indoor corridor scenario. Over 4,000 power delay profiles (PDP) were observed overall bands using an omnidirectional Tx antenna and a highly directional horn Rx antenna in co- and cross-polarized setups. After that, a new PL model was developed to account for frequency attenuation due to distance, termed the frequency attenuation (FA) PL model, which included a frequency-dependent attenuation factor. Additionally, a more generic and simpler method for estimating the cross-polarization discrimination (XPD) factor of close-in reference distances using XPD (CIX) and ABG with XPD (ABGX) PL models was proposed to avoid the computational complexity associated with the MMSE approach. Small-scale metrics were considered to describe multipath channel dispersion, including RMS-DS, mean excess delay, dispersion factors, and maximum excess delay.

Additionally, multiple RMS-DS statistical distributions were investigated. The results implied that the proposed models are more physically based and simpler than other well-known models. RMS-DS values ranged from 0.2 to 13.8 ns, with dispersion factors less than one for all measured frequencies.

In contrast, [125], [134], [160]–[162] focused on the evaluation of outdoor channel models. For instance, [134] demonstrated the large-scale propagation characteristics of 5G in an outdoor parking lot scenario with several end users. As such, a new CI-based PL model was proposed, including a parking lot compensation factor. The PL was evaluated using several

models and observations at 28 and 38 GHz for various scenarios. [160] discussed measurement campaigns in a tropical climate for an outdoor 5G network operating at 32 GHz, considering the distance, polarization, and antenna type. For the LOS scenario, highly directional horn antennas with Co- and Cross-polarizations were used for Tx and Rx.

Meanwhile, horn and omnidirectional antennas were utilized on the receiver side for NLOS. Finally, the CI and FI PL models were evaluated based on the outdoor data. The results in [134] indicated that the PLE values were almost similar. Meanwhile, the compensation factor suggested for 28 GHz and 38 GHz was 10.6-23.1 dB and 13.1-19.1 dB, respectively. They did, however, show that additional compensation factors are required for more scattered objects, particularly at 28 GHz. According to the findings in [160], the PLE for LOS and NLOS scenarios ranged between 3.4 and 6.7. Additionally, the FI PL model was unsuitable for the NLOS scenario, shown by the large divergence between the slope lines of the horn-horn and horn-omnidirectional cases. Likewise, the results indicated that co-polarization decayed faster than cross-polarization in LOS scenarios.

Similarly, [125], [161] evaluated the potential capability of mmWave PL models using measurements taken in outdoor tropical environments. While both studies evaluated the CI and FI models at 38 GHz, [161] included the CIF and ABG models and extended the evaluation to include 20-38 GHz frequency bands. The authors in [161] then proposed a new PL model for 20 GHz and 30 GHz frequency bands. Meanwhile, [125] examined network performance in LOS and NLOS scenarios with co- (vertical-vertical) and cross-polarization (vertical-horizontal). The results in [161] showed that the proposed model was both reliable and straightforward in terms of frequency and environment signal attenuation, suggesting its usefulness for establishing suitable communication links for the scenarios studied. Reference [125] showed that the CI PL model predicted significant NLOS outcomes and better network performance in the LOS case. Also, the results showed that the FI PL model was unsuitable for the NLOS scenario, particularly for V-V polarization. Additionally, the simulation results indicated that user throughputs decreased faster with cross-polarization than with co-polarization in both LOS and NLOS scenarios.

Finally, in [162], the authors presented a brief simulation analysis of rain fading using simultaneous one-minute rain rate measurements and its effects on a short 38 GHz experimental link. The PDP was also generated for omnidirectional and directional scenarios by observing the received power and PL using Malaysia's environmental characteristics. Rain attenuation of up to 15 dB was measured for a 300 m path at a rain rate of roughly 125 mm/h, indicating that 0.001% and 0.011% of outages must be considered for 38 GHz. Moreover, the received power dropped by 33.1 dB for NLOS scenarios. When considering rain attenuation, it was also found that received power dropped by 6.4 dB for Malaysia compared to a temperate area communication link due to increased PL at 38 GHz. Thus, the study implies that further research is required to model 5G channels in tropical environments.

Machine learning techniques are capable of mining high-dimensional data and extracting the required information to learn the structural relationship between data in complex environments. As a result, ML may be a powerful tool for extracting radio wave characteristics and developing channel models from measurement data. However, integrating channel modeling and ML is challenging, and research in this subject is still in the exploration stage. On the other hand, artificial neural network (ANN) is a significant branch of ML that benefits from adaptability, self-learning, and robustness and may be used to predict PL. Recently, [163], [164] introduced PL models based on ANNs and Levenberg-Marquardt backpropagation (BP), respectively. The results indicate that when compared to conventional PL models, the proposed methods can significantly enhance the accuracy of PL prediction. However, the methods' input set consists of signal parameters that describe the channel's properties, with the impact of the environment being ignored.

Providing geometrical information is a complicated procedure. The environment type can be valuable in this sense, as it can provide useful information for describing the environment [165]. In [166], a PL prediction model based on the multilayer perceptron (MLP) neural network (NN) and environment types is established, with BS and Rx, digital images, and satellite maps as inputs. To simplify 3D environment modeling, principal component analysis (PCA) was utilized to extract low-dimensional environmental features from the limited environmental types. An ANN dataset was constructed to train and evaluate the PL prediction model by combining measured information from the BS and receiver, including 3D locations, frequency, Tx/Rx power, antenna data, feeder loss, and other environmental features. The measurement campaigns were done at 2.5 GHz in Hangzhou, China, covering 20 different environmental types like suburban areas, urban areas, high-raised buildings, irregular buildings, green land, wetland, and forest. Three BSs with heights of 30 m, 42 m, and 62 m were considered, with the Rx placed on a vehicle with a height of 2 m. The CI and A-B models were used to fit the measurement data for PL prediction and then compared to predicted results in terms of the absolute value of mean error (AME), mean absolute error (MAE), STD error, and correlation coefficient (R). The comparison showed that the proposed model could achieve a higher prediction accuracy. However, the accuracy of ANN-based prediction methods can be improved at the expense of the ANN architecture's complexity. This study also examined the impact of ANN architectures, dimension, and training sample percentage on PL prediction models, finding that 60% of training samples from training sets is sufficient for a high-efficiency and stable PL prediction model.

Convolutional neural networks (CNN) is a well-known deep learning (DL) model that may be used to solve a wide variety of classification and regression problems with little pre-processing and feature extraction. Reference [167]

proposed a method for 28 GHz mmWave PL modeling based on CNNs for the suburban scenario. The measurement campaign considered 13 scenarios using a fixed Tx at 3 m, and an Rx mounted on the rooftop of a moving car. Four directional antennas were utilized on the receiver side to investigate the mmWave system's characteristics in various environmental scenarios. The method was built assuming that the CNN could generate relevant environmental features from map imagery. Thus, two-dimensional (2-D) Google map images were used to extract geometrical information about buildings and street objects. The Enhanced local area multi-scanning (ELAMS) algorithm was proposed to build a training set for the CNN. The algorithm extracts environmental data between Tx and Rx from pre-processed map images. A CNN was constructed with four subnetworks and 20 neurons, with each subnetwork learning the same propagation and environmental information from the ELAMS images. A feature sharing layer was introduced between convolutional layers to concatenate the activation map of the previous layer as an input to the next layer. It was claimed that the addition of feature-sharing layers did not increase the model's complexity but rather aided in the backpropagation of loss from each antenna to the entire network. The comparison results showed that the proposed CNN model outperforms both the CI and ABG models in accuracy and complexity, with an RMSE of 8.59 dB for PL prediction in the test scenarios.

Although prior research has demonstrated potential channel characterizations for some 5G bands under various setup scenarios, this technology is still in its initial deployment in many countries. As a result, most of these studies are primarily experimental or simulation-based, focusing on high-power devices and high-gain antennas, and do not consider the requirements of IoT-based applications. Thus, future research and characterization must incorporate IoT parameters into the modeling process and optimize the performance of such applications.

Other studies have evaluated the channel characterization of traditionally utilized cellular-based IoT technologies, including narrowband-IoT (NB-IoT) and cellular-based D2D communication. In [168], the authors proposed an empirical PL model for NB-IoT in urban areas using a large-scale measurement campaign conducted in Oslo, Norway. Three datasets in the LTE band from two cellular operators were included, considering three different scenarios: outdoor, indoor, and deep indoor. The ABG and CI PL models were used to characterize the PL, with model parameters statistically characterized from known distributions. The shadowing effect was further studied, and a statistically extended model for inter-cell shadowing distribution and distance correlation was provided. The proposed PL model was verified across NB-IoT and LTE operators, and the findings indicated that it outperforms state-of-the-art NB-IoT PL models in terms of estimation accuracy.

To develop a suitable channel model for D2D IoT communication technologies, the authors of [169] presented two log-distance-based PL models (frequency-independent PLE and frequency-dependent PLE), as well as a new statistical distribution of the DS for IoT communications, based on quasi-simultaneous wideband channel measurements in the VHF/UHF frequency bands (37.8–370 MHz) in Halifax, Canada. The results indicated that both models achieved similar estimation results, with PLE values ranging from 4.13 to 4.8 and shadow fading standard deviation values ranging from 8.87 to 10.96 dB. As a result, they emphasize that existing VHF/UHF propagation models are unsuitable for IoT communications with low Tx and Rx antenna heights.

By contrast, the authors of [54], [170] concentrated on NB-IoT connectivity in a rural forest with low antenna heights. Both measurement campaigns were done at a range of 2.5 km, utilizing LTE band 8 at a frequency of 917.5 MHz, with a special focus on PL and coverage evaluation in a D2D communication scenario. [170] noted that previous PL studies for 900 MHz near-ground scenarios lag of the 164 dB PL specified in the NB-IoT standard. As a result, measurements were made with a custom-built 180 dB dynamic measurement instrument. According to the measurements, a D2D system with Tx and Rx antennas at 1.5 m height could achieve a range of around 2 km when employing the NB-IoT 164 dB PL limit. Meanwhile, in [54], the authors evaluated the effects of various antenna heights by utilizing similar measurement equipment and placing antennas 1.5 m, 2.5 m, and 3.5 m above the ground.

Additionally, measured data were compared to known foliage excess loss models and related PL models to determine suitable models for NB-IoT D2D communication. The results indicated that the antenna height had no significant influence on the received power in the given setting. Additionally, the results indicated that the dominant propagation path for the first km was through the foliage, resulting in foliage excess loss being the dominant loss factor in this area. Thus, the measured received power obeys the fourth-power law after the first km, implying that the dominant loss factor is the distance-dependent PL. Additionally, the comparison revealed that only two models accurately anticipated the level of foliage excess loss. Thus, they stated that by combining these excess loss models with PL models, the estimated total PL might be modeled with an RMSE of less than 10 dB. This was achieved using either the Tewari model or combining a 2-Ray PL model with an ITU-R P.2108 clutter loss model. However, for all models compared, foliage excess losses were modeled only from 200 m onwards.

In [171], [172], the authors followed DL or ML approaches to model the PL. Accordingly, [171] incorporated tabular data and images as inputs for CNN to perform PL prediction in urban areas. Hence, the vectors of tabular data were first manipulated and transformed into images, and then each feature was spread across several pixels, proportional to its calculated importance. Then, pseudo images were created by mixing synthetic images (tabular data transformed) with images depicting selected regions of the area's map. The pseudo images were then used as inputs for a CNN that predicts the PL value at a certain point within the considered

area. The results indicated that the presented approach outperforms models using a single input mode.

In contrast, [172] proposed combining two ML algorithms, ANN and Random Forests, with three types of input data to estimate PL for NB-IoT operating at 900 and 1800 MHz. Both approaches were trained and validated using the same sets of area architectural attributes for comparison. It was concluded that data inputs are critical for predicting PL using ML approaches. Further, it was determined that when the transmitter is mounted above the building rooftops, LOS data is more significant than site-specific information, while combining both types of data results in even higher performance. Additionally, for the 900 MHz scenario, PL predictions were more precise for all input types and ML approaches.

Finally, developing a PL model for the deep-indoor scenario is challenging, and existing PL models are inaccurate in such cases. Studies in such scenarios may also be motivated because many critical IoT scenarios, such as telemedicine or the monitoring of important assets, require a robust long-range communication network to perform well. Guarantees of QoS and high availability are also necessary for such harsh radio environments, where tracked objects or patients may move to difficult-to-locate locations, such as a basement. As a result, developing accurate channel models for these scenarios is a major process toward crucial IoT. In this context, the authors of [128] conducted an experimental measurement campaign to determine the attenuation of NB-IoT deep indoor signals at known points.

Additionally, they showed how deep indoor scenarios impacted RSSI and evaluated the effect of indoor distance to the outermost wall on various indoor scenarios. The findings indicated that indoor signal transmission varies significantly between underground and above-ground scenarios. The findings indicated that the 3GPP TR 38.901 indoor PL model accurately predicted the above-ground indoor scenario but mispredicted the underground tunnel measurements. The latter implied that theoretical models are inapplicable to all indoor scenarios, as the overall link budget is far too complicated to be fully characterized by linear dependence. They emphasize, however, that additional experiments are needed to verify this concept.

In comparison, the authors of [173] proposed an empirical outdoor to deep-indoor PL model for NB-IoT at sub-GHz frequencies. The deep-indoor environment considered is an underground tunnel, where distance-related (Tx-Rx distance) and tunnel-related features (such as the closest corridors, the distance and angle to the farthest tunnel corner, and the distances to the tunnel walls and ceiling) were characterized to develop the empirical PL model. It was determined that the 2-D indoor distance and the distance to the tunnel walls are the most relevant parameters for RSRP prediction. A linear and a Gaussian process model were also constructed for the indoor PL prediction. The derived models outperformed the 3GPP TR 38.901 model by 1.8 and 4.1 dB.

In conclusion, few studies have explored the propagation modeling of such cellular-based IoT technologies. These studies focused on specific areas, utilizing experimental hardware equipped with limited omnidirectional Tx and Rx antennas. As a result, additional study is needed to determine the applicability of various existing channel models, propose new models that consider different scenarios and commercially available devices, and assess the limitations of such cellular-based IoT technologies. To summarize the studies evaluated in this section, Table 3 includes a detailed description of each study's modeling approaches, analysis metrics, key findings, and limitations.

B. SHORT-RANGE BASED WIRELESS IoT CHANNEL MODELING AND CHARACTERIZATION

Numerous studies have attempted to provide practical lower bounds on the accuracy of PL model prediction due to the high need for baseline performance values. Additionally, a well-established error bound for more sophisticated PL modeling and coverage mapping approaches is required to verify their accuracy. As a result, the authors in [123] described and implemented 30 different propagation models, considering data from networks operating at 2.4 GHz, 5.8 GHz, and 900 MHz in rural and urban areas. They concluded from the results that the PL model environment is uncertain. As a result, these models' typical best-case performance accuracy is in the range of 12–15 dB RMSE, and it can be substantially worse in practice. However, adjustable models and specific data fitting approaches may reduce the RMSE to 8-9 dB. These constraints on modeling error remain relatively constant over various environments and frequency ranges.

As such, the author suggested using a few well-accepted and well-performing models, such as Okumura-Hata or Hata-Davidson, in scenarios requiring priority predictions, and if possible, well-validated, measurement-driven methods. They emphasize, however, that the most critical concerns for a researcher are having a reasonable expectation of error and picking a model that allows replication and comparison of findings.

As previously noted, most of the PL models currently used in WSN were initially developed to provide signal prediction in conventional high-power wireless systems, such as satellite and personal communication systems, which differ significantly from WSN environments. As a result, the authors in [30], [119] used RF measurements to characterize the propagation behavior of WSNs in outdoor scenarios and subsequently developed an LNSPL-based model. The focus of [30] was on WSN deployed on concrete surfaces, whereas the focus of [119] was on PL modeling of WSN nodes scattered across a sand terrain environment. Both studies compared observed and predicted PL values to those obtained from FSPL, 2-Ray, and models developed for WSNs deployed in long-grass and sparse-tree environments. Reference [30] showed a significant difference in the PL and model parameters between the proposed model, previous studies, FSPL, and 2-Ray models. Additionally, the MAPE was 36% and 22% for the FSPL and 2-Ray models, confirming their inaccuracy

TABLE 3. A summary of the reviewed cellular-based wireless IoT channel modeling and characterization studies.

Ref	Environment/ Scenario	F.	RAT	Targeted application	Modeling approach & used input parameters	Comparison Models	Analysis Metrics	Key Findings	Limitations
[156]	Indoor LOS/NLOS	4.5, 28, 38 GHz	5G	General 5G applications	Hybrid probabilistic PL model based on CI. Use spectrum analyzer power measurements.	Single frequency, CI & FI, and multi-frequency, ABG.	N/A Compare in terms of best fit to PL	Showed that the PL might be modeled more accurately utilizing the proposed model with a single parameter (PLE) than well-known models.	Limited to indoor. Do not consider other indoor models for comparison.
[158]	Indoor LOS/NLOS	40 GHz	5G	General 5G applications	CI & FI parameters calculation. Use spectrum analyzer power.	FSPL (baseline), CI, FI, & 2-Ray.	Use MATLAB for analysis. Metrics are not listed.	Showed that CI & FI are most suitable for indoor PL modeling. FI provides the best minimum error fit.	Limited to indoor. Do not consider other indoor models for comparison. Do not consider multiple floors.
[132]	Indoor LOS/NLOS	3.5, 28 GHz	5G	5G-based smart city	CI, FI, CIF, & ABG model. Use PDP & Rx power from a spectrum analyzer.	Estimated vs. measured data.	RMS-DS, excess delay & PDP. Diffraction loss & frequency drop.	The results indicated that the 5G channel has excellent PL performance and a very small DS, enabling future real-world deployments of 5G-based smart city IoT networks.	Limited to indoor. Do not consider other indoor PL models for comparison.
[159]	Indoor LOS/NLOS	6.5, 10.5, 15, 19, 28, 38 GHz	5G	General 5G applications	CI, CIX, FI, FA, ABG, & ABGX. Use PDP from a spectrum analyzer.	Modeled vs. measured data & previous studies.	RMS-DS & STD.	PL models for single/multi-frequency, RMS-DS, & excess delay statistics were presented and modeled.	Limited to indoor. Different indoor/outdoor & time-varying dynamic environments need to be investigated.
[134]	Outdoor Parking lot	28, 38 GHz	5G	General 5G applications	CI model with a parking lot compensation factor added.	CI, FI, & ABG.	Mean variation in compensation factor.	Showed that more compensation factors are required for more scattering objects, especially at 28 GHz.	Further investigation is required, considering indoor/ underground/ proximity parking environments.
[160]	Outdoor LOS/NLOS	32 GHz	5G	General 5G applications	CI & FI. Use power from a spectrum analyzer.	Measurements vs. CI & FI.	N/A	Investigate the impacts of PL concerning distance, polarization, and antenna type. FI is shown to be unsuitable for NLOS.	No statistical analysis. Limited to indoor & consider only two models.
[161]	Outdoor Tropical urban LOS/NLOS	26, 28, 36, 38 GHz	5G	General 5G applications	Hybrid probabilistic PL model based on CI, FI, CIF, & ABG. Use Rx power from a handheld spectrum analyzer.	CI, FI, CIF, ABG models & modeled parameters from previous studies	STD	Showed that the proposed model is acceptable for considered scenarios	Further investigation is required to incorporate tropical terrain, foliage, and weather impact, especially rain and fog.
[125]	Outdoor LOS/NLOS	38 GHz	5G	General IoT applications	CI & FI.	N/A	N/A	CI & FI were evaluated under several scenarios (LOS V-V, V-H, NLOS V-V). CI predicted significant NLOS outcomes & better network performance in the LOS case. FI is unsuitable for NLOS (V-V).	Simulation-based. Limited for outdoor with no comparisons. To study the influence of various beam-forming effects & analyze their outcome.
[162]	Outdoor Urban LOS/NLOS	38 GHz	5G	N/A	Rain Attenuation. Use PDP from simulation.	N/A	The decrease in Rx power for different scenarios.	Showed that further research is needed to model 5G channels in tropical areas.	Simulation-based with limited analysis.
[166]	Outdoor Urban, suburban, forest, green-/wet-land. LOS/NLOS	2.5 GHz	4G	General	CI & A-B [using P_{Rx}] ANN [use environmental features combined with Tx/Rx information].	Measured PL vs. CI, A-B, & ANN model.	AME, MAE, STD, R, & training efficiency.	The impact of environmental features, ANN architectures, dimension, & training sample percentage on PL prediction models was investigated.	Environmental features cannot accurately reflect propagation characteristics without height information, affecting the PL model prediction accuracy.
[167]	Outdoor Suburban LOS/NLOS	28 GHz	N/A	General	CNN. Extract features from image data sets. Empirical PL is calculated from RSS.	CI & ABG.	RMSE	A feature sharing layer between convolutional layers was added to benefit backpropagation without increasing complexity.	The PL model was developed using a 2-D street map without regard for object heights or vegetation.
[168]	Outdoor Urban LOS/NLOS & O2I.	800-900 MHz	NB-IoT	General IoT applications.	ABG & CI models. Use RSRP.	Okumura-Hata, 3GPP TR 45.820, & UMa. FSPL (baseline).	RMSE, empirical PDF, & statistical distributions like GEV & Weibull.	They claim their models can simulate NB-IoT PL in multi-cell urban deployments like Oslo, improving PL estimation accuracy.	Site-specific, i.e., PL model is limited to Oslo-like urban environments.
[169]	Outdoor Urban city LOS/NLOS	37.8 - 370 MHz	N/A	General D2D IoT	PL / DS models based on log-distance PL model & DS statistical distribution. Use Rx power and APDP.	Statistical analysis & best fit.	PL, DS, RMS-DS, mean excess delay, & cross-correlation coefficient.	Points out that existing VHF/UHF propagation models are unsuitable for IoT communications with low Tx & Rx antenna heights.	Other models are not considered to compare the accuracy of developed models
[170]	Outdoor Rural forest Terrain	917.5 MHz.	NB-IoT	Sports (forest hiking tracking & monitoring).	No PL modeling. Calculate PL from spectrum analyzer power readings.	Measured PL vs. FSPL & 2-Ray models	N/A	Showed that a D2D system with 1.5 m Tx/Rx antennas could reach 2 km using the NB-IoT 164 dB PL limit.	Limited to max distance & PL evaluation. Further research is needed using physical NB-IoT EDs.
[54]	Outdoor Rural forest/ terrain.	917.5 MHz	NB-IoT	Sports (forest hiking tracking & monitoring).	Comparison only & combine PL and foliage excess loss models, Tewari model.	2-Ray, Tawari, FSPL. Above 1km (reasonable loss prediction): ITU-R P833-9, P2108-0, FITU-R. Combined PL between 2-Ray & ITU-R P.1546.	RMSE	The antenna height had no significant effect on the Rx power. The dominant propagation path for the 1st km was through the foliage, resulting in the dominance of foliage excess loss. This suggests a 4th-power law for measured Rx power beyond 1 km. Two models had RMSE less than 10dB: Tewari or 2-Ray combined with ITU-R P.2108.	All models compared only modeled foliage excess losses from/above 200 m.
[171]	Outdoor Urban	900 MHz	N/A	General IoT applications	DL approach. Use a mix of tabular & images data as two diverse inputs types for DL CNN to predict PL.	CNN-based models with single-mode input	MAE	Proposed compound pseudo images as a fusion of transformed tabular & images (area map). Outperformed DL models with single-mode inputs.	Simulation-based. There are no comparisons with conventional PL models. No statistical analysis.
[172]	Outdoor Urban area	900 & 1800 MHz	NB-IoT	General	ANN & Random Forests (RF) based PL models using three input types.	N/A	MAE, RMSE, & mean absolute percentage error (MAPE)	Both ML models performed very similarly. Conclusions: 1) data inputs are critical in predicting PL using ML. 2) LOS data is more crucial than site-specific data when the Tx is located on a building roof, although integrating both improves performance.	No models are considered for comparison. No experimental data (ray-tracing simulations only). Limited description of simulation parameters.
[128]	Deep Indoor Indoor to Outdoor (I2O)	820.5 MHz	NB-IoT	Remote metering or asset tracking	Modeled based on a simple I2O model. Use RSSI.	3GPP TR 39.901	Power heatmap & RSSI vs. distance.	Showed the impact of deep indoors on RSSI & analyzed the impact of indoor distance to the outermost wall. 3GPP TR 38.901 well-matched the above-ground indoor scenario but not the underground tunnel. Thus, theoretical models may be unsuitable for all indoor scenarios.	Limited to RSSI measurement with no calibration. Considers one model for comparison, and there is no statistical analysis. Do not provide Tx power, antenna specs, and height of Tx & Rx.
[173]	Deep-indoor	868 MHz	NB-IoT	Underground scenarios	Linear regression & Gaussian process (GPR). Use RSRP measurements with a set of distance & tunnel-related features.	3GPP TR 38.901 [UMa].	RMSE & MAE.	Showed that the 3GPP distance-based model fits fairly well NB-IoT measurement above the ground while performs poorly in underground deep-indoor scenarios.	Need more data in diverse scenarios to improve model accuracy, including more environment features, obstacle distribution, & detailed tunnel geometry.

in predicting PL in concrete surface environments. Similar outcomes were reported in [119], indicating that the compared PL models were inaccurate in sand terrain. However, the proposed model does not consider the electrical ground properties of sandy terrain or the placement of Tx/Rx at various heights.

In contrast, [62], [71], [139] analyzed the influence of foliage attenuation on wireless signal and the applicability of existing PL models in a variety of scenarios. The authors of [71] studied signal attenuation in a rice field environment at node antenna heights of 0.8 m, 1.2 m, 1.6 m, and 2.0 m during the tillering, joining, and grain filling stages of rice fields. Also, they evaluated PL fluctuation over a range of distances and compared the measured PL to the predicted PL using FSPL and a 2-Ray model. Then, a one-slope log-distance model was established using regression analysis, and a modified two-slope log-distance model was proposed.

The authors of [139] analyzed and developed a new linear regression model for predicting PL in greenhouse environments. A combination of foliage effects, reflections (from the ground or tree canopy), diffraction, and traveling wave scattering were used to model propagation loss. Numerous empirical measurements were done at 2.425 GHz utilizing an IEEE 802.15.4-based WSN to determine the influence of growing tree components on PL at various Tx/Rx heights. Finally, [62] analyzed experimental data from a real-world ECOMESH test-bed in a native woodland environment, emphasizing propagation issues in a dense foliage area and along a pathway over four vegetation growth seasons. Several theoretical and empirical foliage models were evaluated, including the FSPL, Fresnel, 2-Ray (PE), W MED, COST-235, and FITU-R models. Then, two empirical models were developed to predict the performance of network attenuation in two different scenarios.

The results in [71] indicated that node height significantly impacted channel propagation characteristics and feasible transmission distance, with RSSI decreasing monotonically as antenna height was changed. Additionally, the wireless channel transmission environment deteriorated concerning the developmental stage of the rice field. As a result, the optimal node antenna height was found to be 2 m above ground. While FSPL was shown to be inappropriate, the 2-Ray model may be used if the antenna height exceeds 1.2 m, as height significantly impacts the 2-Ray model prediction. On the other hand, the one-slope log-distance model performed better, although its estimated relative error (RE) was greater than 3%. Finally, the modified two-slope log-distance model outperformed the one-slope log-distance model in all heights, with an estimated RE of less than 2%, and was more applicable to the complicated rice field environment. As a result, the authors claim that the latter will aid in developing efficient rice field WSNs while also improving the quality of wireless transmission.

The results in [139] indicated that the most important vegetation effects occur at 1.5 m tree height. Likewise, the results proved that PL prediction using FSPL and 2-Ray models is inaccurate in certain environments due to their simplistic and optimistic nature. Additionally, results indicated that the combined COST-235 and FSPL models provided the best results compared to other foliage models. However, the latter model is not ideal, as the MAPE was 10.69%. In contrast, the proposed model MAPE has a MAPE of 2.75 %, suggesting that it is the most efficient model for representing greenhouse vegetation loss. Finally, the authors noted in [62] that a proper propagation model, such as those proposed, that enables network performance evaluation enables QoS optimization and can be used as part of a QoS guarantee management platform for native Irish trees and dense woodland applications.

The authors in [104] proposed a channel model for rural smart agricultural WSNs operating in near-ground conditions in the soil, short grass, and tall grass fields. The measurements considered Tx and Rx antennas mounted at 0.2 and 0.4 m above ground and utilized three frequency bands, 868 MHz, 2.4 GHz, and 5.8 GHz. The PL was then calculated and adapted using a three-slope log-normal PL model. The second experiment used RSSI measurements from commercial ZigBee nodes at 2.4 GHz to predict link performance. Accordingly, two sensor nodes were mounted at identical heights to those in the previous experiment, but only in a short grass field scenario. The QoS efficiency was estimated using theoretical BER values for various digital modulations. It was indicated that the Tx-Rx separation could be divided into three regions, defined by two critical points and a break or cross-over point. According to the QoS analysis, the near-ground scenario was more constrained than an obstructed LOS. As a result, it may be necessary to use more robust digital modulation schemes or error correction codes to suit the performance of LOS-based networks. The consequence of more accurate characterization and formulation of near-ground systems would be a significant improvement in their applications, particularly in the near future of 5G-IoT.

The focus of [70] was on the effective deployment of wireless sensors for applications such as tracking cow grazing behavior on grass or track sporting events. As such, an LNSPL-based model was proposed, considering experimental data from natural, short, and tall-grass fields. The empirical PL models were then compared to theoretical PL models such as FSPL and 2-Ray. The findings indicated that theoretical models differ by 12% to 42% from proposed models. Compared to the proposed model in the short grass field, measured data from comparable environments revealed a MAPE of 1.1% and a Ts of 5.6. As a result, they concluded that theoretical models are inappropriate for estimating the PL for WSN application in dense grass fields with a height of less than 1 m. Additionally, comparisons to similar past studies indicated a significant difference in PL and the parameters of empirical models.

In addition to prior work, the authors of [44] highlight that there are currently no accurate and reliable propagation models that ensure the successful and practical deployment of IoT devices in mountainous terrain. As a result, they examined the effect of mountain terrain on the efficiency of tracking

devices and wireless sensor nodes, conducting measurement campaigns involving IoT devices operating at 900 MHz and 2.4 GHz. They then proposed and compared log-distance-based PL models to FSPL, 2 Ray, and log-distance PL models. A variance of 8 dB to 38 dB was observed, indicating that such models significantly underestimated the performance of IoT systems in such environments. Additionally, tests revealed that mountains and rocks cause an average signal loss of 8 dB. As a result, it was concluded that existing models are unsuitable, and some are proposed based on FSPL and 2-Ray models to support high-power systems in a tree or wooded areas.

In order to analyze and enhance RSSI-based PL models, the authors in [117] identified several factors that have an undeniable negative influence on measured RSSI and, thus, on the performance of derived PL models. They classify these factors as intrinsic, resulting from transceivers, connectors, antennas, or extrinsic, resulting from the number of measurements, coexisting interfering devices, packet length, ED battery level, temperature, and environmental impacts. As a result, a set of adjustment models and computational procedures was developed to resolve the disturbances above for three well-known technologies: MicaZ, Iris, and Waspmote. They then compared two RSSI-derived models (a base model, LNSPL, with no adjustments to raw RSSI measurements and an adjusted model, using proposed tools and procedures) to an electrical substation ground-truth VNA-based PL model. The average prediction error was reduced by around 91.76 %, indicating a significant improvement in network simulation accuracy. As a result, operational expenses are reduced and estimating quality and network planning for critical industrial environments are improved. Overall, the findings indicated that when intrinsic and extrinsic RSSI-affecting variables are included, RSSI-based models can be useful, precise, and cost-effective for WSNs.

Finally, [114] aimed to determine the distance between a bicycle and a coach using a mobile ZigBee sensor node and a ZigBee anchor node in outdoor and indoor scenarios. Due to the difficulty of precisely calculating the location of a mobile node due to channel impairments caused by multipath, NLOS, fading, or other interference issues, they consider two methods for estimating distance. The first method was based on LNSPL, whereas the second method used a proposed hybrid particle swarm optimization–artificial neural network (PSO–ANN) algorithm to improve the accuracy of distance estimate. The LNSPL parameters were estimated using RSSI measurements in outdoor and indoor scenarios. The distance between the mobile and coach locations was then computed using the hybrid PSO-ANN and LNSPL algorithm to optimize the precision of the predicted distance. The results indicated that when compared to LNSPL and previous works, the hybrid PSO-ANN algorithm significantly improved distance estimate accuracy. Additionally, the hybrid PSO-ANN algorithm achieved an MAE of 0.022m and 0.208m for outdoor and indoor scenarios, respectively.

As in the previous sub-section, we summarize the reviewed studies in this sub-section, as shown in Table 4, with a detailed description of each study's modeling approaches, analysis metrics, key findings, and limitations. In conclusion, it is worth noting that most of the research covered in this sub-section either evaluates the performance of these wireless systems in terms of coverage and propagation limits or proposes channel models based on relatively simple models such as 2-Ray, FSPL, and LNSPL. These studies were mostly limited to near-ground deployment scenarios utilizing low-power omnidirectional antennas. Furthermore, none of the studies reviewed considered more complex propagation scenarios or evaluated other models available in the literature, such as deterministic ray-tracing-based models. As a result, it can be concluded that more study is needed to assess the suitability of alternative models for diverse implementation scenarios, such as the influence of different Tx/Rx deployment heights and varied, challenging climate conditions, to examine the full boundaries of such technologies and propose more accurate models.

C. LPWAN BASED WIRELESS IoT CHANNEL MODELING AND CHARACTERIZATION

In recent years, the rapid expansion of ICT and the rapid development of new technologies have increased the importance of rapid and accurate planning and deployment of emerging LPWAN wireless IoT technologies [148]. However, such technologies' success relies on signal propagation robustness, especially in complex terrain and irregular elevation profiles [52], [174]. For example, LoRa offers a wide range of coverage options; it can span hundreds of meters or tens of kilometers, depending on its surroundings and the factors influencing its performance directly [118], [126], [175]. In contrast, widely used LoRa channel models do not identify this high variability, and typical on-site measurement options are inaccurate given the huge geographic areas covered [118], [126]. As a result, several studies have been undertaken in this domain.

For instance, [22] described two smart city testbeds developed in Italy for public lighting based on IEEE 802.15.4 and smart buildings based on LoRa. The latter was then investigated using measurement campaigns and simulations to assess LoRa's coverage and performance in an urban scenario. Similarly, in [25], the authors analyzed the feasibility of using LoRa-based WSNs in smart public transports to collect pollution data and meteorological parameters. They also investigated propagation and network architecture for possible practical network realization.

According to [22], LoRa's maximum coverage in dense urban areas was 1-2 km, far less than the 15 km claimed by manufacturers and vendors of LoRa. This record was achieved in favorable conditions, with a GW height of 71 m AGL and the highest SF. Coverage is expected to be reduced even further if such criteria are not fulfilled. Finally, the findings indicated that it is wise to deploy several LoRa GWs

or equip a single GW with multiple receivers, operate on multiple channels, and use a larger SF to cover larger areas. The analysis in [25], on the other hand, showed that the proposed WSN is suitable for integration in a city's public transportation network since theoretical propagation performance, based on the Okumura-Hata model, shows that LoRa delivers adequate outdoor urban coverage areas. As a result, they concluded that the experimental results would provide significant indications concerning the deployment of LoRa and testing on propagation and networking while accounting for the Doppler effect.

In contrast, the authors of [26] used commercial LoRa devices to determine and analyze LoRa coverage in Oulu, Finland. Measurements were made utilizing a node on the ground, mounted to a car's roof rack, or on the water, mounted to a boat's radio mast, transmitting data to a GW. They then presented an LNSPL-based model for the 868 MHz band at 14 dBm Tx power and maximum SF. Results showed that the PLE for the on-ground scenario was greater than the PLE for the FSPL scenario due to the presence of buildings and other obstacles in the path between the end device and GW. Meanwhile, for the boat scenario, it was 1.76, below that of FSPL.

Interestingly, they achieved higher coverage ranges, reaching over 15 km on the ground and nearly 30 km on water. However, they found that for on-ground, the PDR tends to be high, over 80%, for ranges up to 5 km then degrades for higher ranges, being lowest for more than 10 km. Meanwhile, PDR was nearly 70% at distances under 15 km for the water scenario. Finally, they claimed that network operators could utilize the derived model to estimate the needed GW density and enable precise LoRa performance analysis.

In [126], the authors presented an automated method for estimating post-deployment coverage of LoRa GWs in outdoor environments without on-site measurements by integrating free multi-spectral images from remote sensing with the correct channel model. The method automatically classifies the type of environment (such as buildings, trees, or open fields) penetrated by a signal with high precision (∼90%) and spatial resolution. The focus was on the empirical Okumura-Hata model, showing that its predictions are close to their observations and that their method can automatically select and configure its parameters. Additionally, the results showed that their approach closely estimates expected signal power (ESP) within a 10 dB error, compared to a 20 dB to 40 dB errors for widely used channel models. Nonetheless, the model ignores the impact of walls when GWs are placed indoors and ignores other signal-influencing parameters (e.g., physical parameters).

In contrast, [176] evaluated the RSSI accuracy of two LoRa chipsets in a laboratory environment. The Longley-Rice Irregular Terrain Model (ITM) was then simulated and evaluated using SPLAT, a software tool, with real-world Digital Elevation Map (DEM) resolution of 1 arc-second (∼30 m) to predict PL. An extensive measurement campaign was conducted in Germany's outdoor suburban environment to verify ITM prediction accuracy and compare it to FSPL as a baseline model and the log-distance-based models proposed in [177] and [26]. The result indicated that there is no perfect model for all environments. Further, the results showed that the chipsets reported significantly different RSSI and terrain data improves prediction accuracy. Finally, they concluded that conventional terrain data-based PL models, predominantly used for mobile or TV broadcasting, cannot be used for LoRa wireless technology.

Researchers in [31], [52], [118] provided a detailed evaluation of the LoRaWAN channel at 868 MHz for various scenarios. Accordingly, [118] conducted detailed measurement campaigns for indoor and outdoor scenarios in Lebanon's urban and rural environments. They then proposed a set of PL models and evaluated their accuracy against commonly used empirical PL models. These models include; (1) ITU-R, COST 231-MWF, 3GPP's Cellular-IoT models for indoor scenarios and (2) Okumura–Hata, COST 231-Hata, and 3GPP-UMa/RMa for outdoor scenarios. They observed that the proposed PL models are better, accurate, and simple to apply in the study area or similar places.

Meanwhile, results showed that a coverage distance of up to 9 km and 47 km could be obtained in urban and rural areas, respectively. The ITU-R model showed lower precision for indoor scenarios with a mean error and standard deviation error of 0.48 dB and 8.3 dB, respectively. Similarly, Cost 231-MWF and 3GPP models underestimated the measured PL and reported a standard deviation error of 8.7 dB and 10.2 dB, respectively.

In [52], the authors provided a detailed performance analysis in urban, suburban, and rural environments. Various PHY layer settings were studied to evaluate the most suitable one based on propagation conditions. Next, they took a different approach, assessing the predicted signal strength in these scenarios using an RF planning tool (Cloud-RF) that uses topographic maps and the Okumura-Hata model. Then, an extensive measurement campaign validated the theoretical findings. In urban and suburban scenarios, coverage ranges of about 6 km were obtained, while a long transmission range of over 18 km with the lowest data rates (DRs) was obtained in the rural scenario. Hence, it was concluded that there is a clear trade-off between link reliability and DR (and therefore packet time-on-air); thus, the LoRaWAN configuration parameters must be adjusted appropriately, based on the propagation conditions and the range between GW and EN. Finally, they examined the same scenarios but in a stationary condition to evaluate the mobility impact on performance, which indicated that LoRaWAN poses a significant Doppler-related vulnerability if using high DRs; however, this impact was far less evident when using low DRs. It was concluded that it is essential to review the deployment scenario's propagation conditions before actual implantation to reach a compromise between network reliability and transmission DR.

In comparison, [31] examined the impact of seasonal weather changes on the signal-to-noise ratio (SNR), RSSI, and SF usage while enabling adaptive data rate (ADR).

TABLE 4. A summary of the reviewed short-range based wireless IoT channel modeling and characterization studies.

Ref	Environment/ Scenario	F.	RAT	Targeted application	Modeling approach & used input parameters	Comparison Models	Analysis Metrics	Key Findings	Limitations
[123]	Outdoor Rural, urban, & suburban. PTP & mesh.	2.4 & 5.8 GHz, 900 MHz	Wi-Fi	General	Comparative (no modeling). Use RSS with some calibration.	30 models, including foundational, basic, supplementary, & terrain models.	RMSE, SC-RMSE, competitive success, accuracy, skewness, rank correlation	Implemented 30 common models. Showed that a limited no of readings can be used to tune & fit basic empirical models. Overall, Okumura-Hata & Hata-Davidson are top performers.	Do not consider ray-tracing models or indoor scenarios.
[30]	Outdoor LOS/NLOS	1.925 GHz	N/A	WSN deployed on a concrete surface.	LNSPL model. Use RSSI.	FSPL, 2-Ray, & two empirical models for long grass / sparse tree.	Average, STD, absolute percentage error (APE), R^2, MAPE.	The PL and empirical models' parameters differed significantly. FSPL & 2-Ray proved to be inaccurate for concrete surfaces.	Modeling is based on simple linear fitting. Do not consider large distances. Mostly LOS.
[119]	Outdoor Sand terrain. LOS (daytime).	1.925 GHz	N/A	General WSN applications in sand terrain.	Linear regression to model LNSPL. Use RSS.	FSPL, 2-Ray, & two empirical models for long grass / sparse tree.	R^2, APE, & MAPE.	Showed the inaccuracy of FSPL & 2-Ray in predicting PL between WSNs deployed in sand terrain.	LOS only. No details on P_{Tx} & Tx/Rx height. Neglect sandy electrical ground properties.
[71]	Outdoor Rice field. Partial LOS.	2.4 GHz	ZigBee IEEE 802.15.4	Agriculture monitoring	One-slope log-distance & propose a modified two-slope log-distance model. Use RSSI.	FSPL, 2-Ray, & one slope log-distance model.	RMSE & RE.	Node height impacted the propagation. The modified two-slope log-distance performed better & claimed to be usable for WSNs in rice fields.	Neglect obstacles, terrain, & weather impact. The study was conducted in a flat rice field during sunny days only.
[139]	Greenhouse environment.	2.4 GHz	ZigBee IEEE 802.15.4	Mango greenhouse monitoring	Linear regression curve-fitting. Use RSSI.	FSPL, 2-Ray, log-distance, W MED, ITU-R, & COST 235.	APE & MAPE.	Foliage models used in conjugation with FSPL & 2-Ray are inaccurate in predicting PL in a greenhouse.	Few considered scenarios. Use a simple linear curve fitting method.
[62]	Outdoor Dense vegetation.	2.4 GHz	IEEE 802.11 & 802.15.4	PA IoT applications	Empirical foliage models. Use Rx power from a spectrum analyzer.	FSPL, Fresnel Zone, PE, W MED, COST 235, & FITU-R.	RMS power, R^2, & P-value statistics.	States that a proper propagation model for network performance evaluation enables QoS optimization.	Need further evaluation, considering other signal influence factors.
[104]	Outdoor Rural (soil, short & tall grass field).	868 MHz, 2.4 & 5.8 GHz	ZigBee	Smart agriculture	Three slop Log-Normal PL model. Use spectrum analyzer power & RSSI for 2.4 GHz (commercial ZigBee).	FSPL & few previous studies PL model.	Analyze the first Fresnel zone obstruction.	Indicates that Tx-Rx separation could be divided into three regions, defined by two critical points and the break or cross-over point.	Terrain, weather, and NLOS impact are not considered. Only a few models are compared.
[70]	Outdoor Short & tall grass. Mostly LOS.	2.4 GHz	ZigBee	Monitor grass growth. Smart irrigation system.	LNSPL. Use RSSI.	Measured vs. proposed, FSPL, 2-Ray, & a few similar studies.	R^2, P-value, F-value, & α-level statistics. MAPE, Ts, MSE, RMSE.	2-Ray is unsuitable for WSN. Theoretical models differ by 12-42% of proposed models and cannot estimate PL in dense grass fields (≤1 m).	Need to consider the casing, electrical properties of grass, terrain, ground, & weather effect on propagation.
[44]	Outdoor Rural (rocky & mountainous terrain).	900 MHz & 2.4 GHz	ZigBee IEEE 802.15.4, & LoRaWAN	IoA (wildlife), D2D/D2M SAR, military, hiking sports.	Log-distance PL model. Use RSSI.	FSPL, 2-Ray, & log-distance PL model.	Mean, MSE, RMSE, MAPE, and P-values.	Having precise PL models saves power, improves node localization, reduces interference, and increases network capacity. Mountains and rocks reduce the signal by 8 dB.	The electrical properties of mountains and rocks were ignored. More study is needed on different empirical/ray-tracing models and IoT RAT.
[117]	Outdoor LOS/NLOS	2.4 GHz	IEEE 802.15.4	IIoT (smart grid).	LNSPL. Use raw & corrected RSSI to derive two models for each platform.	Compared against a ground truth LNSPL derived from high-end VNA measurements.	MSE, RMSE, mean network delay, & mean network lifetime.	RSSI-based models could be useful, precise, & cost-effective when including intrinsic & extrinsic RSSI-affecting variables. The proposed scheme improves real-world SG characterization accuracy.	Limited to the outdoor scenario & do not consider ray-tracing models. Do not provide details of mounting height of used equipment and Tx power.
[114]	Outdoor & Indoor. Cycling fields.	2.4 GHz	ZigBee IEEE 802.15.4	WPAN (localization of cycling sports)	LNSPL. Use RSSI.	Compare distance estimation accuracy against related studies.	R^2, RMSE, MAE to assess predicted distance accuracy	Used hybrid PSO-ANN & LNSPL to model the outdoor/indoor propagation & improve the estimated distance.	Do not consider other PL models. Highly dependent on RSSI.

Additionally, they evaluated Okumura-Hata and ITM models using Cloud-RF to see how they fit real-world measurements. They observed that results gain from cold weather since low temperatures increase noise intensity, resulting in a higher SNR. In contrast, the battery drains more quickly in cold temperatures. Further, the findings indicated that the combination of long distances and snow negatively impacted LoRaWAN performance. As a result, snow must be considered while designing the deployment of sensors and GWs to reduce the effect of snow on signal transmission. When measured RSSI was compared to Cloud-RF predictions, Okumura-Hata was the best, whereas the ITM model seemed to overestimate RSSI. As a result, they indicated that propagation models should be optimized by taking weather into account when tuning the models. It was also concluded that temperature should be considered while designing a LoRaWAN implementation strategy due to its effect on battery life, propagation conditions, and noise behavior, all of which impact coverage and transmission rates.

In contrast, [178] evaluated the P2P LoRa coverage and proposed a log-distance-based PL model based on measurements conducted in urban, forest, and coastal areas, utilizing low-height nodes of 1.5 m at 868MHz. The PER was then computed based on the predicted PL parameters to quantify P2P link quality. In all scenarios, 80% of the data were successfully received at around 200 m. While, for the LOS scenario, a range of over 4 km was achieved. Given the urban scenario's unfavorable radio propagation and heavily forested areas, a 1 km distance was achieved. They observed relatively high variation around the standard deviation (σ) of shadowing samples in the coastal area due to handheld device usage, resulting in higher PER at shorter distances. They also indicated that the Okumura–Hata model significantly overestimates PL, whereas the modified Cost 231-Hata model and the model derived in [26] underestimated PL. They also observed that the aligning trees acted as waveguides yielding a PLE near the PLE of FSPL for the forest scenario. Finally, the derived PL model based on a maximum-likelihood approach outperformed the least-square method and existing empirical models for all studied environments.

Authors in [175] performed an experimental study to evaluate the performance of LoRa by considering various topographical areas on-campus sites and discussing impacting factors such as the Doppler effect, Fresnel zone, environmental factors, and interference. The results indicated that the GW location, environmental scenarios, and topology must

be considered during deployment to improve performance. Furthermore, an outdoor experimental study was performed to test LoRa's coverage and performance, based on RSSI and PDR, by applying different SF in different terrain and environmental scenarios. The findings indicated that terrain impacts LoRa signal propagation, limiting coverage and reducing PDR by half.

In [127], the authors evaluated the RSSI measurements of the LoRaWAN network implemented in Skelleftea, Sweden. Then, they compared it to data obtained from Cloud-RF based on ITM, Irregular Terrain with Obstructions Model (ITWOM), and the Okumura-Hata model. These models were used since Okumura-Hata is a well-known model for large cellular networks, while ITM and ITWOM are recommended by the planning tool. The data were obtained from five sensors mounted along a wooden bridge with various SF configurations (7, 10, and 12). Hence, results showed that ITWOM accuracy was nearest to measured values due to ITWOM improvements that include the adoption of Radiative Transfer Engine (RTE) rather than the classical theory of diffraction. They, therefore, concluded that ITWOM performed the best, followed by ITM and then Okumura-Hata. However, the study considered only outdoor scenarios and did not consider SNR values to infer channel conditions. The study also indicated that terrain profile, environment, and transmission distance are significant when selecting a planning tool's specific propagation model.

To run WSN all year round and provide a comprehensive communication range of several tens of kilometers, authors of [179] used LoRa technology in Antarctica's outdoor polar area to implement these nodes with minimal power consumption. They studied the system propagation channel conditions within 30 km of the Belgian Princess Elisabeth Antarctic Station. Hence, they verified the usefulness of LoRa technology in polar regions and found that installing directional antennas at the BS would achieve a maximum range of 30 km in both the 434 MHz and 868 MHz bands for the LOS scenario. Besides, the dominant factor affecting propagation was varying terrain elevation, often obstructing the LOS path. Finally, they suggested that NLOS links are possible but require field measurements or ray-tracing simulation to determine optimal antenna locations.

In [148], the authors explored the Lee propagation model's potential use and optimization for 868MHz LoRa network planning, design, and management. The analysis was based on RSSI field measurement comparison with model calculations. Hence, based on results, RMSE averaged 6.71731 dB for Tokyo, 15.0949 dB for Philadelphia, and 19.5495 dB for Newark. These analyses showed the accuracy of the Lee PL model for urban areas. Nonetheless, they point out that further measurements and comparisons with the Lee model should be carried out.

In contrast, the authors in [180] evaluated foliage attenuation and its overall contribution to PL and link budget estimates. Accordingly, the attenuation impact of five tree types was studied for different path crossings (e.g., trunk, tree-top, and branches). For this evaluation, the Okumura-Hata, LNSPL, and foliage models were used as references. Both LOS and NLOS (across tree) tests are considered through RSSI measurements for horizontal and slant paths. After that, both horizontal and slant paths RSSI reading over a tree are taken. Various measurements also determined LoRa communication coverage in a campus area. They found that the Mimusops Elengi tree, characterized by its large size and leaf density, provided the highest foliage attenuation of up to 20 dB. Trunks showed higher attenuation than tree-tops and branches. The study also showed that the Okumura-Hata model failed to capture the foliage effect compared to measurements. However, the study did not consider the effect of thick foliage, especially in a dense jungle area, where attenuation is expected to exceed 20 dB. Also, it does not consider other impacting factors such as weather and being a limited evaluation based purely on RSSI measurements.

On the other hand, the authors in [181] evaluated LoRaWAN propagation in an outdoor-indoor scenario based on RSSI measurements and compared it to commonly used propagation models such as log-distance and indoor COST231-MWM models. They also adjusted the COST231-MWM model for better accuracy. However, these models did not accurately estimate outdoor–indoor propagation characteristics. Thus, a novel hybrid propagation estimation method was developed and examined. This hybrid model consists of ANN and an Optimized COST231-MWM, thus showing higher predictive accuracy and reduced initial COST231-MWM MSE from 21 to 11.23.

Similarly, for LoRa channel characterization and link performance analysis, an autonomous LoRa-compatible node was presented in [182] for both 434 MHz and 868 MHz bands. They showed that the LoRa node provided a significantly more extensive dynamic range by applying stepped attenuators controlled by a dynamic attenuation adjustment algorithm. The node was calibrated to accurately measure the received signal power in dBm based on SNR measurements. Findings showed a correlation between a sudden drop in signal and an event of rainfall, whereas outdoor temperature fluctuation showed no correlation with measured signal levels. Finally, indoor measurements showed that people's presence in a building also has a measurable influence on the LoRa link quality, where 2 dB and 3 dB difference in standard deviation values were found between day and night measurements, respectively.

Different buildings have different communication constraints due to varying sizes, shapes, and structures. Therefore, the authors in [28] conducted a detailed study to investigate the large-scale fading characteristics, temporal fading (TF) characteristics, coverage, and energy consumption of LoRa technology in four types of multi-floor buildings. They also conducted an RSSI adjustment experiment and observed a constant 2 dB shift between the measured RSSI of the LoRa node (mDot) and spectrum analyzer-measured RF power. The PL characterization results showed that a non-fixed intercept model has significantly larger

intercept PL(d0) and smaller PLE than the fixed intercept model. Also, standard deviations for non-fixed intercept and fixed intercept fit well, although it is somewhat larger for a fixed intercept. Therefore, concluding that using a non-fixed intercept PL model is better than using a fixed-intercept model. A Kolmogorov-Smirnov (K-S) goodness-of-fit test was conducted on one-slope shadow fading samples to determine log-normality.

They concluded that a one-slope PL model can estimate PL in indoor scenarios but can only be used as a first-order prediction. Hence, they indicate that an attenuation factor (AF) model is needed to attain more accurate PL prediction in a multi-floor building. A site-specific model should also be considered since building materials, structure, and other factors could significantly affect the PL. Also, the decorrelation distance in a multi-floor building is small, suggesting that the large-scale fading is almost independent of one area to another. Results also showed that TF met a Rician distribution with Rician K-factors of 12 dB to 18 dB. Hence, link budget analysis should consider a fade margin of 9 dB and 7 dB for tested scenarios. The study also showed that energy consumption would vary up to 145 times, using different parameter configurations. Such results highlight the importance of selecting parameters and enabling LoRa's adaptive data rate feature in energy-limited applications.

Moving forward, the authors in [40] presented measurement campaign results to evaluate empirical characterization and mathematical modeling of the radio channel for a wearable LoRaWAN node for different operating ranges across different environments such as urban, suburban, and rural. Furthermore, anechoic measurements were also carried out to evaluate body shadowing effects for this technology. Findings showed that the best fit model for all measured received signal strength, using the Akaike information criterion, is the Nakagami distribution with mu $= 0.52$ and $\Omega = 662.13$. Furthermore, anechoic measurement showed typical additional effects regarding the user orientation concerning the GW location.

As mentioned in previous sections, advances in wireless sensor technology and MEMS have enabled dairy cow health conditions to be monitored remotely using the IoT and WBAN. While on-cow measuring devices are energy-constrained, adequate characterization of the wireless off-body link between the on-cow sensor nodes and the back-end GW is needed for the improved operation of these networks in barns. Thus, authors in [74] characterized the 868 MHz off-body wireless channel for dairy cows in three different barns. LoRa motes investigated both PL and TF. RSSI calibration was also performed, resulting in a constant 6dB adjustment between measured RSSI and actual RF power. Results showed that a one-slope LNSPL model could be suitable for the large-scale fading characterization. It was also shown that the maximum PL increase of around 4 dB resulted from the cow body wearing the sensor node.

Meanwhile, other cows had less influence of about 1 dB. The TF was statistically characterized by Rician distributions with an average K-factor of 8 dB. Finally, the authors claim that study findings could enable reliable IoT cow monitoring systems with optimized network planning and energy consumption.

In contrast, in [75], the authors characterized the in-to-out body PL between an antenna inside the cows' rumen and a specific GW at 433 MHz. Measurements were conducted on seven different fistulated cows using a signal generator and a spectrum analyzer. Later free space antenna measurement was conducted to evaluate PL increase due to the cow body. Results showed an average PL increase of 45.5 dB (all cows), with 39.7 dB and 51.1 dB variability. Also, an LNSPL model matched the measured PL as a transmitter-receiver distance function in a dairy barn. The observed models were then used to evaluate a LoRa-based network range. Therefore, using the highest LoRa transmit power of 20 dBm, the range reached up to 100 m with the least DR, whereas using the highest DR, the range was limited to 11 m. Therefore, they concluded that coverage could be increased by using a lower DR with a higher transmit power while reducing the battery life and data collected.

The authors in [183] proposed a LoRa-based positioning algorithm for search and rescue operations in the mountain environment. The positioning algorithm was developed based on the PL measurement. Hence, a PL model was developed according to the measured SNR and RSSI. The measurements were conducted in three relevant mountain scenarios: canyon (with maximum width, length, and depth of 40 m, 8 km, and 400, respectively), LoRa Tx over the snow, and Tx buried under 1 m of snow. In measurements, Tx was fixed and placed on/under the ground (depends on the considered scenario), and Rx was mobile and put inside a volunteer's jacket. For the measurements, two LoPy-4 expansion boards were used that operated in the 868 MHz frequency band with a bandwidth of 125 kHz, spread factor of 7, the coding rate of 4/5, and Tx power of 14 dBm. The results showed that although the communication range of LoRa decreased from kilometers to hundreds of meters, the operation range of the proposed method is at least five times greater than the golden standard technologies such as ARVA.

Wireless underground communication (WUC) has numerous ecology, agriculture, health care, and environment preservation applications. However, the propagated signal is severely attenuated as it travels across the ground due to the soil composition. Hence, a PL prediction model would play a vital role in designing a WUC system. In [184], the authors proposed a WUC PL model for precision agriculture, in which, first, the underground communication was simplified to a generic model. The developed model was then integrated with an accurate prediction of the complex dielectric constant (CDC), called the Mineralogy-Based Soil Dielectric Model (MBSDM). The integrated method can predict PL in different scenarios, underground-to-underground (UG-UG), underground-to-aboveground (UG-AG), and aboveground-to-underground (AG-UG). The PL model considers reflective and refractive wave attenuation according to each scenario's

sensor node burial depth. To further validate the reliability of the proposed method, intensive experiments were conducted in a real environment with two different pairs of wireless transverses, nRF905 and LoRa SX1278. The results showed that the proposed model outperforms the existing PL models in different communication types and soil conditions, where the proposed model can be used on a real cheap sensor with 87.13% precision and 85% balanced accuracy.

On the other hand, [60] presented the PL analysis of underground wireless communications in urban UIoT for wastewater tracking. They demonstrated that an underground transmitter, communicating through a 10 cm thick asphalt layer, could achieve a range of up to 4 km with PL less than 100 dB and 10 km with PL of 107 dB. The propagation loss was also less than 5 dB with a layer thickness below 1 m. However, as the layer thickness increases, it can reach up to 15 dB for the 4 m asphalt layer. It was also observed that RSSI drops with distance, with dramatic drops for distances below 2 km. It decreases gradually afterward. Finally, at a communication distance of 4 km, the −80 dBm RSSI demonstrates that underground devices in urban UIoT could communicate effectively with urban roadside wireless communication infrastructure.

Finally, for Sigfox devices, their location is predicted and stored on the Sigfox cloud platform. However, the location prediction accuracy is unsatisfactory, where, in some cases, the distance error between predicted and actual location may exceed 20 km or 30 km, with average distance error ranging from 2 km to 10 km, as indicated by authors of [185]. Accordingly, they proposed a new ML-based localization method to estimate the Sigfox device location. The method divides the area around each BS into a few sectors and trains a more precise PL model, based on LNSPL, for each sector to represent their site-specific multipath propagation environment. Hence, the proposed method used RSSI measurements and a multi-sector training and predicting method with four 90-degree sectors. The experimental data observed in a big city utilizing 30 Sigfox devices showed that the proposed method's maximum distance errors are often smaller compared to the official localization service of Sigfox.

As in the previous sub-section, we summarize the reviewed studies in this sub-section, as shown in Table 5, with a detailed description of each study's modeling approaches, analysis metrics, key findings, and limitations.

In conclusion, it can be noted that among the several LPWAN technologies, LoRa/LoRaWAN has gotten the most interest from researchers because of its unique characteristics. As a result, most studies evaluated this technology's performance and proposed channel models for various deployment scenarios. However, these studies mostly used simple models like LNSPL and Okumura-Hata models and primarily focused on urban and suburban implementation scenarios. As a result, we anticipate a significant gap in channel modeling and characterization for these technologies, particularly in areas with complex terrain and harsh climate conditions, such as tropical regions. Although some studies considered utilizing more accurate ray-tracing methodologies or simulation tools, these did not explore the entire limitations of LPWAN technologies. On the other hand, the low-resolution maps available limited most of these studies, making them site-specific and impractical for reuse in other deployment areas.

In this regard, many future work directions may be possible in wireless channel modeling and characterization for LPWAN technologies. Among these, it is believed that measurement-based and comparative analysis studies are of utmost desire to understand such technologies' behavior environments accurately. Other modeling approaches may incorporate new ML-based and hybrid prediction approaches that combine well-known stochastic or deterministic modeling techniques with ML. Nonetheless, any of these approaches may provide a tremendous opportunity, with the potential to have a significant impact on a wide variety of critical applications.

VI. CHALLENGES AND OPPORTUNITIES IN WIRELESS IoT CHANNEL MODELLING

Choosing an accurate channel model to represent the actual real-world wireless IoT deployment is a difficult task due to imperfections in the deployment area, such as varied terrain, the presence of large objects such as tall trees, and the varying speeds of moving objects. In other words, the actual wireless IoT performance varies when used in environments that have different channel conditions from the original development environment.

Although many academics have considered addressing the problem of channel modeling, it can be concluded that a significant gap remains, and additional research is required to resolve the crux of the problem. On the other hand, the proposed models primarily focus on empirical and site-specific modeling methodologies that may not apply to other locations or environments. Hence, despite the high demand for wireless channel modeling, numerous challenging issues must be resolved to achieve more accurate modeling.

Other limiting factors in certain studies include used equipment and deployment scenarios that are far from ideal or commercial use scenarios. The reviewed studies revealed that the research primarily focused on specific cellular-based IoT technologies, utilizing experimental hardware with low height Tx and Rx with omnidirectional antennas. Meanwhile, the research has mostly focused on near-ground deployment scenarios for short-range IoT technologies utilizing low gain omnidirectional antennas.

Interestingly, it was also noted that, among the numerous existing LPWAN technologies, LoRa/LoRaWAN had attracted substantial interest from the research community due to its unique features. As a result, most LPWAN research focused on the performance evaluation of this technology and channel model proposals for various implementation scenarios. However, most of this research used simple propagation models like LNSPL and Okumura-Hata models and concentrated on urban and suburban implementation scenarios. As a

TABLE 5. A summary of the reviewed LPWAN based wireless IoT channel modeling and characterization studies.

Ref	Environment/ Scenario	F. (MHz)	RAT		Targeted application	Modeling approach & used input parameters	Comparison Models	Analysis Metrics	Key Findings	Limitations
			BW (kHz)	SF						
[22]	Outdoor Urban	868	LoRa		Smart City (Smart lightning & buildings).	One-slope log-distance model. Use RSSI.	No comparison Performance evaluation (practical & simulation data).	RMSE & PDR	LoRa's maximum coverage is ≤ 2 km in dense urban, only achievable at favorable conditions (max SF & GW at ≥71m).	Do not consider terrain, weather impact & other models for comparison. It is purely based on RSSI.
			125	R.W. 12 Sim. 7-12						
[25]	Outdoor Urban	868	LoRa		Smart City (Pollution & meteorological).	Okumura-Hata (theoretical).	N/A	Evaluation of maximum range.	Demonstrated LoRa as an ad-hoc network solution for public transport.	Based on a theoretical evaluation only.
			N/A	N/A						
[26]	Outdoor Urban (city & over water).	868	LoRaWAN		Automotive & intelligent transportation.	LNSPL (derive parameters using linear polynomial fit). Use RSSI & SNR.	Measured vs. predicted PL. FSPL (baseline).	N/A	Claim that the derived model can be used to estimate needed GW density & analyze LoRa performance.	Do not compare to other PL models. Based on simple linear fitting.
			125	12						
[126]	Outdoor Urban & rural. LOS/NLOS.	868	LoRaWAN		General IoT applications.	FSPL for the balloon tests. LNSPL & Okumura-Hata for remaining. Use ESP derived from RSSI & SNR.	Prediction vs. data extracted from TTN, FSPL, & [186].	Estimation error (average & STD).	Automated coverage estimation method utilizing free remote sensing multi-spectral images with a channel model.	Do not consider other impacts (e.g., physical parameters) or comparison with other known models.
			125	7						
[176]	Outdoor Suburban	868	LoRa		General IoT applications.	Simulated ITM using SPLAT with DEM of 1 arc-second (~30m) resolution.	Measured vs. ITM, FSPL (baseline), models in [177] & [26] (based on log-distance).	RSSI false positive prediction.	RSSI accuracy evaluation showed a significant difference. No model fits all environments, & terrain data increases prediction accuracy.	RSSI-based. Low-resolution DEM, ignoring the reflection & diffraction impact of buildings or small terrain.
			125	12						
[118]	Outdoor/indoor Rural, urban, & suburban. LOS/NLOS	868	LoRaWAN		General IoT applications.	Indoor: ITU-R & COST231-MWF. Outdoor: LNSPL. Use RSSI & SNR.	FSPL (baseline). Indoor: ITU-R, COST 231-MWF, & 3GPP. Outdoor: Okumura–Hata (urban/rural), 3GPP-UMa, 3GPP-RMa & COST231-Hata (urban).	CDF, mean error, STD error, & PDR analysis.	Extensive measurements in three environments. The proposed PL models are better, more accurate & simple to apply in the study area or similar places. Evaluated LoRaWAN PDR/SNR & confirmed its reliability for many IoT applications.	Outdoor modeling uses simple linear fitting. Do not compare to ray-tracing models. More study is needed on LoRaWAN adaptability and scalability, network planning, and energy efficiency.
			125	12						
[52]	Outdoor Rural, urban, & suburban.	868	LoRaWAN		Smart city, farm, & goods monitoring.	No modeling Uses RSSI data	Examine expected signal using Okumura-Hata.	Range & PDR evaluation at a varied payload.	Present a detailed LoRaWAN performance analysis in three typical outdoor environments.	No model was proposed, limited to outdoor scenarios and RSSI-based evaluation.
			125	7-12						
[31]	Outdoor Urban LOS/NLOS	868	LoRaWAN		Smart city.	No modeling. Use RSSI & SNR.	Measured vs. Okumura-Hata & ITM, simulated in Cloud-RF®.	SF histogram, RSSI CDF vs. Cloud-RF® estimates, RSSI vs. SNR, SNR CDFs & ADR.	Examine how seasonal weather changes impact SNR, RSSI, & SF usage while enabling ADR. Low temperatures increased noise intensity, leading to better SNR. Long distances & snow reduce LoRaWAN performance. Okumura-Hata was the best, while ITM seems to overestimate RSSI.	Do not consider building impact, power consumption, PDR, & PL modeling. The simulation lacked clutter & knife-edge features, resulting in lower accuracy. Need further research on how snow influences signal transmission at different distances.
			125	7, 10, 12 & ADR						
[178]	Outdoor Urban (campus / city) & rural (forest / coastal).	868	LoRa P2P		General IoT applications.	Log-distance PL. Use RSSI & SNR.	Okumura-Hata, COST 231-Hata, & [26] vs. derived PL models.	RMSE & MAE.	Okumura-Hata significantly overestimated PL. Modified COST 231-Hata & [26] underestimated PL.	Tx/Rx height is limited at 1.5m. Do not consider irregular terrain or ray-tracing models.
			N/A	N/A						
[175]	Outdoor Mixed.	923	LoRa		General IoT applications.	N/A Use RSSI.	N/A	RSSI & PDR for coverage & performance analysis.	Indicated that terrain impacts LoRa signal propagation, limiting coverage & reducing PDR by half. Also, GW location, environmental scenarios, & topology must be considered during deployment to improve performance.	Suggest further research on optimal coverage, tropical regions, e.g., Malaysia, rain impact on LoRa performance, & required mitigation strategies to increase performance.
			125	7-10						
[127]	Outdoor City of mixed Suburban/rural areas.	868	LoRaWAN		Pollution & dust bin sensors.	No modeling. Use RSSI for comparison	Measured RSSI vs. predicted from Cloud-RF® (Okumura-Hata, ITM, ITWOM).	Error in dB.	Terrain, environment & distance are significant factors for PL model selection of planning tool. ITWOM was the best, followed by ITM, & Okumura-Hata.	Do not consider SNR, TF, weather & other models. Limited to RSSI comparison.
			N/A	7, 10, & 12						
[179]	Outdoor Antarctic LOS/NLOS	434 & 868	LoRa		Environment monitoring.	No modeling (propagation limits). Use calibrated SNR to calculate P_R(dBm).	No comparison Consider log-distance & FSPL.	SNR & P_g calibrated.	Environment factors did not impact signal & terrain was the dominant factor influencing the propagation.	Do not consider propagation modeling or comparison.
			125	12						
[148]	Outdoor Urban	868	LoRa		Smart city.	Lee PL Model. Use RSSI.	N/A	MSE & RMSE.	Based on experimental measurements.	RSSI-based. Limited to Lee model without comparisons & statistical analysis.
			N/A	N/A						
[180]	Outdoor Foliage LOS/NLOS	915	LoRa		General IoT applications.	Foliage excess attenuation loss. Use RSSI.	Okumura-Hata & LNSPL.	N/A	It was shown that Okumura-Hata fails to capture the effect of foliage in the tropical areas under consideration.	Few measurements. Purely RSSI-based. Other foliage models & signal influencing factors are not considered.
			125	10						
[181]	Outdoor-to-indoor Urban	868	LoRaWAN		General IoT applications.	ANN, adjusted COST231, & optimized COST231-MWM. Use RSSI.	Log-distance, COST231, & Cost231-MWM.	MSE	Outdoor-to-Indoor propagation has a shorter range. COST231 & log-distance are inaccurate. With the proposed model, the COST231-MWM MSE dropped from 21 to 11.23.	Purely RSSI-based.
			125	9						
[182]	Outdoor/Indoor Urban LOS/NLOS	434 & 868	LoRa		General IoT applications.	Propagation limits & people presence impact. Use calibrated SNR to calculate P_R(dBm). Outdoor coverage simulated in Radio Mobile.	N/A	Mean & STD [day & night data].	A sudden drop in signal correlated with a rain event, while temperature fluctuations had no impact. The indoor study showed a 2-3 dB difference in STD between day & night readings when people are present in a building.	Do not consider modeling PL, terrain impact, foliage impact, & comparison with other models.
			125	12						
[28]	Indoor Obstructed LOS/ LOS/ NLOS	915, 919, 923, & 928	LoRaWAN		Gas meter, smart home & buildings.	Large-scale fading: One slop or LNSPL. TF: Rician distribution. Floor impact: AF model. Use calibrated RSSI & Rx power.	FSPL & compare large-scale calculation methods (non-fixed & fixed intercept).	Mean/standard Error. Auto-correlation. PDR & power consumption.	Investigate large-scale fading, TF, coverage, & energy consumption in four multi-floor building types. There was a constant 2 dB difference between the LoRa node's RSSI & the spectrum analyzer's RF power.	Do not compare with other Indoor PL models. Limited to indoor propagation modeling.
			125, 250, & 500.	7-10						
[40]	Outdoor LOS/NLOS	868	LoRaWAN		Medical bleeder.	Based on CDF, maximum likelihood (ML), & Nakagami. Use RSSI.	N/A	N/A	The anechoic measurement revealed typical user orientation effects concerning GW location. They show LoRaWAN as a viable wearable wireless technology.	Further investigation and comparison with other models are required.
			N/A	N/A						

TABLE 5. *(Continued.)* **A summary of the reviewed LPWAN based wireless IoT channel modeling and characterization studies.**

[74]	Indoor Rural (three dairy cattle brans).	868	LoRa N/A	N/A	IoA (health tracking of dairy cows).	LNSPL & TF to evaluate cows' movement impact on signal strength. Use calibrated RSSI.	Measured PL vs. modeled PL, FSPL (baseline), & TF evaluation.	R^2 & mean.	A constant 6dB shift was found. TF was statistically described by Rician distribution with an average K-factor of 8 dB. They argue that their results may enable reliable dairy cow IoT, optimizing network planning and energy consumption.	Based on a simple one-slope empirical model. Do not consider other models for comparison.
[75]	Agriculture with/without Cow.	433	LoRa N/A	N/A	IoA (health tracking of dairy cows).	LNSPL. Use measured signal power from a spectrum analyzer.	Compare PL between with & without cow case. Consider FSPL.	R^2 & STD.	They characterized PL between a GW & an antenna inside a cow's rumen. The average PL increase was 45.5 dB (all cows), with 39.7-51.1 dB variability. PL well fits LNSPL, & depending on the Tx power & DR, 100 m range was achieved.	Do not use actual LoRa hardware. Based on a simple PL model with linear fitting.
[183]	Outdoor Rural (mountain) LOS/NLOS	868	LoRa 125	7	Search and Rescue	LNSPL. Use RSSI & SNR.	Measured vs. estimated PL & FSPL.	STD	Developed a PL model for LoRa in a harsh mountain environment and considered the effect of human body shadowing on wearable Tx.	Need further experiments in different scenarios. Only compared with FSPL & lacks statistical analysis.
[184]	Underground WSN	433	LoRa N/A	N/A	Precision agriculture	Based on the Friis model, the α and β are modified based on MBSDM.	Conventional/NC modified Friis.	RMSE, MAE, & MAPE.	The model covers different scenarios, UG-UG, UG-AG, & AG-UG.	Further studies are required in different types of soil.
[60]	Urban Underground communication	433	N/A N/A	N/A	UIoT	Statistical model, considering losses caused by two stages: FSPL & through asphalt losses. Use RSSI.	N/A	Evaluate the temperature & asphalt thickness impact on signal loss.	Showed that an underground Tx could communicate up to 4 km across a 10 cm thick asphalt layer. The PL is less than 5dB for layers under 1m thick. It rises with layer thickness, reaching 15dB for 4m asphalt.	It does not provide a detailed description of the measurement setup; limited to signal loss analysis, with no comparison.
[185]	Outdoor Urban city	N/A	Sigfox N/A	-	Smart meter & assets tracking.	ML localization model based on LNSPL. Hata & Okumura-Hata were trained to obtain dummy data to increase ML accuracy. Use RSSI.	ML model prediction vs. the location reported by Sigfox cloud.	Average distance error.	Proposes using ML with RSSI to improve Sigfox localization accuracy. Improves localization accuracy by using a multi-sector (four 90°) training & prediction design. This method's maximum distance errors are often lower than the official Sigfox localization service.	Do not provide details on antenna specs & Rx height. Limited to the usage of uncalibrated RSSI & outdoor scenarios.

result, we anticipate a significant gap in channel modeling and characterization for these technologies, particularly in areas with complex terrain and harsh climate conditions, such as tropical regions.

Although several studies have considered utilizing more accurate ray-tracing methodologies or simulation tools, these did not explore the entire limitations of LPWAN technologies. On the other hand, the low-resolution maps available limited most of these studies, making them site-specific and impractical for reuse in other deployment areas.

The recent trend of using low-altitude platforms (LAP) and high-altitude platforms (HAP) such as UAVs have tremendous future opportunities, particularly for rural and difficult-to-reach IoT deployments. Furthermore, with recent improvements in IoT, cloud & edge computing, and wireless communication technologies, UAVs are becoming more maneuverable and smarter. As a result, the IoD is emerging as one of the promising technologies and use cases for UAVs. Despite recent work on developing channel models for UAV communications, more comprehensive models for air-to-air (A2A) and air-to-ground (A2G) scenarios are still required. The communication channel utilized by UAVs has characteristics that are significantly different from those used by conventional models. The most notable characteristics are: (i) highly dynamic propagation channel characteristics due to high UAV velocity, (ii) extreme temporal and spatial channel variation due to UAV mobility, (iii) different LOS propagation probability than terrestrial communication due to different flight heights, and (iv) additional shadowing effects from the aircraft body and propellers. As a result, the characteristics of UAV channels must be thoroughly investigated across a wide range of propagation environments, altitudes, and flying speeds. Thus, more accurate analytical models are required to characterize large-scale fading, direct and multipath components, and spatial-temporal characteristics in non-stationary channels. Additionally, developing empirically-based channel models is critical for validating or disproving theoretical models.

On the other hand, having a reliable A2A communication link is critical in multi-hop UAV networking. Although the A2A channel appears to be like the free space channel due to its high LOS conditions, the dynamic environment and ground reflections have different effects. As a result, issues such as antenna orientation and Doppler spectrum must be investigated in various A2A propagation scenarios.

Finally, ML techniques have advanced significantly in wireless channel modeling, and the reviewed studies have demonstrated that ML-based methods can significantly improve the accuracy of PL prediction compared to conventional PL models. However, most proposed methods rely on small input sets and ignore the impact of multiple KPIs and other critical parameters such as topological information. A rich training set covering a wide range of required information with high resolution plays a vital role in exploiting the potential of ML techniques and extracting the structural relationship between collected data from complex environments.

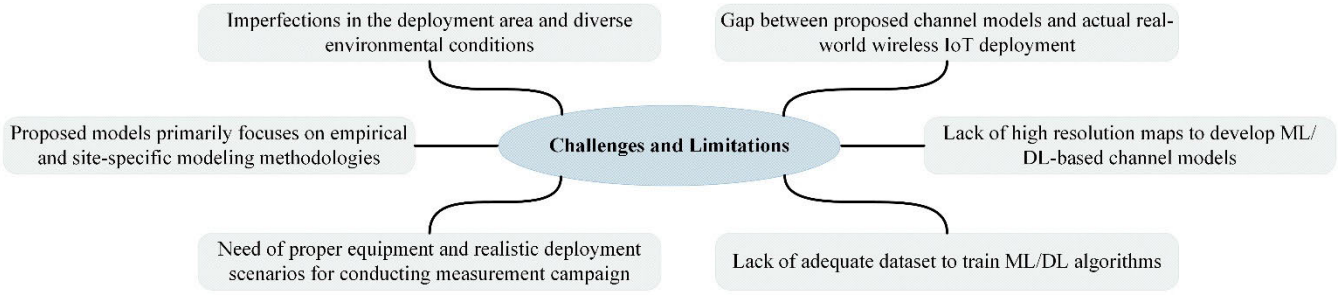

FIGURE 4. Challenges and limitations in wireless IoT channel modeling.

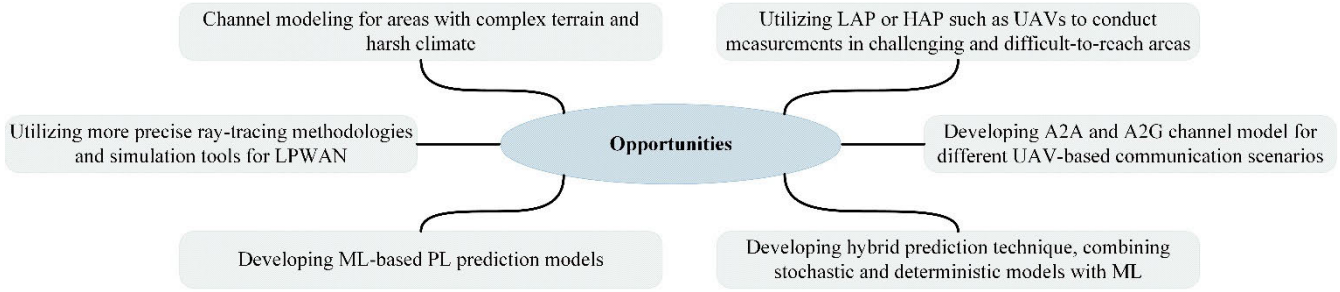

FIGURE 5. Opportunities in wireless IoT channel modeling.

Given the diversity and dynamic nature of environmental conditions in IoT communications, providing rich measurement campaigns for various environments and scenarios is crucial for developing accurate DL-based channel models.

Many future work directions in wireless channel modeling and characterization of IoT technologies, in general, and LPWAN in particular, may be viable in this regard. Among these, it is believed that measurement-based and comparative analysis studies are of utmost desire to understand such technologies' behavior in real-world environments accurately. The latter is also crucial to validate the performance of existing channel models and identify their suitability for a wide range of actual deployments and the need for further optimization or new models implementation. Other modeling approaches may integrate emerging machine learning-based and hybrid prediction techniques, combining popular stochastic or deterministic modeling techniques with ML. Nonetheless, any of these approaches may represent a significant opportunity, with the potential to have a significant impact on a broad range of critical applications. Figs. 4 and 5 summarize the challenges and opportunities in wireless IoT channel propagation modeling, respectively.

VII. CONCLUSION

For any communication system, the wireless channel characteristics are a critical parameter that directly affects the wireless signal traveling from the transmitter to the receiver antenna through the channel. Wireless transmission has recently become the core for enabling wireless IoT applications. As a result, it is crucial to investigate the propagation channel characteristics that directly impact wireless transmission performance. Failure to do so will harm the planning and deployment of any IoT application. As such, this review addresses wireless channel characterization and modeling for wireless IoT technologies, including a comprehensive review of recent advancements and studies in this area. To properly understand this issue, the study begins by briefly reviewing several innovative wireless IoT-based applications and then highlighting the most crucial challenges associated with them.

The study also includes a brief description of channel modeling and a generalized form of commonly used channel models. It also lists 34 well-known path loss models for wireless IoT technologies, with a thorough description of each model's modeling parameters, limitations, and operating conditions. Finally, the study reviews recent advances in channel modeling for wireless IoT technologies, describes gaps in existing research, and suggests future research directions towards addressing these gaps.

Although many researchers have considered addressing the problem of channel modeling, it can be concluded that a significant gap remains, and additional research is required to resolve the crux of this problem. Moreover, to improve modeling accuracy, many challenging issues must be resolved. On the other hand, it was observed that, among the numerous existing LPWAN technologies, LoRa/LoRaWAN had gained significant research attention due to its unique features. While much research has been done on LPWANs, it can be observed that there is still a big gap in channel modeling and characterization of these technologies, especially in areas with complex

terrain and harsh climates like tropical regions. Further, the use of more precise ray-tracing methodologies or simulation tools in some research has not investigated the full potential of LPWAN technology. Meanwhile, the low-resolution maps available constrained most, making such studies site-specific and impractical for usage in other deployment areas.

Among many directions forward to tackle the channel modeling and characterization for wireless IoT technologies, especially LPWANs, it is believed that measurement-based and comparative analysis studies are crucial for fully understanding the behavior of such technologies in the real-world. The latter is also crucial to validate the performance of existing channel models and identify their suitability for a wide range of actual deployments and the need for further optimization or new models implementation. Other modeling approaches may integrate emerging machine learning-based and hybrid prediction techniques, combining popular stochastic or deterministic modeling techniques with ML. Nonetheless, any of these approaches may represent a significant opportunity, with the potential to have a significant impact on a broad range of critical applications.

REFERENCES

[1] I. R. Gomes, C. R. Gomes, H. S. Gomes, and G. P. D. S. Cavalcante, "Empirical radio propagation model for DTV applied to non-homogeneous paths and different climates using machine learning techniques," *PLoS ONE*, vol. 13, no. 3, Mar. 2018, Art. no. e0194511, doi: 10.1371/journal.pone.0194511.

[2] B. S. L. Castro, M. R. Pinheiro, G. P. S. Cavalcante, I. R. Gomes, and O. D. O. Carneiro, "Comparison between known propagation models using least squares tuning algorithm on 5.8 GHz in Amazon region cities," *J. Microw., Optoelectronics Electromagn. Appl.*, vol. 10, no. 1, pp. 106–113, Jun. 2011, doi: 10.1590/S2179-10742011000100011.

[3] S. I. Popoola, A. A. Atayero, O. D. Arausi, and V. O. Matthews, "Path loss dataset for modeling radio wave propagation in smart campus environment," *Data Brief*, vol. 17, pp. 1062–1073, Apr. 2018, doi: 10.1016/j.dib.2018.02.026.

[4] A. A. Jimoh, N. T. Surajudeen-Bakinde, N. Faruk, A. A. Ayeni, O. O. Obiyemi, and O. W. Bello, "Performance analysis of empirical path loss models in VHF & UHF bands," in *Proc. 6th Int. Conf. Inf. Commun. Syst. (ICICS)*, Apr. 2015, pp. 194–199, doi: 10.1109/IACS.2015.7103226.

[5] H. M. Rahim, C. Y. Leow, T. A. Rahman, A. Arsad, and M. A. Malek, "Foliage attenuation measurement at millimeter wave frequencies in tropical vegetation," in *Proc. IEEE 13th Malaysia Int. Conf. Commun. (MICC)*, Nov. 2017, pp. 241–246, doi: 10.1109/MICC.2017.8311766.

[6] S. M. Aldossari and K.-C. Chen, "Machine learning for wireless communication channel modeling: An overview," *Wireless Pers. Commun.*, vol. 106, no. 1, pp. 41–70, May 2019, doi: 10.1007/s11277-019-06275-4.

[7] A. Habib and S. Moh, "Wireless channel models for over-the-sea communication: A comparative study," *Appl. Sci.*, vol. 9, no. 3, p. 443, Jan. 2019, doi: 10.3390/app9030443.

[8] W. Khawaja, I. Guvenc, D. W. Matolak, U.-C. Fiebig, and N. Schneckenburger, "A survey of air-to-ground propagation channel modeling for unmanned aerial vehicles," *IEEE Commun. Surveys Tuts.*, vol. 21, no. 3, pp. 2361–2391, 3rd Quart., 2019, doi: 10.1109/COMST.2019.2915069.

[9] J. C. Silva, G. L. Siqueira, and P. V. G. Castellanos, "Propagation model for path loss through vegetated environments at 700–800 MHz band," *J. Microw., Optoelectron. Electromagn. Appl.*, vol. 17, no. 1, pp. 102–120, 2018, doi: 10.1590/2179-10742018v17i11183.

[10] L. E. C. Eras, D. K. N. Silva, F. B. Barros, L. M. Correia, and G. P. S. Cavalcante, "A radio propagation model for mixed paths in Amazon environments for the UHF band," *Wireless Commun. Mobile Comput.*, vol. 2018, Nov. 2018, Art. no. 2850830.

[11] A. Al-Hourani, S. Kandeepan, and A. Jamalipour, "Modeling air-to-ground path loss for low altitude platforms in urban environments," in *Proc. IEEE Global Commun. Conf.*, Dec. 2014, pp. 2898–2904, doi: 10.1109/GLOCOM.2014.7037248.

[12] W. Wang, S. L. Capitaneanu, D. Marinca, and E.-S. Lohan, "Comparative analysis of channel models for industrial IoT wireless communication," *IEEE Access*, vol. 7, pp. 91627–91640, 2019, doi: 10.1109/ACCESS.2019.2927217.

[13] S.-H. Hwang and S.-Z. Liu, "Survey on 3GPP low power wide area technologies and its application," in *Proc. IEEE VTS Asia Pacific Wireless Commun. Symp. (APWCS)*, Aug. 2019, pp. 1–5, doi: 10.1109/VTS-APWCS.2019.8851631.

[14] N. Poursafar, M. E. E. Alahi, and S. Mukhopadhyay, "Long-range wireless technologies for IoT applications: A review," in *Proc. 11th Int. Conf. Sens. Technol. (ICST)*, Dec. 2017, pp. 1–6, doi: 10.1109/ICSensT.2017.8304507.

[15] M. Shahidul Islam, M. T. Islam, M. A. Ullah, G. Kok Beng, N. Amin, and N. Misran, "A modified meander line microstrip patch antenna with enhanced bandwidth for 2.4 GHz ISM-band Internet of Things (IoT) applications," *IEEE Access*, vol. 7, pp. 127850–127861, 2019, doi: 10.1109/ACCESS.2019.2940049.

[16] W. Ayoub, A. E. Samhat, F. Nouvel, M. Mroue, and J.-C. Prévotet, "Internet of mobile things: Overview of LoRaWAN, DASH7, and NB-IoT in LPWANs standards and supported mobility," *IEEE Commun. Surveys Tuts.*, vol. 21, no. 2, pp. 1561–1581, 2nd Quart., 2019, doi: 10.1109/COMST.2018.2877382.

[17] R. Sharan Sinha, Y. Wei, and S.-H. Hwang, "A survey on LPWA technology: LoRa and NB-IoT," *ICT Exp.*, vol. 3, no. 1, pp. 14–21, Mar. 2017, doi: 10.1016/j.icte.2017.03.004.

[18] K. Mekkia, E. Bajica, F. Chaxela, and F. Meyerb, "A comparative study of LPWAN technologies for large-scale IoT deployment," *ICT Exp.*, vol. 5, no. 1, pp. 1–7, Mar. 2019, doi: 10.1016/j.icte.2017.12.005.

[19] Y. Moon, S. Ha, M. Park, D. Lee, and J. Jeong, "A methodology of NB-IoT mobility optimization," in *Proc. Global Internet Things Summit (GIoTS)*, Jun. 2018, pp. 1–5.

[20] L. Wan, Z. Zhang, Y. Huang, Y. Yan, and J. Wang, "Performance analysis of NB-IoT technology for indoor IoT applications," in *Proc. Int. Conf. Comput. Technol., Electron. Commun. (ICCTEC)*, Dec. 2017, pp. 1365–1369, doi: 10.1109/ICCTEC.2017.00299.

[21] H. A. H. Alobaidy, J. S. Mandeep, R. Nordin, N. F. Abdullah, C. G. Wei, and M. L. S. Soon, "Real-world evaluation of power consumption and performance of NB-IoT in Malaysia," *IEEE Internet Things J.*, early access, Nov. 29, 2021, doi: 10.1109/JIOT.2021.3131160.

[22] G. Pasolini, C. Buratti, L. Feltrin, F. Zabini, C. De Castro, R. Verdone, and O. Andrisano, "Smart city pilot projects using LoRa and IEEE802.15.4 technologies," *Sensors*, vol. 18, no. 4, p. 1118, 2018, doi: 10.3390/s18041118.

[23] H. A. H. Alobaidy, J. S. Mandeep, R. Nordin, and N. F. Abdullah, "A review on ZigBee based WSNs: Concepts, infrastructure, applications, and challenges," *Int. J. Electr. Electron. Eng. Telecommun.*, pp. 189–198, 2020, doi: 10.18178/ijeetc.9.3.189-198.

[24] T.-H. Kim, C. Ramos, and S. Mohammed, "Smart city and IoT," *Future Gener. Comput. Syst.*, vol. 76, pp. 159–162, Nov. 2017, doi: 10.1016/j.future.2017.03.034.

[25] S. Bertoldo, L. Carosso, E. Marchetta, M. Paredes, and M. Allegretti, "Feasibility analysis of a LoRa-based WSN using public transport," *Appl. Syst. Innov.*, vol. 1, no. 4, p. 49, Dec. 2018, doi: 10.3390/asi1040049.

[26] J. Petajajarvi, K. Mikhaylov, A. Roivainen, T. Hanninen, and M. Pettissalo, "On the coverage of LPWANs: Range evaluation and channel attenuation model for Lora technology," in *Proc. 14th Int. Conf. ITS Telecommun. (ITST)*, Dec. 2015, pp. 55–59, doi: 10.1109/ITST.2015.7377400.

[27] M. Sidorov, P. V. Nhut, Y. Matsumoto, and R. Ohmura, "LoRa-based precision wireless structural health monitoring system for bolted joints in a smart city environment," *IEEE Access*, vol. 7, pp. 179235–179251, 2019, doi: 10.1109/ACCESS.2019.2958835.

[28] W. Xu, J. Y. Kim, W. Huang, S. S. Kanhere, S. K. Jha, and W. Hu, "Measurement, characterization, and modeling of Lora technology in multifloor buildings," *IEEE Internet Things J.*, vol. 7, no. 1, pp. 298–310, Jan. 2020, doi: 10.1109/JIOT.2019.2946900.

[29] A. Heller, "The sensing internet—A discussion on its impact on rural areas," *Future Internet*, vol. 7, no. 4, pp. 363–371, Sep. 2015, doi: 10.3390/fi7040363.

[30] A. Alsayyari, I. Kostanic, and C. E. Otero, "An empirical path loss model for wireless sensor network deployment in a concrete surface environment," in *Proc. IEEE 16th Annu. Wireless Microw. Technol. Conf. (WAMICON)*, Apr. 2015, pp. 1–6, doi: 10.1109/WAMICON.2015.7120311.

[31] N. S. Bezerra, C. Åhlund, S. Saguna, and V. A. de Sousa, "Temperature impact in LoRaWAN—A case study in Northern Sweden," *Sensors*, vol. 19, no. 20, p. 4414, Oct. 2019, doi: 10.3390/s19204414.

[32] J. Guo, "Smartphone-powered electrochemical biosensing dongle for emerging medical IoTs application," *IEEE Trans. Ind. Informat.*, vol. 14, no. 6, pp. 2592–2597, Jun. 2018, doi: 10.1109/TII.2017.2777145.

[33] A. H. Mohd Aman, W. H. Hassan, S. Sameen, Z. S. Attarbashi, M. Alizadeh, and L. A. Latiff, "IoMT amid COVID-19 pandemic: Application, architecture, technology, and security," *J. Netw. Comput. Appl.*, vol. 174, Jan. 2021, Art. no. 102886, doi: 10.1016/j.jnca.2020.102886.

[34] N. Naren, V. Chamola, S. Baitragunta, A. Chintanpalli, P. Mishra, S. Yenuganti, and M. Guizani, "IoMT and DNN-enabled drone-assisted covid-19 screening and detection framework for rural areas," *IEEE Internet Things Mag.*, vol. 4, no. 2, pp. 4–9, Jun. 2021, doi: 10.1109/IOTM.0011.2100053.

[35] V. Chamola, V. Hassija, V. Gupta, and M. Guizani, "A comprehensive review of the COVID-19 pandemic and the role of IoT, drones, AI, blockchain, and 5G in managing its impact," *IEEE Access*, vol. 8, pp. 90225–90265, 2020, doi: 10.1109/ACCESS.2020.2992341.

[36] B. Mathieu, C. Westphal, and P. Truong, "Towards the usage of CCN for IoT networks," in *Internet of Things (IoT) in 5G Mobile Technologies* C. X. Mavromoustakis, G. Mastorakis, and J. M. Batalla, Eds. Cham, Switzerland: Springer, 2016, pp. 3–24.

[37] L. M. Vela, H. Kwon, S. B. Rutkove, and B. Sanchez, "Standalone IoT bioimpedance device supporting real-time online data access," *IEEE Internet Things J.*, vol. 6, no. 6, pp. 9545–9554, Dec. 2019, doi: 10.1109/JIOT.2019.2929459.

[38] G. Xu, "IoT-assisted ECG monitoring framework with secure data transmission for health care applications," *IEEE Access*, vol. 8, pp. 74586–74594, 2020, doi: 10.1109/ACCESS.2020.2988059.

[39] M. Cicioglu and A. Calhan, "Internet of Things-based firefighters for disaster case management," *IEEE Sensors J.*, vol. 21, no. 1, pp. 612–619, Jan. 2021, doi: 10.1109/JSEN.2020.3013333.

[40] P. A. Catherwood, S. McComb, M. Little, and J. A. D. McLaughlin, "Channel characterisation for wearable LoRaWAN monitors," in *Proc. Loughborough Antennas Propag. Conf. (LAPC)*, 2017, pp. 6–9, doi: 10.1049/cp.2017.0273.

[41] H. Tan and I. Chung, "Secure authentication and group key distribution scheme for WBANs based on smartphone ECG sensor," *IEEE Access*, vol. 7, pp. 151459–151474, 2019, doi: 10.1109/ACCESS.2019.2948207.

[42] P. Vijayakumar, M. S. Obaidat, M. Azees, S. H. Islam, and N. Kumar, "Efficient and secure anonymous authentication with location privacy for IoT-based WBANs," *IEEE Trans. Ind. Informat.*, vol. 16, no. 4, pp. 2603–2611, Apr. 2020, doi: 10.1109/TII.2019.2925071.

[43] Z. Munadhil, S. K. Gharghan, A. H. Mutlag, A. Al-Naji, and J. Chahl, "Neural network-based Alzheimer's patient localization for wireless sensor network in an indoor environment," *IEEE Access*, vol. 8, pp. 150527–150538, 2020, doi: 10.1109/ACCESS.2020.3016832.

[44] T. O. Olasupo, "Wireless communication modeling for the deployment of tiny IoT devices in rocky and mountainous environments," *IEEE Sensors Lett.*, vol. 3, no. 7, pp. 1–4, Jul. 2019, doi: 10.1109/LSENS.2019.2918331.

[45] H. Xu, W. Yu, D. Griffith, and N. Golmie, "A survey on industrial Internet of Things: A cyber-physical systems perspective," *IEEE Access*, vol. 6, pp. 78238–78259, 2018, doi: 10.1109/ACCESS.2018.2884906.

[46] M. W. Condry and C. B. Nelson, "Using smart edge IoT devices for safer, rapid response with industry IoT control operations," *Proc. IEEE*, vol. 104, no. 5, pp. 938–946, May 2016, doi: 10.1109/JPROC.2015.2513672.

[47] J. Huang, L. Kong, G. Chen, M.-Y. Wu, X. Liu, and P. Zeng, "Towards secure industrial IoT: Blockchain system with credit-based consensus mechanism," *IEEE Trans. Ind. Informat.*, vol. 15, no. 6, pp. 3680–3689, Jun. 2019, doi: 10.1109/TII.2019.2903342.

[48] R. Ajith, A. Tewari, D. Gupta, and S. Tallur, "Low-cost vibration sensor for condition-based monitoring manufactured from polyurethane foam," *IEEE Sensors Lett.*, vol. 1, no. 6, pp. 1–4, Dec. 2017, doi: 10.1109/LSENS.2017.2773652.

[49] T. Nguyen, R. G. Gosine, and P. Warrian, "A systematic review of big data analytics for oil and gas industry 4.0," *IEEE Access*, vol. 8, pp. 61183–61201, 2020, doi: 10.1109/ACCESS.2020.2979678.

[50] R. Morello, C. De Capua, G. Fulco, and S. C. Mukhopadhyay, "A smart power meter to monitor energy flow in smart grids: The role of advanced sensing and IoT in the electric grid of the future," *IEEE Sensors J.*, vol. 17, no. 23, pp. 7828–7837, Dec. 2017, doi: 10.1109/JSEN.2017.2760014.

[51] S. Chen, H. Wen, J. Wu, W. Lei, W. Hou, W. Liu, A. Xu, and Y. Jiang, "Internet of Things based smart grids supported by intelligent edge computing," *IEEE Access* vol. 7, pp. 74089–74102, 2019, doi: 10.1109/ACCESS.2019.2920488.

[52] R. Sanchez-Iborra, J. Sanchez-Gomez, J. Ballesta-Viñas, M.-D. Cano, and A. F. Skarmeta, "Performance evaluation of LoRa considering scenario conditions," *Sensors*, vol. 18, no. 3, p. 772, 2018, doi: 10.3390/s18030772.

[53] S. Proto, E. Di Corso, D. Apiletti, L. Cagliero, T. Cerquitelli, G. Malnati, and D. Mazzucchi, "REDTag: A predictive maintenance framework for parcel delivery services," *IEEE Access*, vol. 8, pp. 14953–14964, 2020, doi: 10.1109/ACCESS.2020.2966568.

[54] J. Hejselbæk, J. Ø. Nielsen, W. Fan, and G. F. Pedersen, "Empirical study of near ground propagation in forest terrain for Internet-of-Things type device-to-device communication," *IEEE Access*, vol. 6, pp. 54052–54063, 2018, doi: 10.1109/ACCESS.2018.2871368.

[55] Z. Huang, Q. Chen, L. Zhang, and X. Hu, "Research on intelligent monitoring and analysis of physical fitness based on the Internet of Things," *IEEE Access*, vol. 7, pp. 177297–177308, 2019, doi: 10.1109/ACCESS.2019.2956835.

[56] O. Postolache, J. D. Pereira, and P. S. Girão, "Wireless sensor network-based solution for environmental monitoring: Water quality assessment case study," *IET Sci., Meas. Technol.*, vol. 8, no. 6, pp. 610–616, Nov. 2014, doi: 10.1049/iet-smt.2013.0136.

[57] S. N. H. Al-Hussaini, A. H. M. J. Al-Obaidy, and A. A. M. Al-Mashhady, "Environmental assessment of heavy metal pollution of diyala river within baghdad city," *Appl. Water Sci.*, vol. 8, no. 3, p. 87, Jun. 2018, doi: 10.1007/s13201-018-0707-9.

[58] I. M. Jasim, A. A. Al-kubaisi, and A. H. M. J. Al-Obaidy, "Test the efficiency of some plants in the tolerant of air pollution within the city of Baghdad. Iraq," *Baghdad Sci. J.*, vol. 15, no. 1, pp. 9–15, Mar. 2018, doi: 10.21123/bsj.15.1.9-15.

[59] Y. Wang, S. M. S. M. Rajib, C. Collins, and B. Grieve, "Low-cost turbidity sensor for low-power wireless monitoring of fresh-water courses," *IEEE Sensors J.*, vol. 18, no. 11, pp. 4689–4696, Jun. 2018, doi: 10.1109/JSEN.2018.2826778.

[60] A. Salam and S. Shah, "Urban underground infrastructure monitoring IoT: The path loss analysis," in *Proc. IEEE 5th World Forum Internet Things (WF-IoT)*, Apr. 2019, pp. 398–401, doi: 10.1109/WF-IoT.2019.8767358.

[61] M. Munoz, J. L. Guzman, J. A. Sanchez, F. Rodriguez, M. Torres, and M. Berenguel, "A new IoT-based platform for greenhouse crop production," *IEEE Internet Things J.*, early access, May 20, 2020, doi: 10.1109/JIOT.2020.2996081.

[62] J. Stewart, R. Stewart, and S. Kennedy, "Internet of Things—Propagation modelling for precision agriculture applications," in *Proc. Wireless Telecommun. Symp. (WTS)*, Apr. 2017, pp. 1–8.

[63] C. A. González-Amarillo, J. C. Corrales-Muñoz, M. Á. Mendoza-Moreno, A. F. Hussein, N. Arunkumar, and G. Ramirez-González, "An IoT-based traceability system for greenhouse seedling crops," *IEEE Access*, vol. 6, pp. 67528–67535, 2018, doi: 10.1109/ACCESS.2018.2877293.

[64] R. G. Vieira, A. M. da Cunha, L. B. Ruiz, and A. P. de Camargo, "On the design of a long range WSN for precision irrigation," *IEEE Sensors J.*, vol. 18, no. 2, pp. 773–780, Jan. 2018, doi: 10.1109/JSEN.2017.2776859.

[65] R. Khan, I. Ali, M. Zakarya, M. Ahmad, M. Imran, and M. Shoaib, "Technology-assisted decision support system for efficient water utilization: A real-time testbed for irrigation using wireless sensor networks," *IEEE Access*, vol. 6, pp. 25686–25697, 2018, doi: 10.1109/ACCESS.2018.2836185.

[66] R. Khan, M. Zakarya, V. Balasubramanian, M. A. Jan, and V. G. Menon, "Smart sensing-enabled decision support system for water scheduling in orange orchard," *IEEE Sensors J.*, vol. 21, no. 16, pp. 17492–17499, Aug. 2021, doi: 10.1109/JSEN.2020.3012511.

[67] A. Goap, D. Sharma, A. K. Shukla, and C. R. Krishna, "An IoT based smart irrigation management system using Machine learning and open source technologies," *Comput. Electron. Agricult.*, vol. 155, pp. 41–49, Dec. 2018, doi: 10.1016/j.compag.2018.09.040.

[68] B. Keswani, A. G. Mohapatra, A. Mohanty, A. Khanna, J. J. Rodrigues, D. Gupta, and V. H. C. de Albuquerque, "Adapting weather conditions based IoT enabled smart irrigation technique in precision agriculture mechanisms," *Neural Comput. Appl.*, vol. 31, no. 1, pp. 277–292, 2019, doi: 10.1007/s00521-018-3737-1.

[69] T. Natori, N. Ariyama, S. Tsuichihara, H. Takemura, and N. Aikawa, "Study of activity collecting system for grazing cattle," in *Proc. 34th Int. Tech. Conf. Circuits/Systems, Comput. Commun. (ITC-CSCC)*, Jun. 2019, pp. 1–4, doi: 10.1109/ITC-CSCC.2019.8793451.

[70] T. Olasupo, C. E. Otero, K. O. Olasupo, and I. Kostanic, "Empirical path loss models for wireless sensor network deployments in short and tall natural grass environments," *IEEE Trans. Antennas Propag.*, early access, Jun. 22, 2016, doi: 10.1109/TAP.2016.2583507.

[71] Z. Gao, W. Li, Y. Zhu, Y. Tian, F. Pang, W. Cao, and J. Ni, "Wireless channel propagation characteristics and modeling research in Rice field sensor networks," *Sensors*, vol. 18, no. 9, p. 3116, Sep. 2018, doi: 10.3390/s18093116.

[72] P. Loreti, A. Catini, M. De Luca, L. Bracciale, G. Gentile, and C. Di Natale, "The design of an energy harvesting wireless sensor node for tracking pink iguanas," *Sensors*, vol. 19, no. 5, p. 985, Feb. 2019, doi: 10.3390/s19050985.

[73] A. Naureen, N. Zhang, S. Furber, and Q. Shi, "A GPS-less localization and mobility modelling (LMM) system for wildlife tracking," *IEEE Access*, vol. 8, pp. 102709–102732, 2020, doi: 10.1109/ACCESS.2020.2997723.

[74] S. Benaissa, D. Plets, E. Tanghe, and J. Trogh, "Internet of animals: Characterisation of LoRa sub-GHz off-body wireless channel in dairy barns," *Electron. Lett.*, vol. 53, no. 18, pp. 1281–1283, Aug. 2017, doi: 10.1049/el.2017.1344.

[75] S. Benaissa, D. Plets, D. Nikolayev, and M. Deruyck, "Experimental characterisation of in-to-out-body path loss at 433 MHz in dairy cows," *Electron. Lett.*, vol. 55, no. 7, pp. 422–424, Apr. 2019, doi: 10.1049/el.2018.8150.

[76] W. Hong, B. Xu, X. Chi, X. Cui, Y. Yan, and T. Li, "Long-term and extensive monitoring for bee colonies based on Internet of Things," *IEEE Internet Things J.*, vol. 7, no. 8, pp. 7148–7155, Aug. 2020, doi: 10.1109/JIOT.2020.2981681.

[77] H. Bello, Z. Xiaoping, R. Nordin, and J. Xin, "Advances and opportunities in passive wake-up radios with wireless energy harvesting for the Internet of Things applications," *Sensors*, vol. 19, no. 14, p. 3078, Jul. 2019, doi: 10.3390/s19143078.

[78] M. Mozaffari, W. Saad, M. Bennis, and M. Debbah, "Mobile unmanned aerial vehicles (UAVs) for energy-efficient Internet of Things communications," *IEEE Trans. Wireless Commun.*, vol. 16, no. 11, pp. 7574–7589, Nov. 2017, doi: 10.1109/TWC.2017.2751045.

[79] M. A. Zulkifley, M. Behjati, R. Nordin, and M. S. Zakaria, "Mobile network performance and technical feasibility of LTE-powered unmanned aerial vehicle," *Sensors*, vol. 21, no. 8, p. 2848, Apr. 2021, doi: 10.3390/s21082848.

[80] M. Behjati, A. B. Mohd Noh, H. A. H. Alobaidy, M. A. Zulkifley, R. Nordin, and N. F. Abdullah, "LoRa communications as an enabler for Internet of Drones towards large-scale livestock monitoring in rural farms," *Sensors*, vol. 21, no. 15, p. 5044, Jul. 2021, doi: 10.3390/s21155044.

[81] C. Luo, J. Nightingale, E. Asemota, and C. Grecos, "A UAV-cloud system for disaster sensing applications," in *Proc. IEEE 81st Veh. Technol. Conf. (VTC Spring)*, May 2015, pp. 1–5, doi: 10.1109/VTCSpring.2015.7145656.

[82] S. J. Kim, Y. Jeong, S. Park, K. Ryu, and G. Oh, "A survey of drone use for entertainment and AVR (augmented and virtual reality)," in *Augmented Reality and Virtual Reality*. Manchester, U.K.: Springer, 2018, pp. 339–352.

[83] D. C. Tsouros, S. Bibi, and P. G. Sarigiannidis, "A review on UAV-based applications for precision agriculture," *Information*, vol. 10, no. 11, p. 349, Nov. 2019, doi: 10.3390/info10110349.

[84] Y. Zhang, X. Yuan, W. Li, and S. Chen, "Automatic power line inspection using UAV images," *Remote Sens.*, vol. 9, no. 8, p. 824, Aug. 2017, doi: 10.3390/rs9080824.

[85] H. Kim, L. Mokdad, and J. Ben-Othman, "Designing UAV surveillance frameworks for smart city and extensive ocean with differential perspectives," *IEEE Commun. Mag*, vol. 56, no. 4, pp. 98–104, Apr. 2018, doi: 10.1109/MCOM.2018.1700444.

[86] S. Sudhakar, V. Vijayakumar, C. S. Kumar, V. Priya, L. Ravi, and V. Subramaniyaswamy, "Unmanned aerial vehicle (UAV) based forest fire detection and monitoring for reducing false alarms in forest-fires," *Comput. Commun.*, vol. 149, pp. 1–16, Jan. 2020, doi: 10.1016/j.comcom.2019.10.007.

[87] M. I. Ahmad, M. H. Ab. Rahim, R. Nordin, F. Mohamed, A. Abu-Samah, and N. F. Abdullah, "Ionizing radiation monitoring technology at the verge of Internet of Things," *Sensors*, vol. 21, no. 22, p. 7629, Nov. 2021, doi: 10.3390/s21227629.

[88] A. Gupta, T. Afrin, E. Scully, and N. Yodo, "Advances of UAVs toward future transportation: The state-of-the-art, challenges, and opportunities," *Future Transp.*, vol. 1, no. 2, pp. 326–350, Sep. 2021, doi: 10.3390/futuretransp1020019.

[89] F. Schiefer, T. Kattenborn, A. Frick, J. Frey, P. Schall, B. Koch, and S. Schmidtlein, "Mapping forest tree species in high resolution UAV-based RGB-imagery by means of convolutional neural networks," *ISPRS J. Photogramm. Remote Sens.*, vol. 170, pp. 205–215, Dec. 2020, doi: 10.1016/j.isprsjprs.2020.10.015.

[90] S. Zeadally, J. Guerrero, and J. Contreras, "A tutorial survey on vehicle-to-vehicle communications," *Telecommun. Syst.*, vol. 73, no. 3, pp. 469–489, Mar. 2020, doi: 10.1007/s11235-019-00639-8.

[91] F. Lyu, M. Li, and X. Shen, "Characterizing urban V2V link communications," in *Vehicular Networking for Road Safety*. Waterloo, ON, Canada: Springer, 2020, pp. 77–99.

[92] H. A. Ameen, A. K. Mahamad, S. Saon, D. M. Nor, and K. Ghazi, "A review on vehicle to vehicle communication system applications," *Indonesian J. Electr. Eng. Comput. Sci.*, vol. 18, no. 1, p. 188, Apr. 2020, doi: 10.11591/ijeecs.v18.i1.pp188-198.

[93] A. Azmoodeh, A. Dehghantanha, and K.-K.-R. Choo, "Robust malware detection for internet of (Battlefield) things devices using deep eigenspace learning," *IEEE Trans. Sustain. Comput.*, vol. 4, no. 1, pp. 88–95, Jan. 2019, doi: 10.1109/TSUSC.2018.2809665.

[94] J. Wang, C. Jiang, Z. Wei, C. Pan, H. Zhang, and Y. Ren, "Joint UAV hovering altitude and power control for space-air-ground IoT networks," *IEEE Internet Things J.*, vol. 6, no. 2, pp. 1741–1753, Apr. 2019, doi: 10.1109/JIOT.2018.2875493.

[95] I. Ullah, Y. Liu, X. Su, and P. Kim, "Efficient and accurate target localization in underwater environment," *IEEE Access*, vol. 7, pp. 101415–101426, 2019, doi: 10.1109/ACCESS.2019.2930735.

[96] V. M. Suresh, R. Sidhu, P. Karkare, A. Patil, Z. Lei, and A. Basu, "Powering the IoT through embedded machine learning and Lora," in *Proc. IEEE 4th World Forum Internet Things (WF-IoT)*, Feb. 2018, pp. 349–354, doi: 10.1109/WF-IoT.2018.8355177.

[97] M. Molefi, E. D. Markus, and A. Abu-Mahfouz, "Wireless power transfer for IoT devices–A review," in *Proc. Int. Multidisciplinary Inf. Technol. Eng. Conf. (IMITEC)*, Nov. 2019, pp. 1–8, doi: 10.1109/IMITEC45504.2019.9015869.

[98] J. Corral-García, F. Lemus-Prieto, J.-L. González-Sánchez, and M.-Á. Pérez-Toledano, "Analysis of energy consumption and optimization techniques for writing energy-efficient code," *Electronics*, vol. 8, no. 10, p. 1192, Oct. 2019, doi: 10.3390/electronics8101192.

[99] F. John Dian, R. Vahidnia, and A. Rahmati, "Wearables and the Internet of Things (IoT), applications, opportunities, and challenges: A survey," *IEEE Access*, vol. 8, pp. 69200–69211, 2020, doi: 10.1109/ACCESS.2020.2986329.

[100] F. Maroto-Molina, J. Navarro-García, K. Príncipe-Aguirre, I. Gómez-Maqueda, J. E. Guerrero-Ginel, A. Garrido-Varo, and D. C. Pérez-Marín, "A low-cost IoT-based system to monitor the location of a whole herd," *Sensors*, vol. 19, no. 10, p. 2298, May 2019, doi: 10.3390/s19102298.

[101] F. Al-Turjman, "Positioning in the Internet of Things era: An overview," in *Proc. Int. Conf. Eng. Technol. (ICET)*, Aug. 2017, pp. 1–5, doi: 10.1109/ICEngTechnol.2017.8308188.

[102] H. Jawad, R. Nordin, S. Gharghan, A. Jawad, M. Ismail, and M. Abu-AlShaeer, "Power reduction with sleep/wake on redundant data (SWORD) in a wireless sensor network for energy-efficient precision agriculture," *Sensors*, vol. 18, no. 10, p. 3450, Oct. 2018, doi: 10.3390/s18103450.

[103] M. Singh and G. Baranwal, "Quality of service (QoS) in Internet of Things," in *Proc. 3rd Int. Conf. Internet Things: Smart Innov. Usages (IoT-SIU)*, Feb. 2018, pp. 1–6, doi: 10.1109/IoT-SIU.2018.8519862.

[104] H. Klaina, A. Vazquez Alejos, O. Aghzout, and F. Falcone, "Narrowband characterization of near-ground radio channel for wireless sensors networks at 5G-IoT bands," *Sensors*, vol. 18, no. 8, p. 2428, Jul. 2018, doi: 10.3390/s18082428.

[105] R. Pita, R. Utrilla, R. Rodriguez-Zurrunero, and A. Araujo, "Experimental evaluation of an RSSI-based localization algorithm on IoT end-devices," *Sensors*, vol. 19, no. 18, p. 3931, Sep. 2019, doi: 10.3390/s19183931.

[106] W. Njima, I. Ahriz, R. Zayani, M. Terre, and R. Bouallegue, "Deep CNN for indoor localization in IoT-sensor systems," *Sensors*, vol. 19, no. 14, p. 3127, Jul. 2019, doi: 10.3390/s19143127.

[107] Y. Bae, "Robust localization for robot and IoT using RSSI," *Energies*, vol. 12, no. 11, p. 2212, Jun. 2019, doi: 10.3390/en12112212.

[108] J. Rezazadeh, K. Sandrasegaran, and X. Kong, "A location-based smart shopping system with IoT technology," in *Proc. IEEE 4th World Forum Internet Things (WF-IoT)*, Feb. 2018, pp. 748–753, doi: 10.1109/WF-IoT.2018.8355175.

[109] S. Sadowski and P. Spachos, "RSSI-based indoor localization with the Internet of Things," *IEEE Access*, vol. 6, pp. 30149–30161, 2018, doi: 10.1109/ACCESS.2018.2843325.

[110] H. Sallouha, A. Chiumento, S. Rajendran, and S. Pollin, "Localization in ultra narrow band IoT networks: Design guidelines and tradeoffs," *IEEE Internet Things J.*, vol. 6, no. 6, pp. 9375–9385, Dec. 2019, doi: 10.1109/JIOT.2019.2931628.

[111] G. Wang, W. Zhu, and N. Ansari, "Robust TDOA-based localization for IoT via joint source position and NLOS error estimation," *IEEE Internet Things J.*, vol. 6, no. 5, pp. 8529–8541, Oct. 2019, doi: 10.1109/JIOT.2019.2920081.

[112] L. Zhao, C. Su, H. Huang, Z. Han, S. Ding, and X. Li, "Intrusion detection based on device-free localization in the era of IoT," *Symmetry*, vol. 11, no. 5, p. 630, May 2019, doi: 10.3390/sym11050630.

[113] F. Zafari, A. Gkelias, and K. K. Leung, "A survey of indoor localization systems and technologies," *IEEE Commun. Surveys Tuts.*, vol. 21, no. 3, pp. 2568–2599, 3rd Quart., 2017, doi: 10.1109/COMST.2019.2911558.

[114] S. K. Gharghan, R. Nordin, M. Ismail, and J. A. Ali, "Accurate wireless sensor localization technique based on hybrid PSO-ANN algorithm for indoor and outdoor track cycling," *IEEE Sensors J.*, vol. 16, no. 2, pp. 529–541, Jan. 2016, doi: 10.1109/JSEN.2015.2483745.

[115] S. K. Gharghan, R. Nordin, A. M. Jawad, H. M. Jawad, and M. Ismail, "Adaptive neural fuzzy inference system for accurate localization of wireless sensor network in outdoor and indoor cycling applications," *IEEE Access*, vol. 6, pp. 38475–38489, 2018, doi: 10.1109/ACCESS.2018.2853996.

[116] Y. Jiang, L. Peng, A. Hu, S. Wang, Y. Huang, and L. Zhang, "Physical layer identification of Lora devices using constellation trace figure," *EURASIP J. Wireless Commun. Netw.*, vol. 2019, no. 1, p. 223, Dec. 2019, doi: 10.1186/s13638-019-1542-x.

[117] R. M. Sandoval, A.-J. Garcia-Sanchez, and J. Garcia-Haro, "Improving RSSI-based path-loss models accuracy for critical infrastructures: A smart grid substation case-study," *IEEE Trans. Ind. Informat.*, vol. 14, no. 5, pp. 2230–2240, May 2018, doi: 10.1109/TII.2017.2774838.

[118] R. El Chall, S. Lahoud, and M. El Helou, "LoRaWAN network: Radio propagation models and performance evaluation in various environments in Lebanon," *IEEE Internet Things J.*, vol. 6, no. 2, pp. 2366–2378, Apr. 2019, doi: 10.1109/JIOT.2019.2906838.

[119] A. Alsayyari, I. Kostanic, C. Otero, M. Almeer, and K. Rukieh, "An empirical path loss model for wireless sensor network deployment in a sand terrain environment," in *Proc. IEEE World Forum Internet Things (WF-IoT)*, Mar. 2014, pp. 218–223, doi: 10.1109/WF-IoT.2014.6803162.

[120] C. Phillips, D. Sicker, and D. Grunwald, "A survey of wireless path loss prediction and coverage mapping methods," *IEEE Commun. Surveys Tuts.*, vol. 15, no. 1, pp. 255–270, 1st Quart., 2013, doi: 10.1109/SURV.2012.022412.00172.

[121] K. S. Muttair, O. A. Shareef, and M. F. Mosleh, "Outdoor to indoor wireless propagation simulation model for 5G band frequencies," in *Proc. IOP Conf., Mater. Sci. Eng.*, vol. 745, Mar. 2020, Art. no. 012034, doi: 10.1088/1757-899X/745/1/012034.

[122] V. Lavanya, G. S. Rao, and B. Bidikar, "Fast fading mobile channel modeling for wireless communication," *Proc. Comput. Sci.*, vol. 85, pp. 777–781, Jan. 2016, doi: 10.1016/j.procs.2016.05.265.

[123] C. Phillips, D. Sicker, and D. Grunwald, "Bounding the practical error of path loss models," *Int. J. Antennas Propag.*, vol. 2012, Jun. 2012, Art. no. 754158, doi: 10.1155/2012/754158.

[124] J. Zhao, Q. Wang, Y. Li, J. Zhou, and W. Zhou, "Ka-band based channel modeling and analysis in high altitude Platform(HAP) system," in *Proc. IEEE 91st Veh. Technol. Conf. (VTC-Spring)*, May 2020, pp. 1–5, doi: 10.1109/VTC2020-Spring48590.2020.9129385.

[125] F. Qamar, M. H. D. Hindia, K. Dimyati, K. A. Noordin, M. B. Majed, T. A. Rahman, and I. S. Amiri, "Investigation of future 5G-IoT millimeter-wave network performance at 38 GHz for urban microcell outdoor environment," *Electronics*, vol. 8, no. 5, p. 495, May 2019, doi: 10.3390/electronics8050495.

[126] S. Demetri, M. Zúñiga, G. P. Picco, F. Kuipers, L. Bruzzone, and T. Telkamp, "Automated estimation of link quality for Lora," in *Proc. 18th Int. Conf. Inf. Process. Sensor Netw.*, Apr. 2019, pp. 145–156, doi: 10.1145/3302506.3310396.

[127] N. S. Bezerra, C. Ahlund, S. Saguna, and V. A. de Sousa, "Propagation model evaluation for LoRaWAN: Planning tool versus real case scenario," in *Proc. IEEE 5th World Forum Internet Things (WF-IoT)*, Apr. 2019, pp. 1–6, doi: 10.1109/WF-IoT.2019.8767299.

[128] K. M. Malarski, J. Thrane, M. G. Bech, K. Macheta, H. L. Christiansen, M. N. Petersen, and S. Ruepp, "Investigation of deep indoor NB-IoT propagation attenuation," in *Proc. IEEE 90th Veh. Technol. Conf. (VTC-Fall)*, Sep. 2019, pp. 1–5, doi: 10.1109/VTCFall.2019.8891414.

[129] S. Kasampalis, P. I. Lazaridis, Z. D. Zaharis, A. Bizopoulos, S. Zettas, and J. Cosmas, "Comparison of ITM and ITWOM propagation models for DVB-T coverage prediction," in *Proc. IEEE Int. Symp. Broadband Multimedia Syst. Broadcast. (BMSB)*, Jun. 2013, pp. 1–4, doi: 10.1109/BMSB.2013.6621780.

[130] F. A. Almalki and M. C. Angelides, "A machine learning approach to evolving an optimal propagation model for last mile connectivity using low altitude platforms," *Comput. Commun.*, vols. 142–143, pp. 9–33, Jun. 2019, doi: 10.1016/j.comcom.2019.04.001.

[131] T. Jawhly and R. C. Tiwari, "Characterization of path loss for VHF terrestrial band in Aizawl, Mizoram (India)," in *Engineering Vibration, Communication and Information Processing*, K. Ray, S. N. Sharan, S. Rawat, S. K. Jain, S. Srivastava, and A. Bandyopadhyay, Eds. Singapore: Springer, 2019, pp. 53–63.

[132] A. M. Al-Samman, T. Abd. Rahman, T. Al-Hadhrami, A. Daho, M. N. Hindia, M. H. Azmi, K. Dimyati, and M. Alazab, "Comparative study of indoor propagation model below and above 6 GHz for 5G wireless networks," *Electronics*, vol. 8, no. 1, p. 44, Jan. 2019, doi: 10.3390/electronics8010044.

[133] S. Sun, G. R. MacCartney, and T. S. Rappaport, "Millimeter-wave distance-dependent large-scale propagation measurements and path loss models for outdoor and indoor 5G systems," in *Proc. 10th Eur. Conf. Antennas Propag. (EuCAP)*, Apr. 2016, pp. 1–5, doi: 10.1109/EuCAP.2016.7481506.

[134] A. Al-Samman, T. Rahman, M. Hindia, A. Daho, and E. Hanafi, "Path loss model for outdoor parking environments at 28 GHz and 38 GHz for 5G wireless networks," *Symmetry*, vol. 10, no. 12, p. 672, Nov. 2018, doi: 10.3390/sym10120672.

[135] S. Sun, T. S. Rappaport, S. Rangan, T. A. Thomas, A. Ghosh, I. Z. Kovacs, I. Rodriguez, O. Koymen, A. Partyka, and J. Jarvelainen, "Propagation path loss models for 5G urban micro- and macro-cellular scenarios," in *Proc. IEEE 83rd Veh. Technol. Conf. (VTC Spring)*, May 2016, pp. 1–6, doi: 10.1109/VTCSpring.2016.7504435.

[136] G. R. MacCartney and T. S. Rappaport, "Rural macrocell path loss models for millimeter wave wireless communications," *IEEE J. Sel. Areas Commun.*, vol. 35, no. 7, pp. 1663–1677, Jul. 2017, doi: 10.1109/JSAC.2017.2699359.

[137] G. R. MacCartney and T. S. Rappaport, "Study on 3GPP rural macrocell path loss models for millimeter wave wireless communications," in *Proc. IEEE Int. Conf. Commun. (ICC)*, May 2017, pp. 1–7, doi: 10.1109/ICC.2017.7996793.

[138] H. M. Rahim, C. Y. Leow, and T. A. Rahman, "Millimeter wave propagation through foliage: Comparison of models," in *Proc. IEEE 12th Malaysia Int. Conf. Commun. (MICC)*, Nov. 2015, pp. 236–240, doi: 10.1109/MICC.2015.7725440.

[139] A. Raheemah, N. Sabri, M. Salim, P. Ehkan, and R. B. Ahmad, "New empirical path loss model for wireless sensor networks in mango greenhouses," *Comput. Electron. Agricult.*, vol. 127, pp. 553–560, Sep. 2016, doi: 10.1016/j.compag.2016.07.011.

[140] J. Ko, S. Hur, Y.-S. Noh, K. Whang, J. Park, D.-J. Park, and D.-H. Cho, "Measurements and analysis of radio propagation at 28 GHz in vegetated areas of typical residential environments," *IEEE Trans. Antennas Propag.*, vol. 68, no. 5, pp. 4149–4154, May 2020, doi: 10.1109/TAP.2020.2968801.

[141] ITU-R, *Propagation Data and Prediction Methods for the Planning of Indoor Radiocommunication Systems and Radio Local Area Networks in the Frequency Range 300 MHz to 450 GHz*, Recommendation, document ITU-R P.1238-10, 2019.
[142] A. B. Zineb and M. Ayadi, "A multi-wall and multi-frequency indoor path loss prediction model using artificial neural networks," *Arabian J. Sci. Eng.*, vol. 41, pp. 987–996, Jun. 2016, doi: 10.1007/s13369-015-1949-6.
[143] M. Lott and I. Forkel, "A multi-wall-and-floor model for indoor radio propagation," in *Proc. IEEE VTS 53rd Veh. Technol. Conf., Spring*, vol. 1, May 2001, pp. 464–468, doi: 10.1109/VETECS.2001.944886.
[144] G. Castellanos and G. Teuta, "Path loss model in Amazonian border region for VHF and UHF television bands," in *Proc. IEEE-APS Top. Conf. Antennas Propag. Wireless Commun. (APWC)*, Sep. 2017, pp. 137–140, doi: 10.1109/APWC.2017.8062262.
[145] V. Armoogum, K. M. S. Soyjaudah, N. Mohamudally, and T. Fogarty, "Propagation models and their applications in digital television broadcast network design and implementation," in *Trends in Telecommunications Technologies*. Rijeka, Croatia: InTech, 2010.
[146] H. K. Hoomod, I. Al-Mejibli, and A. I. Jabboory, "Analyzing study of path loss propagation models in wireless communications at 0.8 GHz," in *Proc. J. Phys., Conf.*, vol. 1003, May 2018, Art. no. 012028, doi: 10.1088/1742-6596/1003/1/012028.
[147] O. Artemenko, A. H. Nayak, S. B. Menezes, and A. Mitschele-Thiel, "Evaluation of different signal propagation models for a mixed indoor-outdoor scenario using empirical data," in *Ad Hoc Networks*, N. Mitton, M. E. Kantarci, A. Gallais, and S. Papavassiliou, Eds. San Remo, Italy: Springer, 2015, pp. 3–14.
[148] D. Dobrilović, M. Malić, D. Malić, and S. Sladojević, "Analyses and optimization of lee propagation model for Lora 868 MHz network deployments in urban areas," *J. Eng. Manage. Competitiveness*, vol. 7, no. 1, pp. 55–62, 2017, doi: 10.5937/jemc1701055D.
[149] M. A. Abu-Rgheff, "mmWave propagation modelling: Atmospheric gaseous and rain losses," in *5G Physical Layer Technologies*, 1st ed. Hoboken, NJ, USA: Wiley, 2019, pp. 241–288.
[150] A. I. Sulyman, A. Alwarafy, G. R. MacCartney, T. S. Rappaport, and A. Alsanie, "Directional radio propagation path loss models for millimeter-wave wireless networks in the 28-, 60-, and 73-GHz bands," *IEEE Trans. Wireless Commun.*, vol. 15, no. 10, pp. 6939–6947, Oct. 2016, doi: 10.1109/TWC.2016.2594067.
[151] V. S. Abhayawardhana, I. J. Wassell, D. Crosby, M. P. Sellars, and M. G. Brown, "Comparison of empirical propagation path loss models for fixed wireless access systems," in *Proc. IEEE 61st Veh. Technol. Conf.*, vol. 1, May 2005, pp. 73–77, doi: 10.1109/VETECS.2005.1543252.
[152] S. Aldossari and K.-C. Chen, "Predicting the path loss of wireless channel models using machine learning techniques in mmWave urban communications," in *Proc. 22nd Int. Symp. Wireless Pers. Multimedia Commun. (WPMC)*, Nov. 2019, pp. 1–6, doi: 10.1109/WPMC48795.2019.9096057.
[153] S. Sun, T. A. Thomas, T. S. Rappaport, H. Nguyen, I. Z. Kovacs, and I. Rodriguez, "Path loss, shadow fading, and line-of-sight probability models for 5G urban macro-cellular scenarios," in *Proc. IEEE Globecom Workshops (GC Wkshps)*, Dec. 2015, pp. 1–7, doi: 10.1109/GLOCOMW.2015.7414036.
[154] J. J. Popoola, A. A. Ponnle, Y. O. Olasoji, and S. A. Oyetunji, "Investigation on need for specific propagation model for specific environment based on different terrain characteristics," *IIUM Eng. J.*, vol. 19, no. 2, pp. 90–104, Dec. 2018, doi: 10.31436/iiumej.v19i2.886.
[155] T. Yilmaz, G. Gokkoca, and O. B. Akan, "Millimetre wave communication for 5G IoT applications," in *Internet of Things (IoT) in 5G Mobile Technologies* C. X. Mavromoustakis, G. Mastorakis, J. M. Batalla, Eds. Cham, Switzerland: Springer, 2016, pp. 37–53.
[156] M. B. Majed, T. A. Rahman, O. A. Aziz, M. N. Hindia, and E. Hanafi, "Channel characterization and path loss modeling in indoor environment at 4.5, 28, and 38 GHz for 5G cellular networks," *Int. J. Antennas Propag.*, vol. 2018, pp. 1–14, Sep. 2018, doi: 10.1155/2018/9142367.
[157] W. Zhang, L. Tian, Z. Wu, J. Zhang, Y. Zheng, and J. Cao, "Dynamic range impact on 3D MIMO channel characteristics in rural-macro scenario at 3.5 GHz," in *Proc. 12th Eur. Conf. Antennas Propag. (EuCAP)*, 2018, p. 47, doi: 10.1049/cp.2018.0406.
[158] A. M. Al-Samman, T. A. Rahman, M. H. Azmi, A. Sharaf, Y. Yamada, and A. Alhammadi, "Path loss model in indoor environment at 40 GHz for 5G wireless network," in *Proc. IEEE 14th Int. Colloq. Signal Process. Appl. (CSPA)*, Mar. 2018, pp. 7–12, doi: 10.1109/CSPA.2018.8368676.
[159] A. M. Al-Samman, T. A. Rahman, M. H. Azmi, M. N. Hindia, I. Khan, and E. Hanafi, "Statistical modelling and characterization of experimental mm-wave indoor channels for future 5G wireless communication networks," *PLoS ONE*, vol. 11, no. 9, Sep. 2016, Art. no. e0163034, doi: 10.1371/journal.pone.0163034.
[160] A. M. Al-Samman, M. N. Hindia, and T. A. Rahman, "Path loss model in outdoor environment at 32 GHz for 5G system," in *Proc. IEEE 3rd Int. Symp. Telecommun. Technol. (ISTT)*, Nov. 2016, pp. 9–13, doi: 10.1109/ISTT.2016.7918076.
[161] M. N. Hindia, A. M. Al-Samman, T. A. Rahman, and T. M. Yazdani, "Outdoor large-scale path loss characterization in an urban environment at 26, 28, 36, and 38 GHz," *Phys. Commun.*, vol. 27, pp. 150–160, Apr. 2018, doi: 10.1016/j.phycom.2018.02.011.
[162] A. A. Budalal, M. R. Islam, M. H. Habaebi, and T. A. Rahman, "Millimeter wave channel modeling—Present development and challenges in tropical areas," in *Proc. 7th Int. Conf. Comput. Commun. Eng. (ICCCE)*, Sep. 2018, pp. 23–28, doi: 10.1109/ICCCE.2018.8539324.
[163] B. W. Domae, R. Li, and D. Cabric, "Machine learning assisted phaseless millimeter-wave beam alignment in multipath channels," 2021, *arXiv:2109.14689*.
[164] N. Xie, L. Ou-Yang, and A. X. Liu, "A machine learning approach to blind multi-path classification for massive MIMO systems," *IEEE/ACM Trans. Netw.*, vol. 28, no. 5, pp. 2309–2322, Oct. 2020, doi: 10.1109/TNET.2020.3008287.
[165] L. Wu, D. He, K. Guan, B. Ai, C. Briso-Rodriguez, T. Shui, C. Liu, L. Zhu, and X. Shen, "Received power prediction for suburban environment based on neural network," in *Proc. Int. Conf. Inf. Netw. (ICOIN)*, Jan. 2020, pp. 35–39, doi: 10.1109/ICOIN48656.2020.9016532.
[166] L. Wu, D. He, B. Ai, J. Wang, H. Qi, K. Guan, and Z. Zhong, "Artificial neural network based path loss prediction for wireless communication network," *IEEE Access*, vol. 8, pp. 199523–199538, 2020, doi: 10.1109/ACCESS.2020.3035209.
[167] H. Cheng, S. Ma, and H. Lee, "CNN-based mmWave path loss modeling for fixed wireless access in suburban scenarios," *IEEE Antennas Wireless Propag. Lett.*, vol. 19, no. 10, pp. 1694–1698, Oct. 2020, doi: 10.1109/LAWP.2020.3014314.
[168] G. Caso, O. Alay, L. De Nardis, A. Brunstrom, M. Neri, and M.-G. Di Benedetto, "Empirical models for NB-IoT path loss in an urban scenario," *IEEE Internet Things J.*, vol. 8, no. 17, pp. 13774–13788, Sep. 2021, doi: 10.1109/JIOT.2021.3068148.
[169] E. Bedeer, J. Pugh, C. Brown, and H. Yanikomeroglu, "Measurement-based path loss and delay spread propagation models in VHF/UHF bands for IoT communications," in *Proc. IEEE 86th Veh. Technol. Conf. (VTC-Fall)*, Sep. 2017, pp. 1–5, doi: 10.1109/VTCFall.2017.8287901.
[170] J. Hejselbæk, J. O. Nielsen, C. Drewes, W. Fan, and G. F. Pedersen, "Propagation measurements for device-to-device communication in forest terrain," in *Proc. 12th Eur. Conf. Antennas Propag. (EuCAP)*, 2018, p. 30, doi: 10.1049/cp.2018.0389.
[171] S. P. Sotiroudis, P. Sarigiannidis, S. K. Goudos, and K. Siakavara, "Fusing diverse input modalities for path loss prediction: A deep learning approach," *IEEE Access*, vol. 9, pp. 30441–30451, 2021, doi: 10.1109/ACCESS.2021.3059589.
[172] S. P. Sotiroudis, S. K. Goudos, and K. Siakavara, "Neural networks and random forests: A comparison regarding prediction of propagation path loss for NB-IoT networks," in *Proc. 8th Int. Conf. Modern Circuits Syst. Technol. (MOCAST)*, May 2019, pp. 1–4, doi: 10.1109/MOCAST.2019.8741751.
[173] K. M. Malarski, J. Thrane, H. L. Christiansen, and S. Ruepp, "Understanding sub-GHz signal behavior in deep-indoor scenarios," *IEEE Internet Things J.*, vol. 8, no. 8, pp. 6746–6756, Apr. 2021, doi: 10.1109/JIOT.2020.3027829.
[174] R. Nordin, H. Mohamad, M. Behjati, A. H. Kelechi, N. Ramli, K. Ishizu, F. Kojima, M. Ismail, and M. Idris, "The world-first deployment of narrowband IoT for rural hydrological monitoring in UNESCO biosphere environment," in *Proc. IEEE 4th Int. Conf. Smart Instrum., Meas. Appl. (ICSIMA)*, Nov. 2017, pp. 1–5, doi: 10.1109/ICSIMA.2017.8311981.
[175] O. Elijah, T. A. Rahman, H. I. Saharuddin, and F. N. Khairodin, "Factors that impact Lora IoT communication technology," in *Proc. IEEE 14th Malaysia Int. Conf. Commun. (MICC)*, Dec. 2019, pp. 112–117, doi: 10.1109/MICC48337.2019.9037503.
[176] H. Linka, M. Rademacher, O. G. Aliu, K. Jonas, B. Rhein-sieg, and S. Augustin, "Path loss models for low-power wide-area networks: Experimental results using LoRa," in *VDE ITG-Fachbericht Mobilkommunikation*. Osnabrück, Germany: VDE Verlag, 2018, pp. 10–14.

[177] P. Jorke, S. Bocker, F. Liedmann, and C. Wietfeld, "Urban channel models for smart city IoT-networks based on empirical measurements of LoRa-links at 433 and 868 MHz," in *Proc. IEEE 28th Annu. Int. Symp. Pers., Indoor, Mobile Radio Commun. (PIMRC)*, Oct. 2017, pp. 1–6, doi: 10.1109/PIMRC.2017.8292708.

[178] G. Callebaut and L. Van der Perre, "Characterization of Lora point-to-point path loss: Measurement campaigns and modeling considering censored data," *IEEE Internet Things J.*, vol. 7, no. 3, pp. 1910–1918, Mar. 2020, doi: 10.1109/JIOT.2019.2953804.

[179] J. Gaelens, J. Verhaevert, H. Rogier, and P. Van Torre, "LoRa mobile-to-base-station channel characterization in the Antarctic," *Sensors*, vol. 17, no. 8, p. 1903, Aug. 2017, doi: 10.3390/s17081903.

[180] N. A. B. Masadan, M. H. Habaebi, and S. H. Yusoff, "LoRa LPWAN propagation channel modelling in IIUM campus," in *Proc. 7th Int. Conf. Comput. Commun. Eng. (ICCCE)*, Sep. 2018, pp. 14–19, doi: 10.1109/ICCCE.2018.8539327.

[181] S. Hosseinzadeh, M. Almoathen, H. Larijani, and K. Curtis, "A neural network propagation model for LoRaWAN and critical analysis with real-world measurements," *Big Data Cognit. Comput.*, vol. 1, no. 1, p. 7, Dec. 2017, doi: 10.3390/bdcc1010007.

[182] T. Ameloot, P. Van Torre, and H. Rogier, "A compact low-power LoRa IoT sensor node with extended dynamic range for channel measurements," *Sensors*, vol. 18, no. 7, p. 2137, 2018, doi: 10.3390/s18072137.

[183] G. M. Bianco, R. Giuliano, G. Marrocco, F. Mazzenga, and A. Mejia-Aguilar, "LoRa system for search and rescue: Path-loss models and procedures in mountain scenarios," *IEEE Internet Things J.*, vol. 8, no. 3, pp. 1985–1999, Feb. 2021, doi: 10.1109/JIOT.2020.3017044.

[184] D. Wohwe Sambo, A. Forster, B. O. Yenke, I. Sarr, B. Gueye, and P. Dayang, "Wireless underground sensor networks path loss model for precision agriculture (WUSN-PLM)," *IEEE Sensors J.*, vol. 20, no. 10, pp. 5298–5313, May 2020, doi: 10.1109/JSEN.2020.2968351.

[185] S.-Y. Wang, Y.-H. Cheng, and J.-H. Tarng, "Improving the localization accuracy for Sigfox low-power wide area networks," in *Proc. IEEE Symp. Comput. Commun. (ISCC)*, Jun. 2019, pp. 1–6, doi: 10.1109/ISCC47284.2019.8969734.

[186] M. C. Bor, U. Roedig, T. Voigt, and J. M. Alonso, "Do Lora low-power wide-area networks scale?" in *Proc. 19th ACM Int. Conf. Modeling, Anal. Simulation Wireless Mobile Syst.*, Nov. 2016, pp. 59–67, doi: 10.1145/2988287.2989163.

HAIDER A. H. ALOBAIDY (Graduate Student Member, IEEE) received the M.Sc. degree in electrical engineering/electronics and communication from the Faculty of Engineering, Mustansiriyah University, Iraq, in 2016. He is currently pursuing the Ph.D. degree with the Department of Electrical, Electronic and Systems Engineering, Faculty of Engineering and Built Environment, Universiti Kebangsaan Malaysia (UKM). His research interests include wireless sensor networks, wireless communication, the IoT, and channel propagation modeling and estimation.

MANDEEP JIT SINGH is a Professor with the Department of Electrical, Electronic and Systems Engineering, Universiti Kebangsaan Malaysia (UKM). He is currently the Advisor of the Engineering Education Technical Division (E2TD), The Institution of Engineers, Malaysia. He is an author and a coauthor of more than 240 research articles in antenna and microwave RF. His research interests include communication antenna design, radio wave propagation, satellite antennas, and the IoT. He received several international and national medal awards for his research and innovation.

MEHRAN BEHJATI received the B.Sc. degree in electrical and electronic engineering from Islamic Azad University, Iran, in 2009, and the M.Sc. and Ph.D. degrees in communication engineering from the National University of Malaysia (UKM), in 2013 and 2017, respectively. He is currently a Postdoctoral Researcher with the Department of Electrical, Electronics, and System Engineering, UKM. His main research interests include advanced multiple-input multiple-output (MIMO) systems, interference management, limited-feedback techniques, aerial wireless communications, the IoT, the Internet of Drone (IoD), and green communications.

ROSDIADEE NORDIN (Senior Member, IEEE) received the B.Eng. degree in electrical, electronic, and systems engineering from Universiti Kebangsaan Malaysia (UKM), in 2001, and the Ph.D. degree in wireless engineering from the University of Bristol, U.K., in 2010. After completing his B.Eng. degree, he worked as an Engineer at Malaysia's telecommunication industry for almost five years. He is currently an Associate Professor of electrical, electronic, and systems engineering with UKM.

NOR FADZILAH ABDULLAH (Member, IEEE) received the B.Sc. degree in electrical and electronics from Universiti Teknologi Malaysia, in 2001, the M.Sc. degree (Hons.) in communications engineering from The University of Manchester, U.K., in 2003, and the Ph.D. degree in electrical and electronic engineering from the University of Bristol, U.K., in 2012. She is currently an Associate Professor with the Department of Electrical, Electronic, and Systems Engineering, Universiti Kebangsaan Malaysia. Her research interests include 5G, millimeter wave, LTE-A, vehicular networks, MIMO, space time coding, fountain code, and channel propagation modeling and estimation.